UNIVERSITY OF OKLAHOMA

GRADUATE COLLEGE

MASS AND CHARGE TRANSPORT IN ALCOHOL AND KETONE

SOLVENTS AND ELECTROLYTE SOLUTIONS

A DISSERTATION

SUBMITTED TO THE GRADUATE FACULTY

IN PARTIAL FULFILLMENT OF THE REQUIREMENTS FOR THE

DEGREE OF

DOCTOR OF PHILOSOPHY

BY

ALLISON M. FLESHMAN
NORMAN, OKLAHOMA
2012

UMI Number: 3522886

UMI

Dissertation Publishing

ProQuest®

MASS AND CHARGE TRANSPORT IN ALCOHOL AND KETONE
SOLVENTS AND ELECTROLYTE SOLUTIONS

A DISSERTATION APPROVED FOR THE
DEPARTMENT OF CHEMISTRY AND BIOCHEMISTRY

BY

_____

Dr. Wai Tak Yip (Chair)

_____

Dr. Roger Frech

_____

Dr. Daniel T. Glatzhofer

_____

Dr. Charles Rice

_____

Dr. John Moore-Furneaux

_____

Dr. Ralph A. Wheeler

Acknowledgements

It is difficult to list the people who have helped me over the past seven years, because there have honestly been so many. The first person to whom I owe so much, of course is **Roger Frech**. I am grateful that even when retirement was getting closer, you said, "just one more student". I am honored that you gave me the opportunity to be part of the select group of students that you mentored (the 21st!) over your incredible science career. I have learned so much from you and I look forward to sharing all of it with students of my own.

Thank you **John Moore-Furneaux**, who gave me a summer research job when I had no clue what I was doing, and then hired me again. Your enthusiasm and passion for understanding all things science (and not) is truly inspiring. I also convinced you to group Bobby and I together in electronics lab. That turned out very well. Thanks for that, too!

I would also like to thank **Ralph Wheeler**. I enjoyed the time we worked together, and learned many things. I gained so much confidence from you and am grateful for our ventures into the world of computational chemistry. I look forward to our paths crossing in the future; I know they will. To the other members of my committee: **Ivan Yip**, **Charles Rice**, and **Dan Glatzhofer**, thank you for sharing your love of science with me and helping me all along the way.

Matt Petrowsky, you are the big brother I never had. You have a work ethic that is uncanny, a drive for understanding that is contagious, and obsessive ways that can be incredibly irritating. But I owe so much of my success to you. You are a great, and

inspiring scientist and will always be my sparkling friend. **Scott Boesch**, thank you for your computational genius and especially your friendship. Both mean so much to me.

Matt Johnson, I have learned so much from you during all of these years, both in the lab and out. Your intense teaching style was difficult to get used to, but rewarding because it worked. Thank you. To **Jeremy Jernigan**, **Roshan Bokalawela**, and **Chris Crowe**; you guys were my wingmen when we set up the automated system. You saved me so many hours of work by dedicating so many of yours, and that will not be forgotten.

I would like to thank **Robert Mantz** and the **Army Research Office**. Your support of our work made some of the most beautiful data possible.

I am in debt to the staff of the **Department of Chemistry and Biochemistry**, especially **Laura Cornell, Carl van Buskirk, Susan Nimmo, Chad Cunningham, and Carol Jones.** Your work and enthusiasm to always help was priceless. Thank you.

To the previous members of the Frech Group (I am the only one left!). I am so lucky to have you all in my academic family and I know the friendships we formed will last for many years: **Varuni Seneviratne, Whitney Booher, Gwen Giffin, Nimali Bopege, Nathalie Rocher, Dilhani Jayathilaka, Chris Burba, Shawna York**, and especially **Rachel Mason**. Thanks also to **Adam Campbell** for years of PChem camaraderie.

To my friends who kept me going: **Kristen & Jef Wagner, John & Carolynn Moore, Brent Johnson, Laura & Jack Lege, Melissa Bruker, Larry Mad-**

dox, **Gail & Jeff Huber, Shayne Cairns, Scarlet Norberg, Sean Krzyzewski, Michele Gressman, Jason Benesh**, et **Stéphane Valladier**. For the others I left off, I thank you too.

I thank my family: **Bob and Jacque Fleshman**, and **Cindi and Mike Jackman** for your love and support, and the countless glasses of wine that helped keep sanity close. Thanks to my sister, **Valerie** and her husband **Kevin** (It's nice not being the only science nerds in the family.)

I would not be a scientist if it weren't, of course, for my parents, **Karen and Steve McCoy**. Both of you instilled in me the importance of education; I hold on to that dearly and will forever be a student. Thank you both.

And finally I want to thank my husband, **Bobby**. For the science part: your computational help and the countless discussions of data over dinner gave me some of the greatest insight into my research. Thank you. For the marriage part: you are my best friend, and the only one who truly knows what went into this whole thing. Thank you for helping me become the best version of myself. *Je t'aimerai toujours.*

I would also like to thank my cat, **Luxor**, because, well, he's my cat and everyone needs a cat.

Table of Contents

List of Tables

List of Figures

Abstract

Experimental data show there is a distinct relationship between the molal conductivity and concentration for electrolyte solutions with low dielectric constants. The molal conductivity decreases with the square root of the concentration to a minimum in the area referred to as "region I", and then increases to a maximum over the concentration range referred to as "region II". This behavior has been attributed to changes in ionic association in the electrolyte. The electrolyte systems used in this study, however, show this behavior but exhibit no spectroscopic evidence of ionic association. Molecular level properties are determined using the compensated Arrhenius Formalism (CAF) that add valuable insight in describing the qualitative behavior of the molal conductivity with concentration. The CAF assumes that transport is a thermally activated process, and uses the dielectric constant as a measure of changes in the intermolecular interactions. This formalism makes it possible to measure the energy of activation for mass and charge transport. Hydrodynamic models that use the solution viscosity as a characteristic system property in describing transport do not paint any picture of these transport mechanisms at the molecular level. Modeling mass and charge transport as a thermally activated process through the use of the CAF agrees with the experimental data. This work uses the dielectric constant as a key component in describing transport. The CAF is applied to mass transport in hydrogen-bonded 1- and 3-alcohol liquids and non-associating 2-ketone liquids, and the differences observed between the systems are explained using the CAF results. The CAF is also applied to a range of concentrations of tetrabutylammonium trifluoromethanesulfonate (TbaTf) dissolved in 1- and

3-alcohol and 2-ketone solvents. The results offer a new interpretation for the qualitative behavior of the molal conductivity with concentration. This work will show that the increase in region II is a complicated relationship between the concentration dependence of the energy of activation and the concentration dependence of the dielectric constant, consistent with the data from multiple electrolyte systems.

Chapter 1

Introduction

1.1 The need for better batteries

The role of portable electronic devices during the day of an average, U.S. citizen has shifted from convenience to necessity over the past decade. Most notable is the cellular phone. According to a recent report given by CNN, 88% of U.S. adults own and use a cell phone, while 46% of those phones are considered "smartphones".[1] A smartphone is a hand-held computer device that offers the user access to the internet as well as the typical features associated with a phone. The limiting factor for the advancement of these devices, however, is the rechargeable battery that powers them. A typical smart phone requires recharging after approximately 12 hours of use, whereas a non-smart phone can remain charged for as long as five days.[a] In 2007, Apple Inc. released the iPhone™, and sold 1.1 million units during the first year of production. In 2010, 35.1 million iPhones™ were sold.[2] The advancement of smartphone technology, however, is limited to the rechargeable battery systems available in the present market. Given the increased demand for these types of phones, and the need for the power necessary to run them, more efficient rechargeable battery systems are needed.

Another justification for the improvement of rechargeable battery systems is the increased demand for electric vehicles. According to the U.S. Department of Energy, the sales of hybrid electric vehicles increased from 50,000 in 2002 to 300,000 in 2010.[3]

---

[a]This data was collected using an iPhone 3GS™ (smart phone) and a Samsung A107 GSM™ (non-smart phone).

The Chevrolet Volt[TM] (a common electric hybrid vehicle) can travel approximately 35 miles on a single charge.[3] The limitation of the distance travelled of this vehicle is, in part, the efficiency of the battery.

1.2   Background information

A schematic of a typical rechargeable lithium battery is shown in **Fig. 1.1**.[4] The battery system contains two electrodes separated by an electrolyte. The anode is most
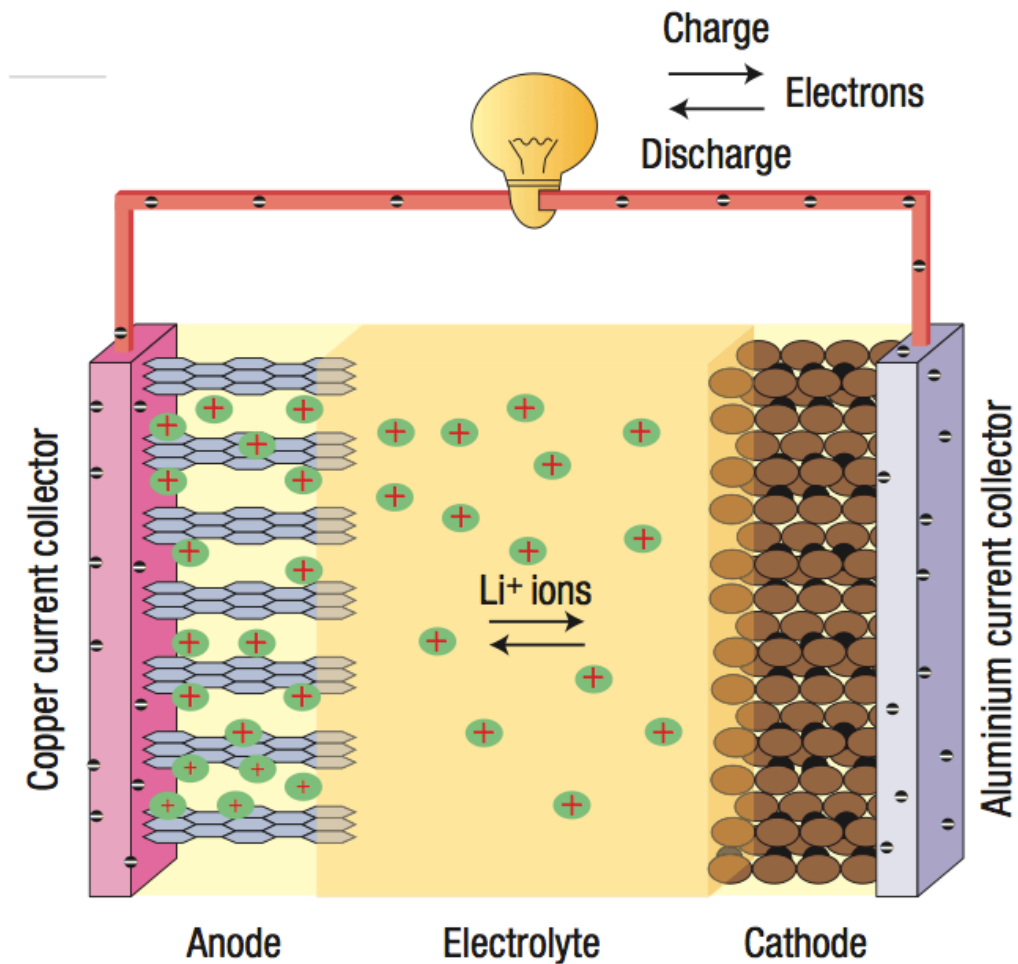
Figure 1.1: Schematic of rechargeable lithium ion battery, with labels described in the text.[4]

commonly comprised of a lithiated carbon material on a copper current collector,[4,5] as labelled in the figure. The cathode contains a lithium metal oxide that covers an aluminum current collector.[4,5] Through the discharge cycle, the cathodic material is oxidized, releasing lithium ions that then migrate to the anodic material where they are reduced. The charging cycle reverses this process. During both processes, the ions flow through the medium separating the two electrodes. To a large extent, this medium governs the mobility of the ions. To maximize the efficiency of this electrolytic material it is essential to have a fundamental understanding of the process of charge transport within the material. Several commercially used electrolytes consist of mixtures of various types of charge carriers and solvents so as to maximize the efficiency of the material.[6] To gain this fundamental understanding of charge transport, it is best to examine simple liquid electrolytes which consist of a single salt dissolved in a single polar solvent. The polar solvent in these simple liquids typically contains only one heteroatom. Reducing the number of components results in fewer types of intermolecular interactions, thereby simplifying the relationships between the type of solvent used, the type of salt, and the amount of salt.

The physical properties of the solvent affect the mobility of the ions. In particular, the migration of the ion will be different in a solvent with strong solvent-solvent interactions (*i.e.*, an associating solvent) as opposed to a solvent that is weakly associated. For example, the conductive properties of water will be very different than those of a non-hydrogen bonding solvent.[7] To better understand the relationship of these solvent-solvent interactions, and their role in the conductive properties of the electrolyte, systems containing associating liquids (*via* hydrogen bonding) will be com-

pared to non-associating solvents. The number of ions present in the electrolyte also plays a vital role in the conductive properties of the material. Therefore, this work will also focus on the concentration dependence of salt in the aforementioned associating and non-associating solvents. The liquid properties of the pure solvents will be used to establish a baseline for comparison to the concentrated electrolyte solutions.

The mechanism governing mass and charge transport in simple liquids is not straightforward and has been debated in the literature for more than a century.[8] The models that have been developed are based on hydrodynamic theory and do not always agree with experimental findings.[8–14] These models are also sensitive to the type of system being described, *e.g.*, aqueous, aprotic, *etc.* In order to improve the performance of materials used in battery systems, it is essential to identify the types of molecular and system properties that should be exploited to maximize the material's electrochemical potential.

A molecular level picture has been developed by Petrowsky and Frech[15] that offers a new interpretation of both charge and mass transport in simple liquid systems. The compensated Arrhenius Formalism (CAF) relates molecular level properties to bulk transport measurements and yields a model of the temperature-dependent transport property that agrees well with experiment.[15–17] The CAF assumes that a major component in describing the temperature dependence of mass and charge transport is the temperature dependence of the dielectric constant of the system.

If a clear molecular level picture of the mechanism governing ion transport can be determined in simple electrolyte systems, then the molecular level properties that enhance the conductivity can be used to design better materials that will improve

the battery performance for electric vehicles, smart phones, and any other portable electronic device.

1.3   Research objectives

The goal of this work is to gain a fundamental understanding of mass transport in pure associating and non-associating liquids and the concentration dependence of charge transport in associating and non-associating electrolyte systems through use of the CAF. The associating solvent systems selected are 1- and 3-alcohol solvent systems. The extent of association is different within these two solvent systems even though they share a similar functional group. The non-associating solvent system used in this study is the 2-ketone solvent group, which offers the unique opportunity to vary the range of dielectric constant such that different behaviors of charge transport with concentration are observed. The CAF will also be applied to mass transport of the pure associating and non-associating solvent systems to understand the fundamental differences between transport properties and liquid structure in the absence of salt.

Several experimental techniques are used throughout this work, including vibrational infrared (IR) spectroscopy, impedance spectroscopy, density measurements, and pulse-field-gradient nuclear magnetic resonance (PFG NMR). A detailed description of the use of these techniques, along with sample preparation and data analysis, is given in **Appendix** A.

1.3.1   Outline of the dissertation

The material in this dissertation is organized as follows:

- Chapter 2 gives background information of mass and charge transport. The compensated Arrhenius formalism is described in detail, including an example of the scaling procedure for ionic conductivity. The CAF scaling procedure is also described for application to temperature-dependent diffusion coefficients.

- Chapter 3 applies the CAF to the temperature-dependent conductivities of 1-alcohol based electrolyte solutions over a broad concentration range. A relationship is established between the concentration dependence of the dielectric constant and the concentration dependence of the exponential prefactor, σ_0.

- Chapter 4 compares the differences of temperature-dependent diffusion coefficients between 1- and 3-alcohol solvents using the CAF. The Kirkwood-Frölich model of the temperature dependence of the dielectric constant is used to explain observed differences in the dielectric constant data, as well as differences in the diffusion coefficient data.

- Chapter 5 applies the CAF to the temperature-dependent conductivities of 3-alcohol based electrolyte solutions over the same concentration range as Chapter 3. The results of the 3-alcohol solutions are compared to the results of the 1-alcohol based electrolyte systems given in Chapter 3.

- Chapter 6 applies the CAF to the temperature-dependent conductivities of 2-ketone based electrolyte solutions over a broad concentration range. The 2-ketones are divided into two groups: high dielectric constant solutions and low dielectric constant solutions. The results of the CAF are compared between the two groups. The CAF is also applied to the diffusion coefficients of the pure solvents of the

two groups and the results are compared.

- Chapter 7 gives concluding remarks for the work presented throughout this disser-
  tation. In particular, the major conclusions concerning the concentration depen-
  dence of charge transport in associating and non-associating electrolyte systems
  are summarized.

The purpose of this work is to demonstrate that the accepted view of charge trans-
port is incomplete, and certain physical properties of the electrolyte that explain the
concentration-dependent conductivity in multiple systems have been overlooked. Fur-
thermore, the use of the compensated Arrhenius formalism provides a direct means to
calculate these important physical properties. The findings of this work contribute to
the fundamental understanding of charge transport. This fundamental understanding
will hopefully result in the design of better electrolytic materials, and therefore, better
battery systems.

Chapter 2

Compensated Arrhenius Formalism

Portions of this chapter have appeared in Fleshman, A. M.; Petrowsky, M.; Jernigen, J. D.; Bokalawela, R. S. P.; Johnson, M. B.; Frech, R. *Electrochimica Acta* **2011**, *57*, 147–152.

2.1   General concepts of charge transport

The movement of a charged species through a medium results from the system's response to an external electric field. The properties governing that response, and specifically, the movement of the ion, have been the subject of study for more than a century.[8] Many of the models proposed to describe the motion of ions through a medium have been based on a hydrodynamic interpretation of ionic movement.[18] It is thought that the moving ion has a drift velocity influenced by a resistive drag based on the interactions between the ion and the surrounding solvent. The solution viscosity is a common solvent property used to describe this resistive drag experienced by the ion.[18] Ion transport models involving the macroscopic viscosity do not always agree with experimental data over a broad concentration range. Most notable is the inconsistency of Walden's rule with concentrated electrolytes.[9–14] Part of the goal for this work is to extend the model of the concentration dependence of ion transport in terms of the compensated Arrhenius formalism, which treats ion motion as a thermally activated process rather than a hydrodynamic process.

The conductivity of electrolyte solutions is also affected by changes in the temperature of the system. The temperature dependence of ionic conductivity in rigid solids is usually described by a simple Arrhenius equation: $\sigma = \sigma_0 \exp(-E_a/RT)$. Consequently, in such systems, transport is a thermally activated process. For liquid electrolytes, as well as polymer electrolytes above the glass transition temperature, the simple Arrhenius expression often inadequately describes the temperature dependence. Several empirical models describe the temperature dependence of the conductivity in systems where the simple Arrhenius relationship fails. The empirical relationship between conductivity and temperature, as proposed by William-Landel-Ferry (WLF)[19] is given below:

$$\log \frac{\sigma(T)}{\sigma(T_s)} = \frac{C_1(T - T_s)}{C_2 + (T - T_s)} \qquad (2.1)$$

Here, σ is conductivity, T is temperature, T_s is a reference temperature, and C_1 and C_2 are empirical constants specific to the electrolyte in use. Another model for the temperature-dependent conductivity, was developed by Vogel, Tamman, and Fulcher (VTF equation), and is given by:

$$\sigma = \sigma_0 T^{-1/2} \exp\left[\frac{-B}{T - T_0}\right], \qquad (2.2)$$

where T is the temperature and B, σ_0, and T_0 are empirical constants.[20–22] Again, the constants in **eq. 2.2** are specific to the system being studied. The use of empirical fitting parameters to model the temperature-dependent data are functional for comparing one system to another, but fail to provide any molecular level insight into the mechanism

of conductivity.

The molecular level picture of charge transport offered by the compensated Arrhenius formalism is based on transport being an activated process; a model accepted for solid electrolytes and polymer electrolytes below the glass transition temperature. Unlike the equations given in **eq. 2.1** and **eq. 2.2**, the CAF offers a model for temperature-dependent conductivity that contains no adjustable fitting parameters. The values determined from the CAF represent molecular properties of the systems studied and are reproducible regardless of the method of interpolation for the experimental data, which is a characteristic not observed with the empirical fitting parameters of previous models.

2.1.1   Concentration dependence of charge transport

The general expression for the conductivity, σ, of an electrolyte is given by

$$\sigma = \sum_{i=1} z_i \, c_i \, F \, \mu_i \tag{2.3}$$

where z_i is the charge of the ith ion, c_i is the concentration of species i, F is Faraday's constant, and μ_i is the ionic mobility of species i.[23] For a simple monovalent electrolyte completely dissociated in solution $z_i = 1$ and $c_+ = c_- = c$, where c is the formal concentration of the electrolyte, simplifying **eq. 2.3** to

$$\sigma = c_+ \, F \, \mu^+ + c_- \, F \, \mu^- = c \, F \, (\mu^+ + \mu^-). \tag{2.4}$$

Dividing **eq. 2.4** by c, results in the familiar expression for the molal conductivity,[a] Λ,

---

[a]Unless noted, units of concentration are in moles of salt per kg of solvent, or molal (abbreviated m) and will be used throughout this work, and not the molar scale (moles of salt per liter of solution,

of our simple electrolyte

$$\Lambda = \frac{\sigma}{c} = F\left(\mu^+ + \mu^-\right). \tag{2.5}$$

The expression for Λ in **eq. 2.5** describes a small number of systems in which the electrolyte is completely dissociated, *i.e.*, both the cation and anion form no ionically associated species. If neutral ion pairs do form, the relationship in **eq. 2.5** becomes more complicated. The systems presented in this work, however, follow **eq. 2.5** allowing us to make the statement that the molal conductivity is directly proportional to the sum of the ionic mobilities, *i.e.*, $\Lambda \propto (\mu^+ + \mu^-)$.

Kohlrausch established the empirical model for the concentration dependence of Λ as a linear relationship with the square root of the concentration[18] given by

$$\Lambda = \Lambda^0 - A\, c^{1/2} \tag{2.6}$$

where Λ^0 is the limiting equivalent conductivity at infinite dilution and A is a constant. The combined work of Debye, Huckel, and Onsager related the constant, A, to the valence of the electrolyte, the temperature, the solution dielectric constant, and the solution viscosity.[18] According to **eq. 2.6**, a plot of Λ versus $c^{1/2}$ will be linear, but this is not the case for the systems presented throughout this work. For electrolytes with a low dielectric constant (generally $\varepsilon_s \lesssim 10$) three distinct regions are observed when Λ is plotted versus the square root of the concentration. A schematic in **Fig. 2.1** illustrates these regions. This behavior is seen in both protic and aprotic liquid electrolytes as

_____

M) as is traditionally used.
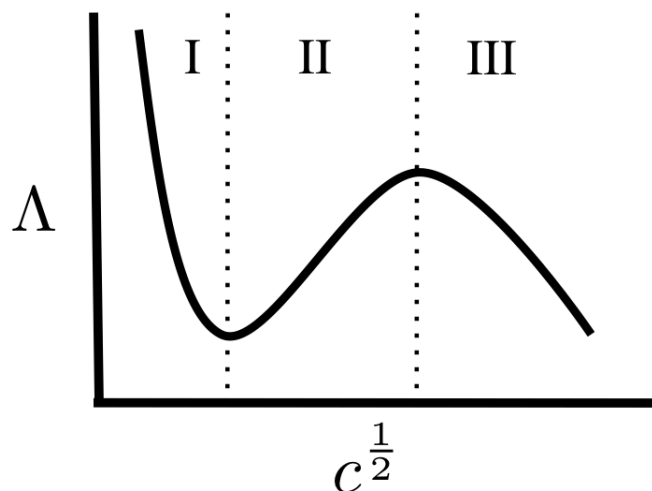
Figure 2.1: Schematic of molal conductivity versus square root of the salt concentration depicting three different regions labelled I, II, & III for a low permittivity electrolyte.

well as polymer electrolytes. An initial decrease to a minimum is observed at low concentrations (labelled region I), then an increase to a maximum (marked region II), followed by a decrease (region III). The three regions are labelled following the notation of Albinsson *et al.*[10] The non-linear relationship between Λ and $c^{1/2}$ supports the need for a more complete understanding of the relationship between molal conductivity and concentration than that offered by Kohlrausch and the works of Debye, Huckel, and Onsager.[18] Given that the molal conductivity is directly proportional to the sum of the mobility of the ions (*i.e.*, the fraction of charged species is unity), the relationship between Λ and concentration becomes a relationship between the ionic mobilities and concentration. Previous works have proposed several explanations for the minimum and maximum behavior of Λ. The decrease in region III is ascribed to an increase in the solution viscosity, which causes a reduction in the molal conductivity.[10,24] This region is not investigated here because of limitations in measuring the dielectric constant at salt concentrations corresponding to region III, as well as solubility limits that are reached

at these concentrations for some of the systems studied. One of the many goals of this work is to explain the decrease of Λ in region I and the increase in region II. The previous interpretations have been primarily based on changes in ionic association, where both the extent of association and nature of associated species varies with concentration. The initial decrease in region I of both polymer electrolytes and organic liquid electrolytes is ascribed to a decrease in the number of "free" ions by the formation of neutral ion pairs.[10,24,25] One explanation for the subsequent increase of Λ in region II is that there is a shift in the association equilibrium from neutral pairs back into "free" ions, which results in a "redissociation" effect.[24,26,27] Another explanation, however, claims that the low dielectric constant allows for the formation of triple ions introducing more charge carriers and thus an increase in Λ.[28,29] Ferry *et al.*,[30] however, determined that the increase in region II in polypropylene glycol $LiCF_3SO_3$ systems is not governed by the variation of population of neutral ion pairs, but postulated that an increase of the ionic mobilities with concentration causes the increase in Λ. Spectroscopic data were used to determine the percentage of "free," contact-ion pair, and aggregate ions across the concentrations corresponding to the increase of Λ in region II. It was concluded that the ionic mobilities must increase over the concentration range, because the percent of "free" and pair remained constant.[30,31] The present work agrees with the interpretation of Ferry *et al.*, that the increase in Λ with concentration is due to an increase in the sum of the ionic mobilities.[30] In addition, this work proposes that conductivity is a thermally activated process and that the concentration dependence of the sum of the ionic mobilities originates from two contributions: the concentration dependence of the energy of activation, and the concentration dependence of the solution dielectric

constant.

2.1.2 Concentration dependence of the static dielectric constant

Previous studies involving aqueous monovalent electrolytes have shown that the dielectric constant decreases with increasing concentration.[32,33] The variation of the dielectric constant in alcohol-based electrolytes is not consistent, however, and depends on the nature of the salt. Gestblom *et al.* measured ε_s in solutions of LiCl and $CaCl_2 \cdot 2H_2O$ in 1-propanol[34] and 1-hexanol[35] and found it to decrease with concentration for LiCl but increase for $CaCl_2 \cdot 2H_2O$. They also reported that ε_s remains constant with increasing concentration of $CaCl_2 \cdot 2H_2O$ in ethanol while it decreases with LiCl and increases with $Ca(NO_3)_2 \cdot 4H_2O$.[35] The use of hydrated salts affects the dielectric constant behavior with concentration differently than the non-hydrated salts. Gestblom *et al.*[34,36] and others[37,38] attribute the increase in ε_s with salt concentration to an increase in the total number of dipoles by the addition of dipoles formed by ion pairs. Sigvartsen *et al.*[38] reported an increase in ε_s with increasing concentrations of tetrabutylammonium perchlorate ($TbaClO_4$) in several different non-aqueous solvents ranging in dielectric constant from $3 - 20$. The properties of Tba^+ will be discussed in detail in § 2.1.3. In brief, Tba^+ is a non-associating cation rendering the claim of increased dipoles due to contact-ion pairs inaccurate.

Much work has been done in studying the effect of the magnitude of ε_s on the conductivity of electrolytes.[27,36,37,39] In several cases, water-dioxane mixtures were used such that ε_s of the mixture could be varied by adjusting the proportions of water to dioxane. The extreme values of ε_s of the pure solvents (water, $\varepsilon_s \approx 80$ and dioxane, ε_s

≈ 2) allowed a broad range of ε_s to be covered. Kraus and Fuoss [39] used tetraisoamy-lammonium picrate as the salt in these water-dioxane mixtures. Benzene and ethylene chloride were also used. It was determined that the conductivity changed greatly with increasing ε_s (increasing per cent of water), and the minimum of Λ shown in **Fig. 2.1** shifted to higher concentration for higher values of ε_s. The reasons for this were based on the value of the dielectric constant alone and not the effect of the solvent. Viscosity arguments were used to interpret variations from using the different solvents, but as previously described, the solution viscosity is a poor descriptor of ion transport. While the work of Kraus and Fuoss [39] was thorough, a more simplistic approach is needed to understand the effect that ε_s has on conductivity. The work presented here does not involve mixtures of solvents in order to avoid the introduction of additional solvent-solvent interactions. Here, ε_s is systematically changed by adding a methylene group to simple liquids with a similar functional group. Additionally ε_s was varied by increasing the temperature, which decreases ε_s. Both methods for changing the dielectric constant offer a new way to develop a molecular level picture of ion transport. The choice of salt in this work also provides a more straightforward means to determine the role of the solvent in these electrolyte solutions.

2.1.3 Tetrabutylammonium Trifluoromethanesulfonate: TbaTf

Only one salt is used throughout this work. Tetrabutylammonium (($[CH_3(CH_2)_3]_4N^+$, abbreviated Tba) trifluoromethanesulfonate ($CF_3SO_3^-$, referred to as triflate, and abbreviated Tf) is unique in that both the cation and anion play integral roles in elucidating the effects of solute on the solvent. TbaTf has been previously shown to exists
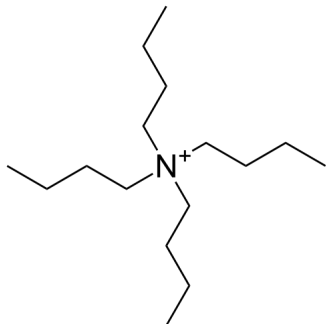
Figure 2.2: Tetrabutylammonium cation $((CH_3CH_2CH_2CH_2)_4N^+$, abbreviated Tba)
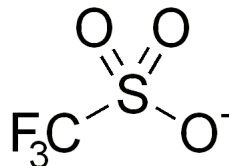
Figure 2.3: Trifluoromethanesulfonate $(CF_3SO_3^-$, referred to as triflate, and abbreviated Tf)

spectroscopically as "free" ions in several solvent systems for a wide range of concentrations[40–44] and further evidence of this will be given throughout the next few chapters for the concentration ranges studied here. The bulky butyl groups of the Tba^+ protect the charge on the nitrogen and hinder association with the anion.

Triflate is a suitable anion for this study in that it is monovalent and has several well-studied, spectroscopically detectable modes whose frequencies are sensitive to cation-anion interactions.[30,45–48] The infrared vibrational frequency of the $\nu_s(SO_3)$ symmetric stretching region of triflate does not overlap any solvent bands studied here and the bands are clearly identifiable as either "free" (≈ 1032 cm^{-1}),[42] or contact-ion pair (≈ 1040 cm^{-1}).[48]

It is important to choose a non-associating salt for these projects, because the majority of the previous arguments for the concentration dependence of Λ and ε_s, as explained in § 2.1.1 and § 2.1.2 respectively, are based on ionic association. As will be shown in the following chapters, TbaTf also shows these concentration dependent behaviors in Λ and ε_s. The interpretation of the data, most notably the concentration

dependence of Λ, can therefore be simplified to only solvent-solvent interactions with minimal solvent-ion interactions. The ion-ion interactions are negligible and cannot be used to explain the concentration dependent behaviors of Λ and ε_s for TbaTf in the solutions presented here, as has been done for several decades.

2.2   The compensated Arrhenius formalism: CAF

2.2.1   General concept

Based on the work of Petrowsky and Frech [15], the compensated Arrhenius formalism (CAF) takes an unconventional view of mass and charge transport that assumes transport to be a thermally activated process. The CAF has been successfully tested with ionic conductivity,[15,17,49–51] dielectric relaxation,[52] and self-diffusion[16,51] of organic liquid electrolytes and pure protic and aprotic solvents.

To give a general overview of the formalism, the ionic conductivity will be discussed, but the formalism will be extended to self-diffusion coefficients in § 2.3. The CAF assumes the temperature-dependent conductivity can be written in an Arrhenius form as

$$\sigma(T) = \sigma_0(T) \exp\left[\frac{-E_a}{RT}\right]. \tag{2.7}$$

Here σ is the ionic conductivity, σ_0 is the exponential prefactor, E_a is the energy of activation, and R and T are the gas constant and temperature. The initial deviation from a simple Arrhenius form is the addition of a temperature dependence in σ_0. It is well known that the conductivity depends on the solution static dielectric constant, ε_s. This formalism postulates that the dielectric constant dependence of the conductivity is

contained in the exponential prefactor along with a temperature dependence, and can be written as $\sigma_0(\varepsilon_s, T)$. The CAF further assumes that the temperature dependence of the exponential prefactor is due to the temperature dependence of the dielectric constant such that **eq. 2.7** becomes

$$\sigma = \sigma_0(\varepsilon_s(T)) \exp\left[\frac{-E_a}{RT}\right]. \tag{2.8}$$

A scaling procedure can be performed that removes the exponential prefactor allowing for the calculation of E_a, which governs the thermally activated process.[15,17,49]

The CAF represents a significant departure from conventional theories describing mass and charge transport. The generally accepted hydrodynamic model of transport assumes that solvent molecules exert a resistive drag on the moving ion/molecule. The CAF proposes a new interpretation of ion transport, unlike those based on hydrodynamic models, that uses the dielectric constant rather than viscosity as the critical parameter characterizing transport. It is well known that the conductivity depends on both the temperature and the dielectric constant[29] of the solution. Several empirical models describe the temperature dependence of the conductivity, but do not take into account the dielectric constant or the temperature dependence therein, as described in § 2.1.[19–22] This work will show that the static dielectric constant dependence in the exponential prefactor, given in **eq. 2.8**, represents a significant part of the temperature dependence of the conductivity and must therefore be included in models of the temperature dependence of ion transport.

2.2.2 Scaling procedure example - 0.035 m TbaTf 1-heptanol

The process of scaling out the dielectric constant dependence contained in σ_0 begins with the identification of a solvent family and the construction of a reference curve. A solvent family is defined as a group of compounds that have similar intermolecular interactions resulting from the presence of the same functional group, but have different dielectric constants. For example, the solvent family chosen for the study in Chapter 3 is the linear 1-alcohol family: 1-hexanol, 1-heptanol, 1-octanol, 1-nonanol, 1-decanol, and 1-dodecanol. The construction of a reference curve here is based on the observation that as the alkyl chain length increases, the dielectric constant decreases at a constant temperature, T_r, which is defined as the reference temperature. The reference curve is simply an isothermal plot of conductivity versus dielectric constant that includes all members of the solvent family. An example of a conductivity reference curve is given in **Fig. 2.4** for the 0.035 m TbaTf 1-alcohol family. The blue diamonds represent the 25°C reference conductivity curve and are labelled according to the number of carbons in their alkyl chain (*e.g.*, (6) hexanol, (7) heptanol, *etc.*). The reference curve is fit to an empirical function that best represents the data for the purposes of accurate interpolation between data points. The resulting function is used to determine the reference conductivities. The function given in **Fig. 2.4** is the most common function used for reference curves. However, the choice of function to represent the reference curve is arbitrary as long as the temperature-dependent conductivity data can be accurately interpolated with the function.

Another example is given in **Fig. 2.5** which shows the same conductivity data and reference curve as **Fig. 2.4**, but a different functional form is used for the reference
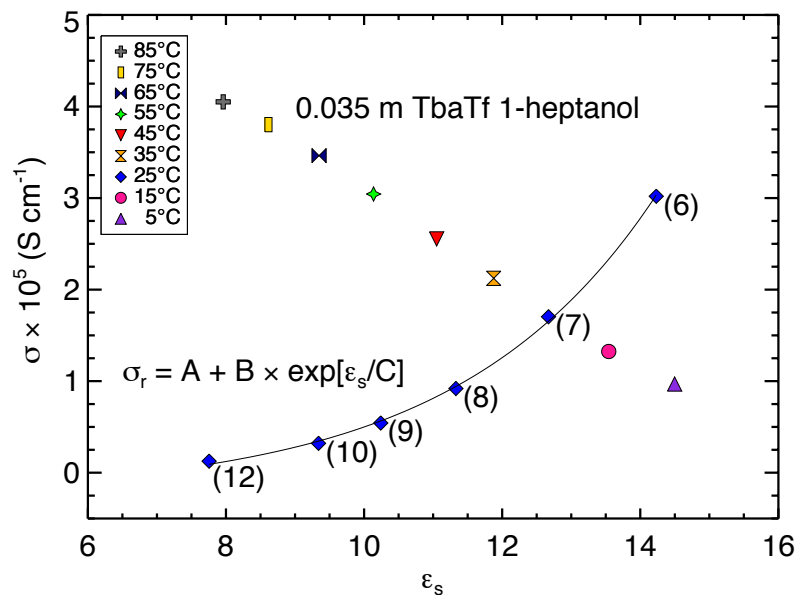
Figure 2.4: Temperature-dependent conductivity versus dielectric constant for 0.035 m TbaTf 1-heptanol. The reference curve for 25°C (blue diamonds) is defined as the isothermal conductivity versus dielectric constant for the 0.035 m TbaTf 1-alcohol solvent family, and is labelled as (6) hexanol (7) heptanol (8) octanol (9) nonanol (10) decanol (11) dodecanol. The best fit line is an empirical fit based on the given equation, where A = -2.5 $\times 10^{-6}$, B = 2.88 $\times 10^{-7}$, and C = 7.87.

curve, and given in the figure. The function used in **Fig. 2.4** yields a slightly better fit to the isothermal data, and is therefore chosen to determine the reference conductivities, but again, either function could be used and will yield accurate results.[a]

Once the function for the reference curve has been determined, it is then used to determine the value of σ_r corresponding to the same value of ε_s for each temperature-dependent conductivity value of the 1-heptanol solution. Next, the measured conductivity, $\sigma(T, \varepsilon_s)$, is divided by the reference conductivity, $\sigma_r(T_r, \varepsilon_s)$, for the selected family member (in this case, 1-heptanol) that, again, corresponds to the *same value of the*

---

[a]The slight deviation in the functional fit of the data in **Fig. 2.5** is incredibly minor and concern should only arise if significant deviations occur in the functional fit of the data. I would be confident to use either function, but for the purposes of this example, the exponential growth was chosen.
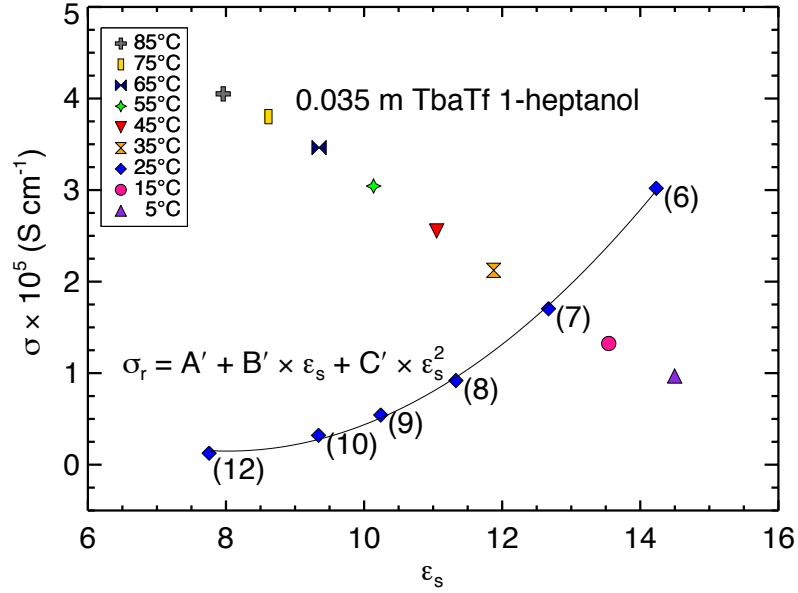
Figure 2.5: Conductivity and dielectric constants for the same system as **Fig. 2.4**, however the best fit line for the reference curve is given by a different function than **Fig. 2.4**. The equation is given in the figure, where A' = 4.91 $\times 10^{-5}$, B' = -1.19 $\times 10^{-5}$, and C' = 7.39 $\times 10^{-7}$.

dielectric constant as the exponential prefactor, $\sigma_0(\varepsilon_s(T))$, shown in **eq. 2.9**.

$$\frac{\sigma(T, \varepsilon_s) = \sigma_0(\varepsilon_s(T)) \, e^{-E_a/RT}}{\sigma_r(T_r, \varepsilon_s) = \sigma_0(\varepsilon_s(T_r)) \, e^{-E_a/RT_r}} \qquad (\mathbf{2.9})$$

Given that $\varepsilon_s(T) = \varepsilon_s(T_r)$, the exponential prefactors cancel and the ratio of the temperature-dependent conductivity to reference conductivity can be plotted as the natural logarithm versus reciprocal temperature to yield an energy of activation that can be calculated from either the slope or the intercept. **Eq. 2.10** is called the compensated Arrhenius equation (CAE) and the resulting plot is referred to as a compensated Arrhenius plot.

$$\ln\left(\frac{\sigma(T, \varepsilon_s)}{\sigma_r(T_r, \varepsilon_s)}\right) = -\frac{E_a}{R}\frac{1}{T} + \frac{E_a}{RT_r} \qquad (\mathbf{2.10})$$

A simple Arrhenius expression contains an exponential prefactor that is not temperature-dependent and can also be plotted versus reciprocal temperature following the equation

$$\ln(\sigma(T)) = -\frac{E_a}{R}\frac{1}{T} + \ln(\sigma_0). \tag{2.11}$$

Throughout this work, **eq. 2.11** is defined as the simple Arrhenius equation (SAE), and the corresponding plot a simple Arrhenius plot. **Fig. 2.6** shows a simple Arrhenius plot (filled circles, left axis) and a compensated Arrhenius plot (open diamonds, right axis) for 0.035 molal TbaTf 1-heptanol over the temperature range $5 - 85°C$. The curvature of the simple Arrhenius plot is due to the temperature dependence of the dielectric constant in the exponential prefactor shown in **eq. 2.8**, and is the primary reason for using the scaling procedure of the CAF. Once this temperature dependence is scaled out using the CAF, the scaled conductivity yields a straight line when plotted as the natural logarithm versus reciprocal temperature (**Fig. 2.6**). The E_a is calculated from the slope (48.5 kJ mol^{-1}) and the intercept (48.7 kJ mol^{-1}), yielding an average E_a of 48.6 kJ mol^{-1}. Using the functional form given in **Fig. 2.5** yields E_a values of 49.0 kJ mol^{-1} (slope) and 49.1 kJ mol^{-1} (intercept). Thus, the choice of the functional form for the reference curve is arbitrary as long as the data can be accurately interpolated.

To better illustrate the individual steps of the scaling procedure, **Table 2.1** gives the necessary data to scale the 0.035 m TbaTf 1-heptanol data using the 25°C reference conductivity curve given in **Fig. 2.4** and create the plots in **Fig. 2.6**. Each column (labelled A to G) will be described systematically from left to right for the scaling procedure. Column A, B, and C are the experimental data (temperature, conductivity,
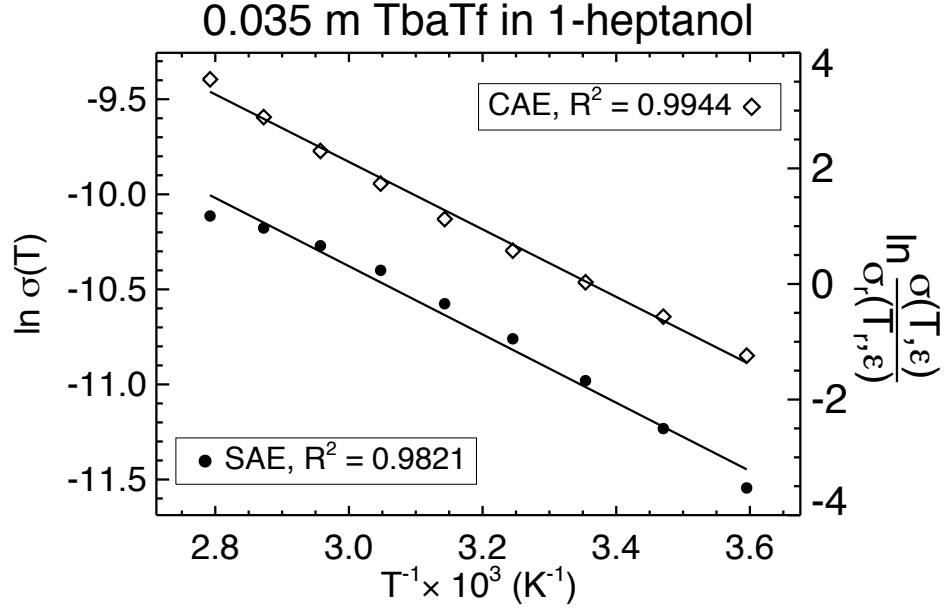
Figure 2.6: Simple Arrhenius plot (Filled circles, left axis) and compensated Arrhenius plot for 0.035 molal TbaTf 1-heptanol with $T_r = 25°C$ (open diamonds). Data are given in **Table 2.1**. Linear best-fit lines are included with corresponding R^2 values.

A	B	C	D	E	F	G
T (°C)	σ (S cm^{-1})	ε_s	σ_r (S cm^{-1})	$\ln\left(\frac{\sigma}{\sigma_r}\right)$	T^{-1} (K^{-1})	$\ln(\sigma)$
5	9.69×10^{-6}	14.50	3.35×10^{-5}	-1.24	3.60×10^{-3}	-11.54
15	1.32×10^{-5}	13.54	2.33×10^{-5}	-0.57	3.47×10^{-3}	-11.23
25	1.70×10^{-5}	12.67	1.65×10^{-5}	0.03	3.35×10^{-3}	-10.98
35	2.12×10^{-5}	11.88	1.19×10^{-5}	0.58	3.25×10^{-3}	-10.76
45	2.55×10^{-5}	11.05	8.31×10^{-6}	1.12	3.14×10^{-3}	-10.58
55	3.04×10^{-5}	10.14	5.36×10^{-6}	1.74	3.05×10^{-3}	-10.40
65	3.46×10^{-5}	9.35	3.47×10^{-6}	2.30	2.96×10^{-3}	-10.27
75	3.80×10^{-5}	8.61	2.12×10^{-6}	2.89	2.87×10^{-3}	-10.18
85	4.05×10^{-5}	7.96	1.17×10^{-6}	3.54	2.79×10^{-3}	-10.11

Table 2.1: Temperature-dependent data for the scaling procedure for 0.035 m TbaTf 1-heptanol using the 25°C reference temperature curve shown in shown in **Fig. 2.4** (blue diamonds). Columns correspond to (A) temperature (B) conductivity (C) dielectric constant (D) reference conductivity using the function given in **Fig. 2.4** (E) natural log of the scaled conductivities, left hand side of **eq. 2.10** (F) reciprocal temperature (G) natural log of the conductivity, left hand side of **eq. 2.11**. Columns E and G are plotted versus Column F in **Fig. 2.6**.

and dielectric constant, respectively) taken for the 0.035 m TbaTf 1-heptanol, and given in **Fig. 2.4**. Column D is the reference conductivity calculated using ε_s from Column C at each temperature with the equation $\sigma_r = A + B \times \exp[\varepsilon_s/C]$, where A, B, and C are given in the caption of **Fig. 2.4**. Column E is the natural logarithm of the scaled conductivities; or the natural log of Column B divided by Column D. Column E represents the left hand side of **eq. 2.10** and is plotted against Column F (the reciprocal temperature) to yield the CAE plot in **Fig. 2.6**. The simple Arrhenius plot is made by plotting Column G (or the natural log of Column B) versus reciprocal temperature. Again, the energies of activation are found from the slope and intercept of the CAE plot following **eq. 2.10**.

The scaling procedure is performed for each member of the alcohol family and the resulting E_a values and corresponding reference temperatures are given in **Table 2.2**. The E_a values calculated from the slope and the intercept are always very close to each other. This is one indication that the conductivity has been compensated correctly.

2.2.3 Selecting an appropriate reference temperature

A plot of the temperature-dependent conductivity versus dielectric constant for the family of 1-alcohols at a concentration of 0.035 molal TbaTf is given in **Fig. 2.7**. As previously mentioned, the non-Arrhenius curvature of the conductivity is due primarily to the temperature dependence of the dielectric constant in the exponential prefactor. To properly compensate the temperature-dependent conductivity data, a reference curve must be chosen with a dielectric constant range that encompasses the temperature-dependent dielectric constants of the selected family member.
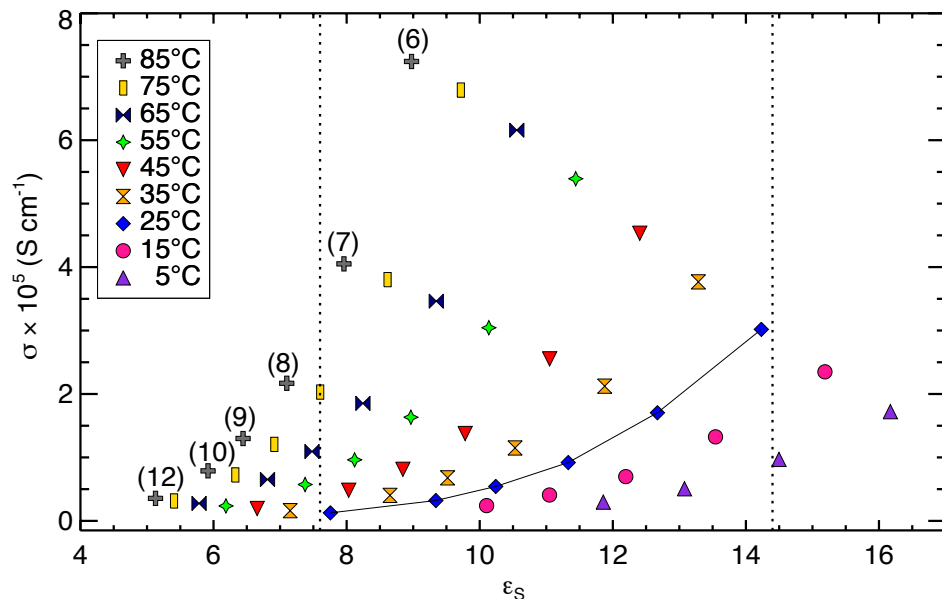
Figure 2.7: Temperature-dependent conductivity versus static dielectric constant for 0.035 molal TbaTf 1-alcohols: (6) 1-hexanol (7) 1-heptanol (8) 1-octanol (9) 1-nonanol (10) 1-decanol (12) 1-dodecanol. The line connecting the 25°C reference curve is a guide to the eye. The vertical dashed lines depict the dielectric constant range available for scaling using the 25°C reference curve.

The 25°C reference conductivity curve (shown connected as a guide to the eye in **Fig. 2.7**) has a dielectric constant range of 7.6–14.2 (the region between the two vertical dashed lines), and can therefore be used to calculate the reference conductivity for each temperature of the 1-heptanol solution (labeled (7)). As previously described in § 2.2.2, scaling the 1-heptanol solution to the 25°C reference curve yields an E_a of 48.5 kJ mol^{-1} from the slope and 48.7 kJ mol^{-1} from the intercept, given in **Table 2.2**. The reference temperature used in the scaling procedure for each temperature-dependent member of the 1-alcohol family along with the resulting E_a values are also given in **Table 2.2**. The 35°C reference curve can also be used to scale the temperature-dependent 1-heptanol data because the dielectric constant range of 35°C is similar to that of 1-heptanol and

System 0.035 molal TbaTf–	T_r (°C)	E_a (slope) (kJ mol^{-1})	E_a (intercept) (kJ mol^{-1})
1-hexanol	15	51 ± 2	51 ± 2
1-heptanol	25	49 ± 1	49 ± 1
1-octanol	45	47.8 ± 0.5	48.1 ± 0.5
1-nonanol	55	48.3 ± 0.9	48.3 ± 0.9
1-decanol	65	50 ± 1	50 ± 1
1-dodecanol	85	52 ± 1	52 ± 1
1-heptanol	75^a	$49.6^a \pm 0.3$	$49.6^a \pm 0.3$
1-dodecanol	35^a	$93^a \pm 17$	$94^a \pm 15$

Table 2.2: Energies of activation, E_a, from the slope and the intercept of the compensated Arrhenius plot. T_r is the corresponding reference temperature of the reference curve used for the scaling procedure. [a]Reference temperatures and E_a values are deemed unreliable, as discussed in Section 2.2.3, and are not used in the calculation of the exponential prefactor.

results in an E_a of 46.9 ± 0.6 kJ mol^{-1} from the slope and 47.1 ± 0.6 kJ mol^{-1} from the intercept, which are comparable to the values from the 25°C reference curve.

Table 2.2 also shows the E_a found by scaling the 1-heptanol solution to the 75°C reference curve, which does not encompass a range of dielectric constant values similar to that for the 1-heptanol solution. Although the E_a values are 49.6 kJ mol^{-1} from both the slope and the intercept, this data point is not included in the calculation of the exponential prefactor because to accurately interpolate the reference conductivities the range of the dielectric constants for the reference curve must cover approximately the same range as the temperature-dependent family member being scaled. A more extreme example is afforded by the use of the 35°C reference curve for scaling the 1-dodecanol solution. This reference curve only includes two of the seven data points of the 1-dodecanol solution which is insufficient for the scaling procedure. Calculating reference conductivities for the 1-dodecanol solution using the 35°C reference curve yields erroneous reference conductivities.[a] The resulting E_a values of 93.5 kJ mol^{-1}

---

[a]The value for the reference conductivity becomes negative for temperatures above 55°C.

(slope) and 94.4 kJ mol^{-1} (intercept) demonstrate the inaccuracy of the extrapolation.

An appropriate choice for 1-dodecanol is the 85°C reference curve, yielding E_a values

of 51.9 kJ mol^{-1} (slope) and 52.3 kJ mol^{-1} (intercept) which are similar to the other

members of the 1-alcohol family at this concentration. The choice of reference curve

depends on the temperature-dependent dielectric constant range of the family member.

As the alkyl-chain length increases, the range of the dielectric constant narrows and

shifts to lower dielectric constant values. This shift can usually be accommodated by

selecting a reference curve corresponding to a higher reference temperature.

2.2.4   Verifying the scaling procedure

One important criterion for validating the choice of reference temperature used in

the scaling procedure is found by considering **eq. 2.9**. For the scaling procedure to be

successful, the ratio of the prefactors must cancel (*i.e.*, $\frac{\sigma_0(\varepsilon_s(T))}{\sigma_0(\varepsilon_s(T_r))}$ must be unity). Once

a T_r is chosen, and the E_a is calculated, the E_a values from the slope and the intercept

can be substituted back into **eq. 2.9**, and the resulting ratio of the prefactors can be

determined at each temperature for each solvent family member, as shown by:

$$\frac{\sigma(T)\, e^{-E_a(intercept)/RT_r}}{\sigma_r(T_r)\, e^{-E_a(slope)/RT}} = \frac{\sigma_0(\varepsilon_s(T))}{\sigma_0(\varepsilon_s(T_r))} \tag{2.12}$$

The E_a values are differentiated by either the slope or the intercept because they

are not identical, and the propagation of the errors of averaging can mask any slight

deviations in the results of the calculation. By rigorously testing each reference temper-

ature and calculating the appropriate prefactor ratios for each family member, the best

T_r can be selected to optimally scale the temperature-dependent conductivity. This additional step in the scaling procedure is useful (and in some cases essential) for solvent systems that do not span a large dielectric constant range, as will be shown in Chapter 4 with the 3-alcohol solvent family. **Table 2.3** gives the prefactor ratios for each temperature calculated using **eq. 2.12** for the example of 0.035 TbaTf 1-heptanol. Only reference temperatures 15, 25, and 65°C are shown, but a typical analysis would require that each reference temperature (5 – 85°C) be considered. The third criterion

Temperature	$\sigma_0(\varepsilon_s(T))/\sigma_0(\varepsilon_s(T_r))$		
T_r (°C)	15	25	65
5	1.660	1.129	1.009
15	1.218	1.070	1.029
25	0.894	0.984	1.005
35	0.676	0.900	0.963
45	0.559	0.857	0.947
55	0.572	0.906	1.009
65	0.709	0.942	1.019
75	3.606	1.030	1.018
85	N/A[a]	1.241	1.004
CAE R^2	0.9055	0.9944	0.9996

Table 2.3: Calculated ratios of exponential prefacators for 0.035 TbaTf 1-heptanol following **eq. 2.12** with reference temperatures 15, 25, and 65°C for each temperature. The CAE R^2 correspond to the goodness of fit of the CAE plot for each respective T_r. [a]The 15°C reference temperature for the 85°C data point resulted in a negative reference conductivity and is therefore invalid.

for selecting an appropriate reference temperature is the resulting linearity of the CAE plots.[a] The R^2 values from the CAE plots using the associated reference temperature are given at the bottom of **Table 2.3**. If the scaling procedure canceled out the entire exponential prefactor, then the ratio of the prefactors would be unity. **Table 2.3** shows quite a variation of prefactor ratios for the 15°C reference temperature. This would not be an appropriate reference temperature to select. Choosing a T_r of 65°C

---

[a]I have arbitrarily used an R^2 value of 0.99 as the lower cut-off value for determining a successful application of the CAF based on the linearity of the CAE plot.

yields values of the prefactor ratio that are quite close to unity, as well as a very linear compensated plot with an R^2 value of 0.9996. However, as shown in **Fig. 2.7**, the reference temperature chosen must correspond to a reference curve that encompasses the range of ε_s of the selected family member. The 65°C reference curve is depicted by the black bow-ties in **Fig. 2.7** and covers a much lower dielectric constant range than the 1-heptanol conductivity data (the curve labelled (7)) and would therefore require extrapolation to determine reference conductivities. The only choice left would be the 25°C reference temperature, which (1) has values of the prefactor ratio close to one, (2) corresponds to a reference curve that encompasses the dielectric constant range spanned by the temperature-dependent conductivity, and (3) yields a linear CAE plot. The 35°C reference temperature could also be chosen as described in § 2.2.3, as it has prefactor ratios close to unity and an R^2 value of 0.9987. However, the range of dielectric constant spanned by the 1-heptanol data is slightly more encompassed by the 25°C reference curve. If two reference temperatures yield comparable prefactor ratios, and both reference curves of the respective T_r values encompass the conductivity data of the selected family member then the reference temperature that yields the most linear CAE plot is selected.

To summarize, three criteria must be met to maximize the accuracy of the CAF:

- The reference conductivity curve must encompass the majority of the dielectric constant range of the temperature-dependent conductivity of the selected family member. (**Fig. 2.7** on page 25)

- The ratio of the prefactors using the calculated E_a value from the chosen T_r must

29

be close to unity. (**eq. 2.12** on page 27)

- The resulting CAE plot must be linear ($R^2 \geqslant 0.99$).

2.2.5 Calculating the exponential prefactor, σ_0
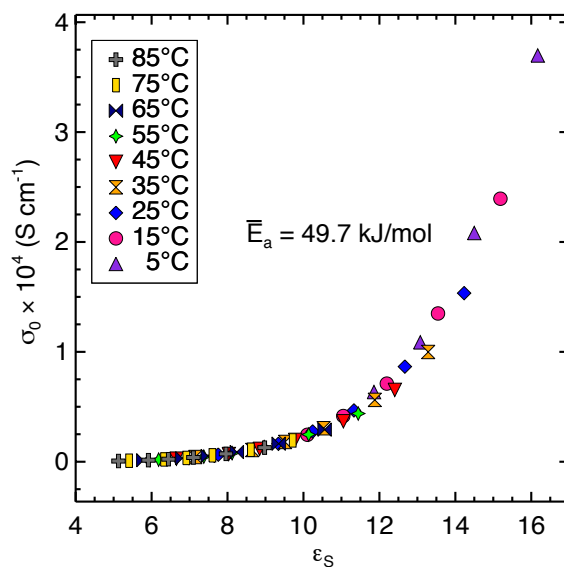
Figure 2.8: Temperature-dependent exponential prefactor versus static dielectric constant for 0.035 molal TbaTf-alcohols. 1-Alcohol members are given in **Fig. 2.7**.

Once an average E_a value is determined, the exponential prefactor, σ_0, can be calculated for each data point using **eq. 2.8**. **Fig. 2.8** shows the exponential prefactor, $\sigma_o(\varepsilon_s(T))$, plotted versus the dielectric constant for 0.035 TbaTf 1-alcohol solutions. All of the data lie on a single master curve, which supports the assumption that the temperature dependence of the exponential prefactor is governed entirely by the temperature dependence of the dielectric constant.

2.2.6 Summary of CAF scaling procedure

The compensated Arrhenius formalism scaling procedure is summarized below:

- Select a solvent family with a similar functional group that can be altered by the addition of a methylene group such that the dielectric constant incrementally changes.

- Create a conductivity reference curve by plotting isothermal conductivity versus dielectric constant of the solvent family members and fit the data to the functional form that allows accurate interpolation between adjacent data points.

- Select a single family member to scale the temperature-dependent conductivity data and determine the most appropriate reference temperature for that member based on the three criteria described in § 2.2.4. The validation of the choice of reference temperature will require completion of the next three steps and can be considered an iterative process.

- Calculate the value of the reference conductivity at each dielectric constant value of each temperature measurement of the selected family member.

- Divide the temperature-dependent conductivity by the appropriate value of the reference conductivity and plot the natural logarithm of this scaled conductivity versus inverse temperature.

- Calculate the E_a from both the slope and the intercept according to **eq. 2.10** and repeat for each member of the solvent family.

- Calculate the exponential prefactor using the average E_a from each family member and plot versus the dielectric constant for the entire temperature range of each family member; the formation of a master curve will correspond to a successful application of the CAF.

- Enjoy the beauty of the master curve.

2.3 Applying the CAF to diffusion coefficients

The same assumptions and scaling procedure of the CAF can be applied to temperature-dependent diffusion coefficients for a family of solvents with a similar functional group that differ by a methylene group.[16] For this, **eq. 2.8** on page 18 becomes

$$D(T, \varepsilon_s) = D_0(\varepsilon_s(T)) \exp\left[\frac{-E_a}{RT}\right] \tag{2.13}$$

where D is the temperature-dependent diffusion coefficient, D_0 is the exponential prefactor for diffusion that contains a temperature dependence due to the temperature dependence of the dielectric constant, and E_a is the energy of activation. Reference diffusion coefficients, D_r, are determined from a plot of the isothermal diffusion coefficients versus the static dielectric constant. The scaling in **eq. 2.14** for diffusion follows **eq. 2.9** for conductivity.

$$\frac{D(T, \varepsilon_s) = D_0(\varepsilon_s(T)) \, e^{-E_a/RT}}{D_r(T_r, \varepsilon_s) = D_0(\varepsilon_s(T_r)) \, e^{-E_a/RT_r}} \tag{2.14}$$

The natural log of the scaled diffusion coefficients are plotted versus reciprocal

temperature and the resulting equation is the compensated Arrhenius equation for diffusion (given by **eq. 2.15**, and the resulting plot, the compensated Arrhenius plot.

$$\ln\left(\frac{D(T, \varepsilon_s)}{D_r(T_r, \varepsilon_s)}\right) = \frac{-E_a}{R}\frac{1}{T} + \frac{E_a}{RT_r} \tag{2.15}$$

Once the E_a is determined from both the slope and the intercept, the exponential prefactor can be determined. A plot of D_0 versus the dielectric constant will result in a master curve just as a plot of σ_0 versus ε_s results in a master curve for conductivity. Note that the same criteria for selecting the appropriate reference temperatures for conductivity given in sections 2.2.3 and 2.2.4 apply to diffusion coefficients.

Throughout this work, the term "applying the compensated Arrhenius formalism", or CAF, to either ionic conductivity or self-diffusion coefficients will refer to utilizing the procedure outlined in the § 2.2 and § 2.3 to determine both an E_a and exponential prefactor for the given systems.

Chapter 3

Concentration dependence of the molal conductivity and dielectric constant of TbaTf 1-alcohol electrolytes

Portions of this chapter have appeared in Fleshman, A. M.; Petrowsky, M.; Jernigen, J. D.; Bokalawela, R. S. P.; Johnson, M. B.; Frech, R. *Electrochimica Acta* **2011**, *57*, 147–152.

3.1   Introduction

The molal conductivity, Λ, of liquid electrolytes with low static dielectric constants ($\varepsilon_s \lesssim 10$) decreases to a minimum from dilute to low concentrations (region I) and increases to a maximum at high concentrations (region II) when plotted against the square root of the concentration, as illustrated in **Fig. 2.1** on page 12. This behavior in Λ with concentration is observed for TbaTf 1-alcohol solutions. The concentration-dependent dielectric constant for these TbaTf 1-alcohol solutions shows similar behavior to that of the molal conductivity with a maximum occurring at higher concentrations. This behavior is investigated by applying the compensated Arrhenius formalism (CAF) to the temperature dependent conductivities over the concentration range 0.00042 m – 0.6 m. Within this concentration range, the simple arrhenius plots for the lower concentrations show non-Arrhenius like behavior,[a] whereas the moderately concentrated to highly concentrated solutions show Arrhenius behavior.[b]

---

[a] A plot of $\ln(\sigma)$ versus T^{-1} is non-linear, as described in § 2.2.1
[b] A plot of $\ln(\sigma)$ versus T^{-1} is linear.

The results presented in this chapter will validate the following claims:

- The CAF results provide an explanation for the non-Arrhenius behavior observed in low concentration 1-alcohol solutions and the Arrhenius-like behavior observed in high concentration 1-alcohol solutions in terms of the inherent temperature dependence of ε_s contained within the exponential prefactor, σ_0.

- The CAF must be applied to the temperature-dependent conductivity regardless of the linearity of the simple Arrhenius plot for 1-alcohol electrolytes in order to determine an "appropriate" energy of activation.

- The CAF can be used to explain the differences between regions I & II, and the cause for the increase in Λ in region II is due to the effect of both the concentration dependence of the dielectric constant *and* the concentration dependence of the energy of activation that combine to form the concentration dependence of the ionic mobilities.

3.1.1 The 1-alcohol solvent family

The 1-alcohol solvent family has been extensively studied using the CAF.[15–17] It is classified as a strongly associating solvent family because of its extended hydrogen bonding network that will be described in greater detail in Chapter 4. An important characteristic for the 1-alcohol solvent family is that the range of dielectric constants of the solvents are low enough such that the molal conductivity demonstrates region II behavior, *i.e.*, Λ decreases to a minimum and then increases with increasing concentration. The 1-alcohol solvent family studied here consists of 1-hexanol, 1-heptanol, 1-octanol,

1-nonanol, and 1-decanol, and the salt is tetrabutylammonium trifluoromethanesul-fonate (TbaTf). The previous interpretation of the increase in Λ with concentration in region II (as discussed in detail in § 2.1.1) is that the conductivity increases because of an increase in the number of charge carriers through an increased population of charged aggregate species,[28,29] or the redissociation of contact-ion pairs back into "free" ions.[24,26,27] Using TbaTf as the salt negates these arguments because the ions exist only as spectroscopically "free" ions, and are therefore, non-associating, even for the lowest dielectric constant solution studied here. To illustrate this, **Fig. 3.1** shows vibrational
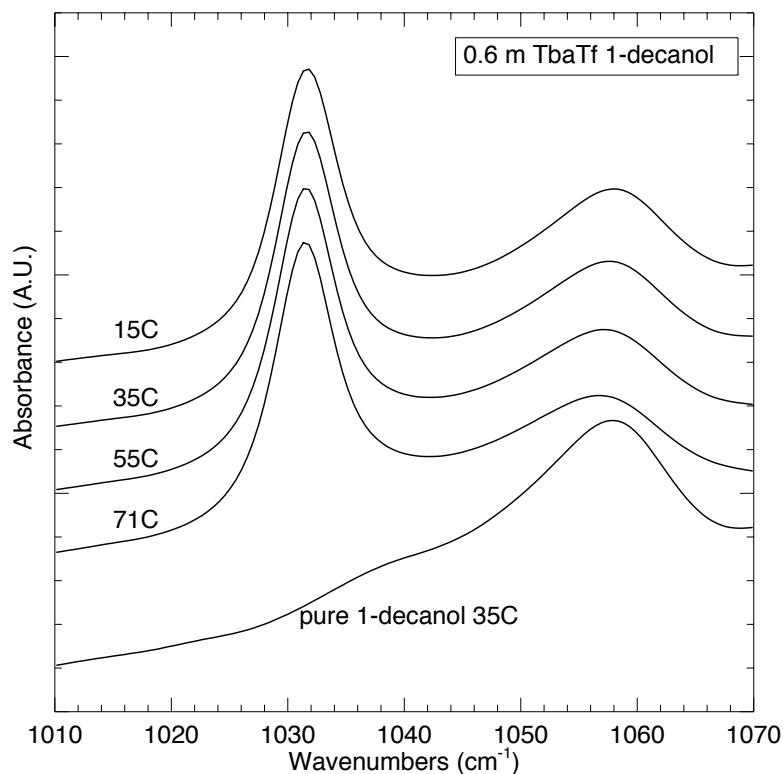
Figure 3.1: IR spectra of 0.6 m TbaTf 1-decanol at 15, 35, 55, and 71°C and pure 1-decanol at 35°C.

infrared spectra for 0.6 m TbaTf 1-decanol.[a] It is widely observed that ionic associa-tion will increase as the dielectric constant decreases.[27,53] 1-decanol is the longest alkyl chain member studied here and has the lowest dielectric constant. A single peak is seen at 1032 cm^{-1} in the $\nu_s(SO_3)$ symmetric stretching region of the Tf$^-$ anion, which has been assigned to the"free" ion.[42] This demonstrates that there is no spectroscopically detectable indication of ionic association of the Tba$^+$ cation in 1-decanol at the highest concentration; it can be assumed that there is no association in the shorter chain alcohol family members, which all have higher dielectric constants. With no spectroscopically detectable ion pairs present, the arguments for the behavior of both Λ and ε_s with concentration described in § 2.1.1 and § 2.1.2 are invalid.

3.2 Concentration dependence of the dielectric constant of TbaTf 1-alcohol solutions

To better understand the concentration dependence of the molal conductivity, it is best to first consider the concentration dependence of the dielectric constant.[b] **Fig. 3.2** shows the dielectric constant versus square root of the concentration for TbaTf solutions of (top) 1-hexanol and (bottom) 1-decanol for 15, 45, and 85°C. The dielectric constant increases from the value of the pure solvent to a maximum and then slightly decreases. For 1-hexanol, the location of the maximum depends on temperature, but it remains at approximately 0.2 m (0.45 m$^{1/2}$) for 1-decanol. Extending the alkyl chain only decreases

---

[a]The instrument and method used for acquiring the vibrational spectra are discussed in Appendix A.4.

[b]The instrument used for acquiring the dielectric constants, as well as the method of calculation are explained in detail in Appendix A.2.

the magnitude of ε_s, as observed by comparing ε_s for 1-hexanol and 1-decanol, but the

general qualitative behavior with concentration is the same.
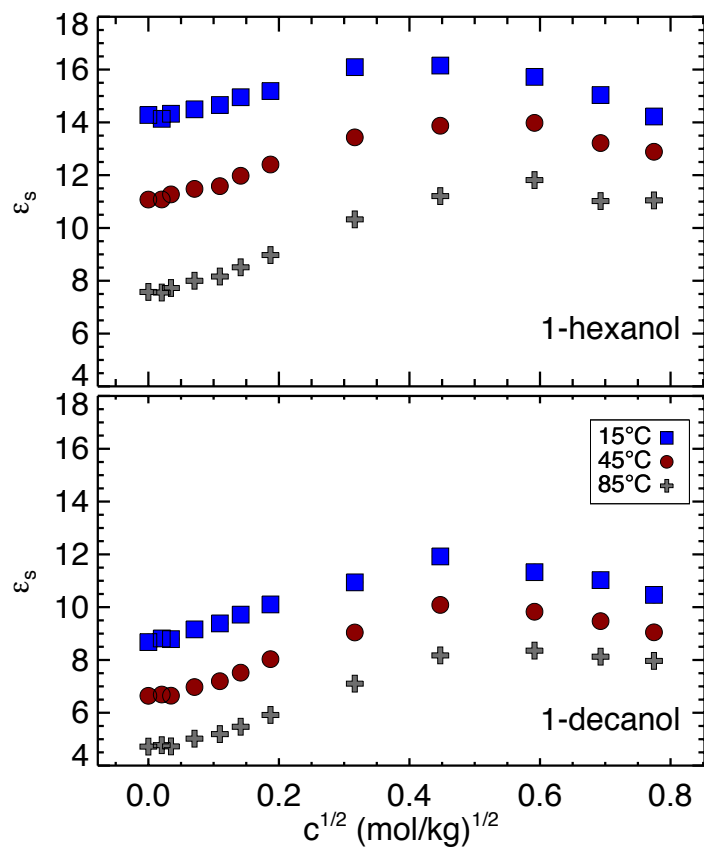
Figure 3.2: Dielectric constant versus square root of concentration for TbaTf 1-hexanol (top) and TbaTf 1-decanol (bottom) for 15°C (blue squares), 45°C (red circles), and 85 °C (gray crosses).

3.3 Concentration dependence of the molal conductivity of TbaTf 1-alcohol solutions

Fig. 3.3 shows the molal conductivity[a] versus square root of the concentration for 1-hexanol (top) and 1-decanol (bottom).[b] The 1-hexanol data at 15 and 45°C do not show region II behavior with increasing concentration, but the 85°C data show a distinct increase in Λ at concentrations greater than about 0.02 m. Λ for 1-decanol at all temperatures demonstrates region I (a decrease with concentration) to 0.07 $m^{1/2}$ and then region II (an increase with concentration). For both solvents, the increase in region II becomes more apparent at higher temperatures. The magnitude of the molal conductivity decreases as the chain length increases, similar to the behavior of the dielectric constant. This same behavior has been observed for solutions of LiTf 1-alcohols at 25°C.[44] Increasing the temperature and extending the chain length of the alcohol enhances the distinct behavior characterizing regions I and II because the dielectric constant, in part, governs the behavior of Λ. It is known that the distinct regions are observed only for low dielectric constant systems, *i.e.*, $\varepsilon_s \lesssim 10$. Increasing the temperature will decrease the dielectric constant, as will using an alcohol with a longer alkyl chain as the solvent. The magnitude of the dielectric constant for 1-decanol, for the majority of the temperatures and concentrations measured, is lower than 10. On the other hand, the dielectric constant for 1-hexanol is below 10 only for the highest temperatures, $75 - 85°C$, so it is to be expected that region II is more pronounced for

---

[a]The instrument used for acquiring the dielectric constants, as well as the method of calculation are explained in detail in Appendix A.2.

[b]Note that the ordinate is $c^{1/2}$ and not c by the convention of Kohlraush.[8] The unique behavior of the minimum is best observed when the data are spread apart in terms of $c^{1/2}$. We make no claim that plotting the data versus $c^{1/2}$ yields any quantitative relationship.
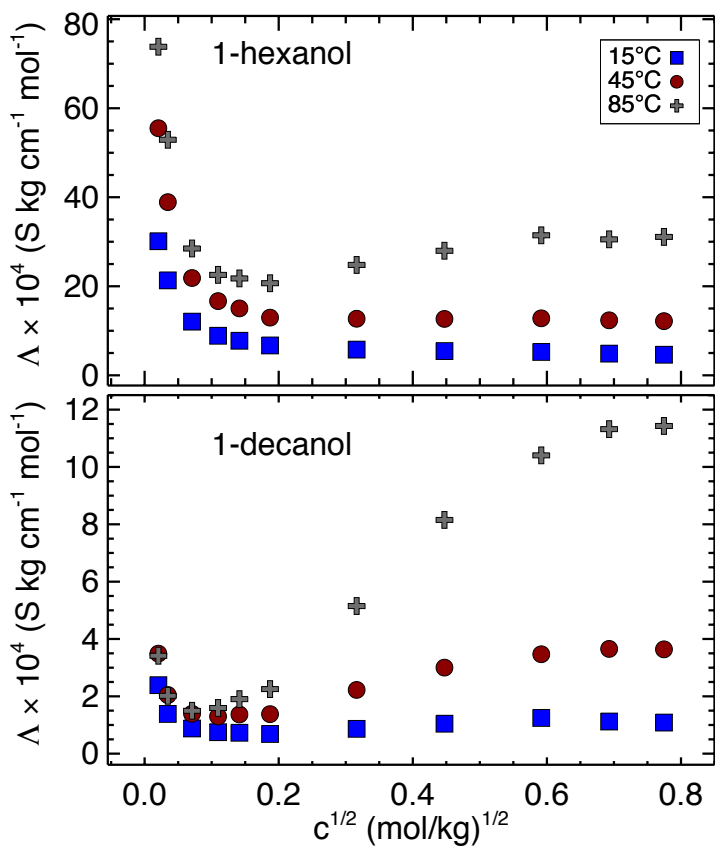
Figure 3.3: Molal conductivity versus square root of concentration for TbaTf 1-hexanol (top) and TbaTf 1-decanol (bottom) for 15°C (blue squares), 45°C (red circles), and 85 °C (gray crosses).

1-decanol than for 1-hexanol. To demonstrate the difference in scale of the increase in region II for 1-hexanol and 1-decanol, **Fig. 3.4** shows Λ plotted versus concentration for 1-hexanol (open diamonds, left axis) and 1-decanol (filled circles, right axis) at 25°C. An increase in region II is not observed for the 1-hexanol data because the range of the dielectric constant over the concentrations is approximately $13 - 15$, whereas the range of dielectric constants for 1-decanol is approximately $8 - 10$. The percent increase in region II is much greater for the 1-decanol, but the magnitude of Λ is still much

smaller than Λ for 1-hexanol. The highest value of Λ for 1-decanol is still lower that the minimum value of Λ for 1-hexanol. This suggests that the magnitude of Λ is directly affected by the value of the dielectric constant, which in turn, affects the concentration dependent behavior.
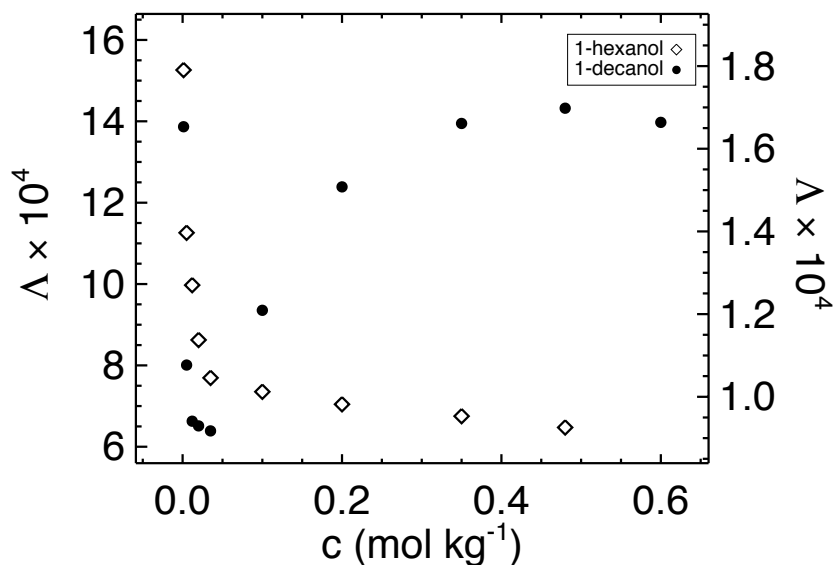
Figure 3.4: Molal conductivity versus concentration for 1-hexanol (open diamonds, left axis) and 1-decanol (filled circles, right axis) at 25°. Units of Λ are (S kg cm^{-1} mol^{-1}).

Comparing **Fig. 3.3** and **Fig. 3.2** one sees that the dielectric constant covers a smaller range with temperature at the higher salt concentrations, which correspond to the concentration range that Λ increases for all members of the 1-alcohol family. The variation in the temperature dependence of ε_s with salt concentration plays an integral role in explaining the increase of Λ in region II, as described in the next section by applying the CAF to the temperature dependent conductivity data and calculating E_a and σ_0 at each concentration.

3.4 Applying the compensated Arrhenius formalism to the conductivity of TbaTf 1-alcohol solutions

3.4.1 CAF: E_a values of $\sigma(T)$

The CAF is successfully applied to the temperature dependent conductivity of TbaTf 1-alcohol solutions over the concentration range 0.00042 – 0.60 m. The scaling procedure for the CAF has been described in detail in § 2.2. E_a values were calculated for each member of the 1-alcohol solvent family at each concentration of TbaTf following **eq. 2.10** on page 21. For comparison, the simple Arrhenius equation (**eq. 2.11** on page 22) was also applied to all TbaTf 1-alcohol solutions.

Fig. 3.5 and **Fig. 3.6** show simple Arrhenius plots (left axis, filled circles, SAE) and compensated Arrhenius plots (right axis, open diamonds, CAE) for four of the eleven concentrations of TbaTf of the two end members of the 1-alcohol family studied here: 1-hexanol and 1-decanol over the temperature range 5 – 85°C (15 – 85°C for 1-decanol). For both solvents the SAE at the lowest concentration shows the greatest deviation from Arrhenius-like behavior with the 1-decanol showing greater curvature than the 1-hexanol. Upon compensation, the non-linearity is corrected and the resulting compensated Arrhenius plots (**Fig. 3.5** and **Fig. 3.6**, right axis) yield Arrhenius-like behavior. As the concentration increases, the non-scaled conductivity becomes more linear, and therefore more Arrhenius-like with increasing correlation coefficients given in the figures. By convention, a linear fit is considered to have a correlation coefficient of 0.990 or greater. The 0.035 m SAE plots show only slight curvature compared to the CAE plots, but they are still considered to follow non-Arrhenius behavior (R^2=0.983
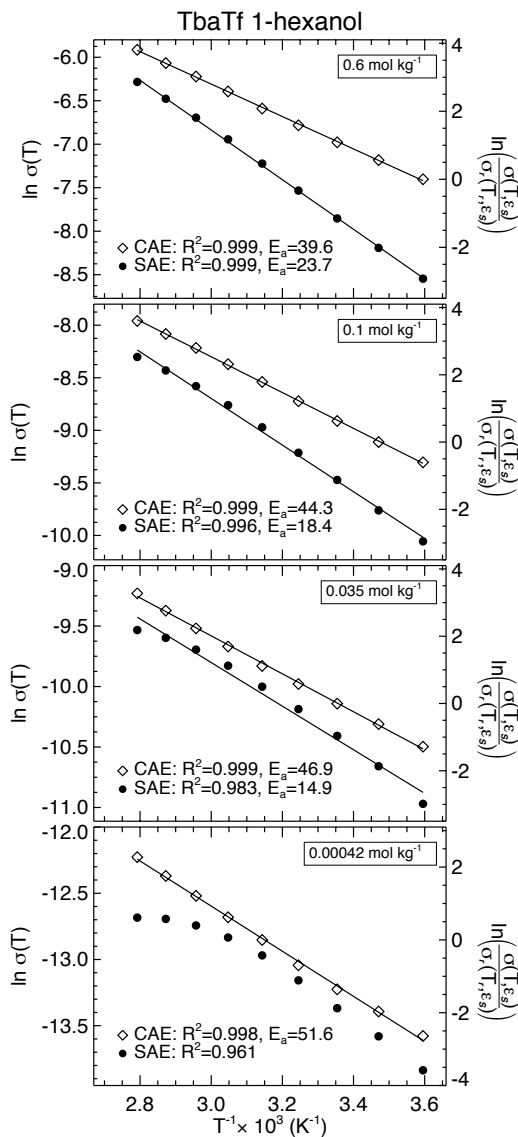
Figure 3.5: Simple Arrhenius plots (left axis, filled circles) and compensated Arrhenius plots (right axis, open diamonds) for X m TbaTf 1-hexanol (X = 0.00042, 0.035, 0.1, and 0.6 as labelled in figure).
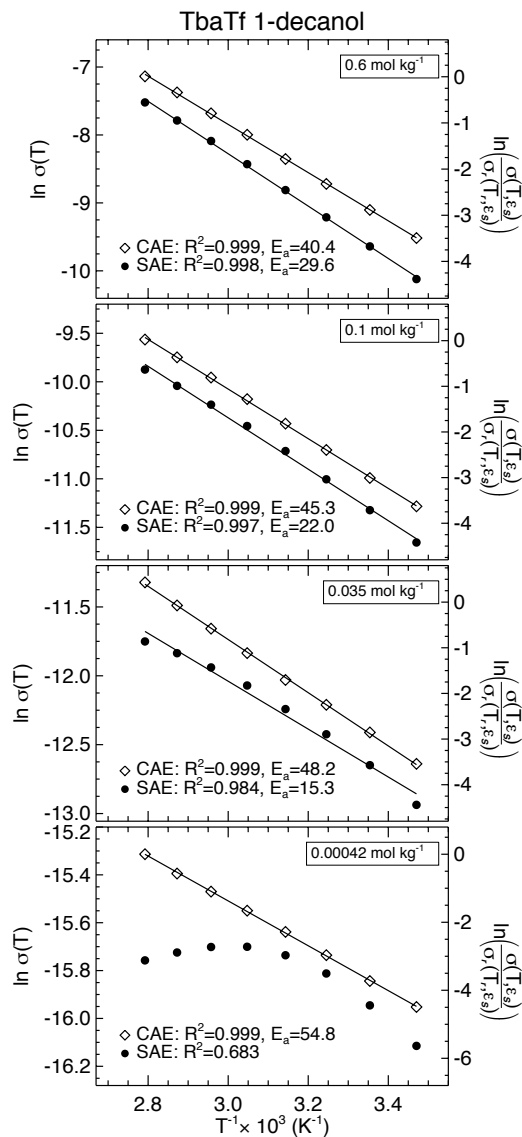
Figure 3.6: Simple Arrhenius plots (left axis, filled circles) and compensated Arrhenius plots (right axis, open diamonds) for X m TbaTf 1- decanol (X = 0.00042, 0.035, 0.1, and 0.6 as labelled in figure).

and 0.984 for 1-hexanol and 1-decanol, respectively). The transition from non-Arrhenius to Arrhenius behavior occurs between 0.035 and 0.1 m for both 1-hexanol and 1-decanol.

Given that ε_s is always lower for 1-decanol than 1-hexanol, we speculate that the extent

of curvature observed in the SAE plots is independent of the magnitude of ε_s, but is related to the temperature dependence of ε_s.

c (m)	$c^{1/2}$ ($\text{m}^{1/2}$)	CAE E_a (kJ mol^{-1})	SAE E_a (kJ mol^{-1})
0.00042	0.02	52.9 ± 0.3	-
0.0012	0.03	51.8 ± 0.5	-
0.005	0.07	49.9 ± 0.3	-
0.012	0.11	48.2 ± 0.5	-
0.02	0.14	47.7 ± 0.4	-
0.035	0.19	47.9 ± 0.2	-
0.1	0.32	44.5 ± 0.2	20.3 ± 0.2
0.2	0.45	42.7 ± 0.3	22.9 ± 0.2
0.35	0.59	41.5 ± 0.2	25.4 ± 0.2
0.48	0.69	39.9 ± 0.2	25.2 ± 0.2
0.6	0.77	39.1 ± 0.2	26.7 ± 0.2

Table 3.1: Average energies of activation for TbaTf 1-alcohols calculated based on the CAE (**eq. 2.10** on page 21) and the SAE (**eq. 2.11** on page 22). E_a values could not be determined from non-linear SAE plots and are intentionally left blank.

The 0.6 m conductivity data show a similar trend to the 0.1 m conductivity data. The simple Arrhenius plot is linear as is the compensated Arrhenius plot. This is seen for the higher concentrations, 0.1 m and above, which all show Arrhenius-like behavior. **Table 3.1** gives average E_a values that are determined from the CAE plots, as well as those from the SAE plots that demonstrate linearity. The E_a values calculated from the CAF are averaged from the slope and the intercept, and then averaged again for all 1-alcohol members with the corresponding concentration. The CAE E_a values are all 10 kJ mol^{-1} or more higher than the SAE E_a values. The E_a values from the SAE were calculated from 0.1 to 0.6 m, which corresponds to the range of 0.316 to 0.775 for $c^{1/2}$ in **Fig. 3.3**. In this concentration range, Λ is increasing, particularly for 1-decanol and 1-hexanol at 85°C. An increasing E_a necessarily results in a decreasing conductivity from the SAE. Hence the SAE provides an especially poor description of the temperature-

dependent conductivity in these (and other) systems. The decrease in E_a observed for the CAE values are consistent with the increase in Λ observed in **Fig. 3.3** on page 40. It is therefore, still necessary to perform the scaling procedure if there is a temperature dependence in ε_s, regardless of the apparent linearity of the simple Arrhenius plot. To further explain this point it is necessary to calculate the exponential prefactor, which will be done in the § 3.4.2. Otherwise, an accurate E_a can not be calculated.[49] The data presented here rather dramatically demonstrate this point.

3.4.2 CAF: exponential prefactor of $\sigma(T)$

The CAF shows that the temperature dependence of the conductivity is due in part to the temperature dependence of the dielectric constant, which changes upon addition of salt. As the salt concentration increases, the temperature dependence of ε_s decreases. For example, ε_s for the 1-hexanol solution in **Fig. 3.2** varies from approximately $15 - 7.5$ for 0.00042 m (0.02 m$^{1/2}$), and $14.7 - 11$ for 0.6 m (0.77 m$^{1/2}$) over the range $15 - 85°$C. The temperature dependence of the exponential prefactor is a result of the temperature dependence of ε_s, which itself has a concentration dependence. The reduction of the temperature dependence of ε_s with concentration plays a significant role in describing the concentration dependence of the conductivity via the exponential prefactor σ_0.

Fig. 3.7 shows the isothermal conductivity data for 0.6 m (top), 0.1 m (middle), and 0.00042 m (bottom) TbaTf 1-alcohol solutions plotted as a function of dielectric constant, which form five curves that correlate to the temperature dependent conductivity of each solvent family member. The curves are labelled according to the number of carbons in the alkyl chain: (6) 1-hexanol (7) 1-heptanol (8) 1-octanol (9) 1-nonanol
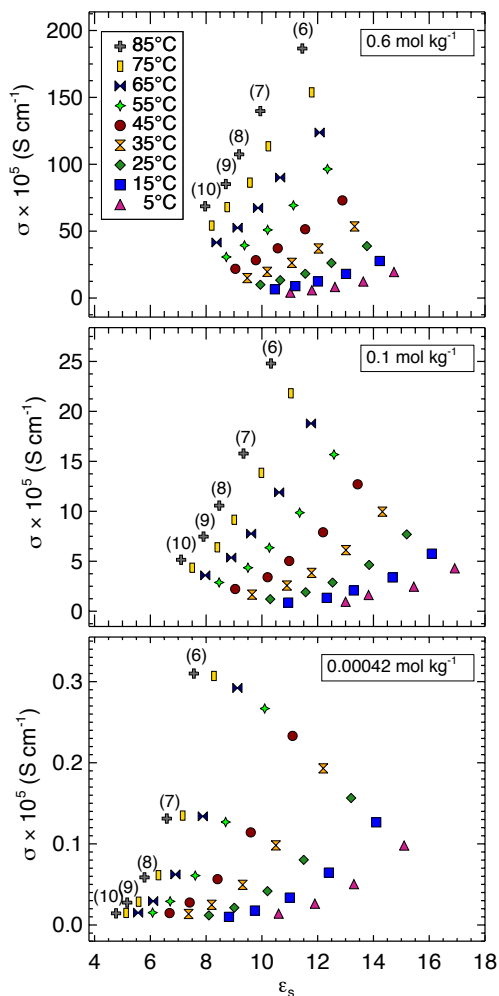
Figure 3.7: Isothermal conductivity versus dielectric constant for (top) 0.6 m (middle) 0.1 m and (bottom) 0.00042 m TbaTf 1-alcohol solutions. The numbers correspond to (6) 1-hexanol, (7) 1-heptanol, (8) 1-octanol, (9) 1-nonanol, (10) 1-decanol.

Figure 3.8: Isothermal exponential prefactors versus dielectric constant for (top) 0.6 m (middle) 0.1 m and (bottom) 0.00042 m TbaTf 1-alcohol solutions. E_a values correspond to average values calculated from the CAE and are given in **Table 3.1**.

and (10) 1-decanol. Each isothermal curve defined by a particular symbol is a reference curve at that reference temperature, T_r, for the given concentration. As an example, in the scaling procedure for 0.6 m TbaTf 1-octanol (the curve labelled 8), T_r was chosen

46

as 45°C (corresponding to the red circles). The addition of salt greatly affects the value of the conductivity by almost three orders of magnitude from the lowest to the highest concentration. The conductivity data change with dielectric constant differently as the concentration increases. The lowest concentration conductivity data (bottom plot) level off at higher temperature, or lower dielectric constant, for each family member. As the concentration increases to 0.1 and 0.6 m, the rate of increase with temperature for the conductivity becomes greater, whereas the reduced temperature dependence of ε_s results in a smaller dielectric constant range. The lowest concentration conductivity data span approximately 11 dielectric constant units, while the highest concentration covers approximately 7 dielectric constant units.

One of the primary assumptions of the CAF is that the temperature dependence of σ_0 is due to the temperature dependence of the dielectric constant. Using the average E_a calculated from the CAF, σ_0 is determined by dividing $\sigma(T)$ by the quantity $\exp[-\overline{E_a}/RT]$, as discussed in § 2.2.5. It has been shown in several studies that the exponential prefactors form a single master curve when plotted versus the dielectric constant, which supports the aforementioned assumption of the CAF.[15–17,49,51,52] **Fig. 3.8** shows the exponential prefactor versus dielectric constant for the same concentrations as **Fig. 3.7** and demonstrates the formation of master curves at each of the concentrations. The master curves all show a similar, exponential-like dependence on the dielectric constant, but the magnitudes vary with concentration. The 0.00042 m data display a similar increase in σ_0 and cover approximately the same ε_s range as the 0.1 m data, however the data are shifted horizontally to higher dielectric constants for the 0.1 m solutions. Following the concentration dependence of ε_s, the 0.6 m ε_s data have

47

a lower concentration range than the 0.1 m data, but the ε_s range is still higher than the 0.00042 m data. As the temperature dependence of the dielectric constant becomes smaller, the temperature dependence of σ_0 also decreases. This can also be seen in **Fig. 3.5** and **Fig. 3.6**. The simple Arrhenius plots for the lowest concentrations have the greatest curvature because the temperature dependence of the dielectric constant is larger, resulting in a larger temperature dependence in σ_0. As the temperature dependence in σ_0 decreases with increasing concentration, the curvature of the simple Arrhenius plots also decreases and the data become more Arrhenius-like. This further supports the assumption previously described: the temperature dependence of σ_0 is due to the temperature dependence of ε_s. A closer look will now be taken at the differences between Arrhenius and non-Arrhenius behavior in the temperature dependence of the conductivity.

3.5 Arrhenius versus non-Arrhenius behavior of $\sigma(\mathrm{T})$

The 0.1 m concentration appears to correspond to the cutoff concentration for observing Arrhenius-like behavior according to the TbaTf 1-hexanol and 1-decanol data in **Fig. 3.5** and **Fig. 3.6** on page 43. Solutions of 0.1 to 0.6 m TbaTf all show Arrhenius-like behavior in the SAE plots. The median concentration of this range, 0.35 m, will now be discussed in detail to distinguish the different characteristics of the CAE and SAE. **Fig. 3.9** compares a SAE plot (top) and CAE plot (bottom) for 0.35 molal TbaTf octanol (open diamonds) and nonanol (filled circles) over the temperature range 5 – 85°C. Note from the values of the correlation coefficients that the conductivity data show Arrhenius-like behavior, which might suggest that the scaling procedure is un-
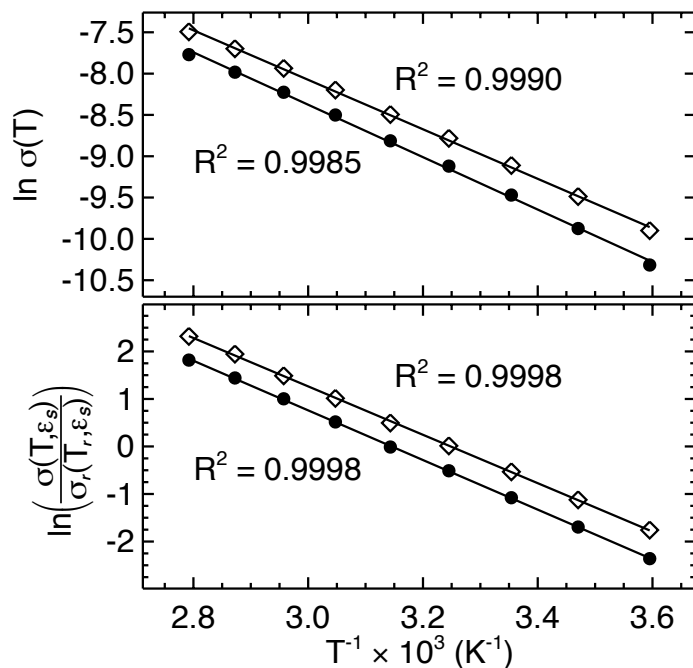
Figure 3.9: (Top) Simple Arrhenius plot of 0.35 molal TbaTf octanol (open diamonds) and nonanol (filled circles). (Bottom) Compensated Arrhenius plot of 0.35 molal TbaTf octanol with $T_r = 35°C$ (open diamonds) and nonanol with $T_r = 45°C$ (filled circles).

necessary. The CAF can still be applied, but negligibly changes the linearity of the data. The E_a values from both the simple Arrhenius plot and compensated Arrhenius plot are given in **Table 3.2**. Regardless of the Arrhenius-like behavior of the simple Arrhenius plot, the scaling procedure will yield strikingly different E_a values. Also note that the SAE E_a values increase with increasing alkyl-chain length, whereas the CAE E_a values are relatively constant. It is unlikely that the addition of a methylene group to a solvent family member would increase the E_a by 2 kJ mol^{-1}, suggesting that the simple Arrhenius model is a poor descriptor of charge transport.

The primary justification for using the CAF, as opposed to the SAE, stems from

| System | Simple Arrhenius | | Compensated Arrhenius | |
| 0.35 molal | E_a | T_r | E_a (slope) | E_a (intercept) |
TbaTf–	(kJ mol^{-1})	(°C)	(kJ mol^{-1})	(kJ mol^{-1})
hexanol	21.7 ± 0.2	15	41.4± 0.4	41.4± 0.4
heptanol	23.4 ± 0.3	25	42.1± 0.3	42.1± 0.3
octanol	24.9 ± 0.3	35	42.3± 0.2	42.4± 0.2
nonanol	26.4 ± 0.4	45	43.4± 0.2	43.5± 0.2
decanol	26.8 ± 0.4	55	43.1± 0.3	43.0± 0.3
dodecanol	28.4 ± 0.3	75	43.8± 0.5	43.7± 0.5

Table 3.2: Energies of activation for 0.35 molal TbaTf 1-alcohols calculated from the SAE (**eq. 2.11**, page 22) and from the CAE (**eq. 2.10**, page 21). CAE reference temperatures are also given with E_a values from both the slope and intercept, as labelled.

comparing the exponential prefactors calculated using the respective E_a values. The exponential prefactor versus dielectric constant for both the SAE (top) and CAE (bottom) is plotted in **Fig. 3.10**. Using the E_a from a simple Arrhenius equation does not yield a master curve, as shown in the top plot. There is a narrow range of E_a values, from 38-46 kJ mol^{-1}, that will produce a single master curve. The median of this range is 42 kJ mol^{-1}, which is approximately the average E_a value (42.7 kJ mol^{-1}) found using the CAE. The formation of a master curve (bottom **Fig. 3.10**) further supports the assumption that the temperature dependence of the exponential prefactor is given by the temperature-dependent dielectric constant and must be compensated for to determine the "proper" E_a. This also supports the claim that conductivity in these alcohol electrolytes is a thermally activated process with an E_a representing an average energy barrier for that transport process. A similar comparison between Arrhenius and compensated Arrhenius E_a values is made for alcohol self-diffusion coefficients.[16]
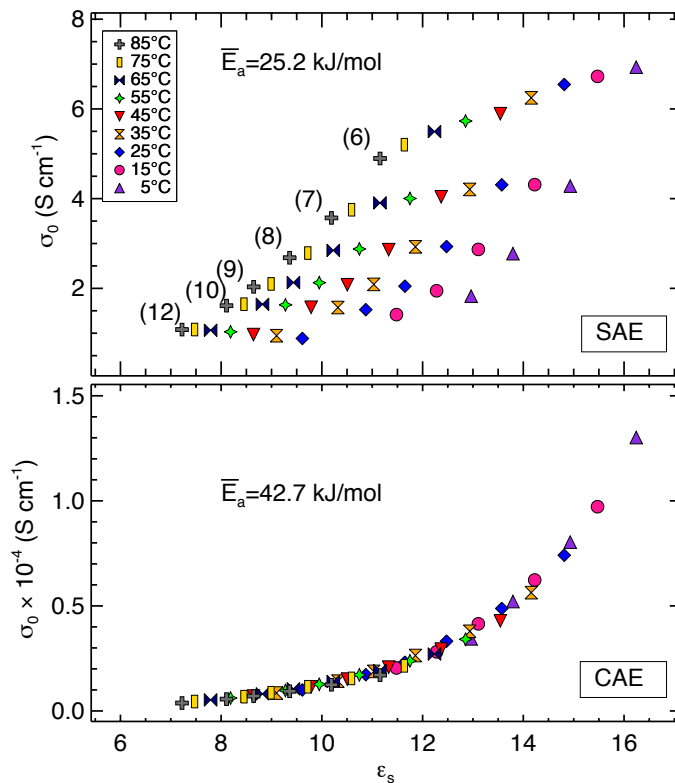
Figure 3.10: (Top) Temperature-dependent exponential prefactor versus dielectric constant for 0.35 molal TbaTf 1-alcohols calculated using simple Arrhenius E_a values specific to each family member according to **Table 3.2**. Numbers correspond to (6) 1-hexanol (7) 1-heptanol (8) 1-octanol (9) 1-nonanol (10) 1-decanol (12) 1-dodecanol. (Bottom) Temperature dependent exponential prefactor versus dielectric constant for 0.35 molal TbaTf alcohols calculated using average E_a (42.7 kJ mol^{-1}) from compensated Arrhenius plot.

3.6 Concentration dependence of the molal exponential prefactor and Boltzmann factor

The primary goal of this chapter is to identify the cause for the increase in Λ with concentration in region II, as shown in **Fig. 3.3** on page 40. **Table 3.1** shows that as the salt concentration increases in region II, the E_a values decrease, which partially

contributes to the increase in molal conductivity with concentration. The behavior of Λ is also affected by the exponential prefactor. **Fig. 3.8** shows a concentration dependence in σ_0, but in order to relate this to the concentration dependence of Λ, one must consider the molal exponential prefactor, Λ_0, which is defined as σ_0/c, where c is the formal concentration introduced in **eq. 2.5** on page 11. The behavior of Λ in region I and II results from both the concentration dependence of E_a and the concentration dependence of Λ_0.

Fig. 3.11 illustrates the concentration dependence of the molal conductivity, Λ (top), molal exponential prefactor, Λ_0 (middle), and Boltzmann factor (bottom) for TbaTf 1-octanol at 5, 45, and 85°C. The molal conductivity plot for 1-octanol looks similar to the 1-hexanol and 1-decanol data of **Fig. 3.3** (page 40) with a minimum separating regions I and II that becomes more distinct as the temperature increases. The molal exponential prefactor decreases with increasing concentration for all three temperatures, however, at the higher temperatures, Λ_0 becomes approximately independent of concentration for the $c^{1/2}$ range of $0.1 - 0.2$ m$^{1/2}$. As the concentration increases beyond this range, Λ_0 decreases at a lower rate than for the dilute concentrations. The isothermal data of Λ_0 at the higher concentrations appear to converge as a result of the decreased temperature dependence of ε_s in the concentrated solutions.

For the lower concentrations up to 0.1 m (0.32 m$^{1/2}$), the temperature dependence of ε_s is relatively constant at each concentration. At approximately 0.1 m, the temperature dependence of ε_s begins to decrease. For example, in **Fig. 3.2** on page 38 the difference between ε_s for 1-hexanol at 15 and 85°C at 0.6 m ($c^{1/2} = 0.77$) is 3.7 while at 0.035 m ($c^{1/2} = 0.19$) $\Delta\varepsilon_s = 7.2$. The range, as well as the magnitude, of the dielectric constant
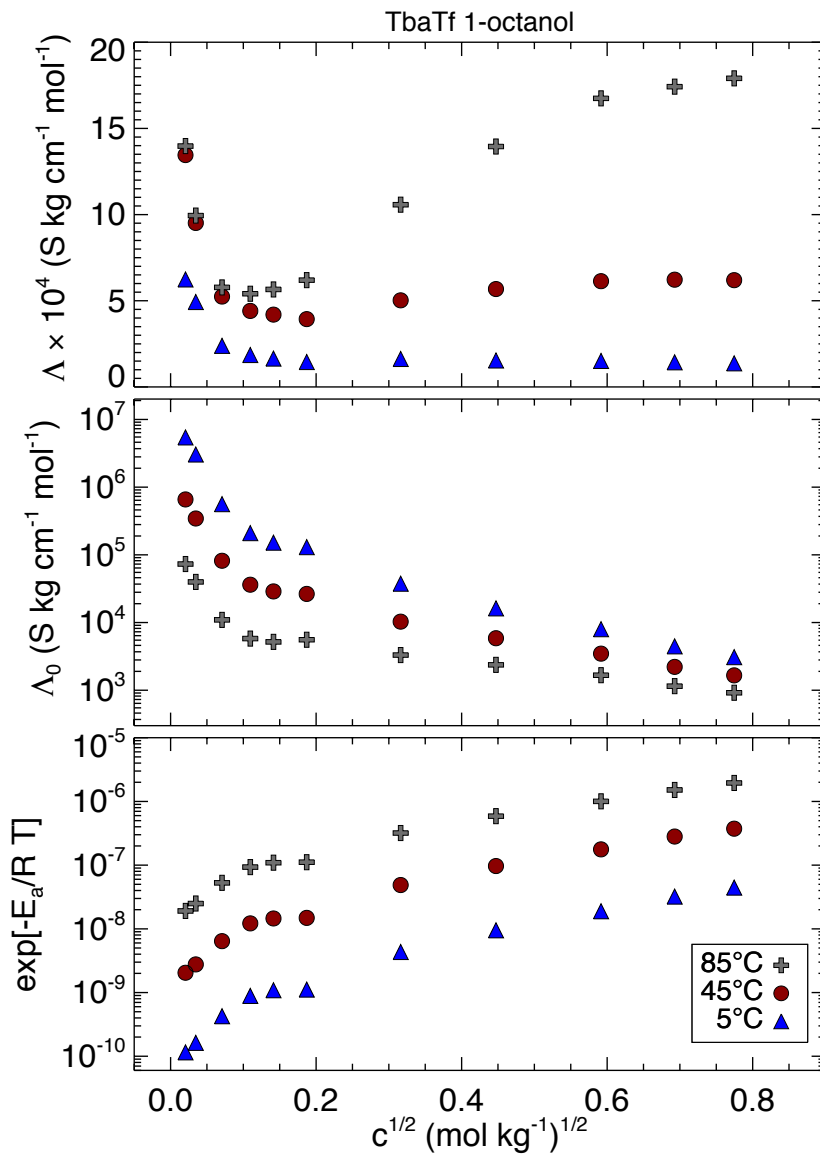
Figure 3.11: Concentration dependence (plotted as $c^{1/2}$) of (top) molal conductivity, (middle) molal exponential prefactor, and (bottom) Boltzmann factor at 5, 45, and 85°C for TbaTf 1-octanol solutions.

is affected by adding salt, which is reflected in the concentration dependence of the molal exponential prefactor.

Comparing the molal conductivity and the molal exponential prefactor, one sees the

$c^{1/2}$ range of Λ_0 that is approximately constant corresponds to the same concentration range of Λ where the minimum is observed. It is well known that the location of the minimum in Λ shifts to lower concentrations with decreasing ε_s.[29] As the temperature increases, ε_s decreases, causing the expected shift in the minimum of Λ due to the lower ε_s. For the 5°C 1-octanol data, the minimum corresponds to 0.18 m$^{1/2}$, while the 85°C has a minimum at 0.11 m$^{1/2}$. The minimums of Λ for 1-hexanol and 1-decanol shown in **Fig. 3.3** (page 40) also shift to lower concentrations with increasing temperature. This range of concentrations that represent the possible minima of Λ are consistent with the concentration range that Λ_0 appears to be independent of concentration.

The Boltzmann factor (bottom of **Fig. 3.11**) increases with increasing concentration as a direct result of the decrease of the E_a values. The same range of $c^{1/2}$ in which Λ_0 is independent of concentration also corresponds to a range that the Boltzmann factor becomes approximately independent of concentration. Unlike Λ_0, the Boltzmann factor does not have an intrinsic temperature dependence due to ε_s. The temperature dependence in the Boltzmann factor is only due to the temperature factor in the denominator of the exponential. Increasing the temperature results in a larger Boltzmann factor that increases the magnitude of Λ. For the higher concentrations, when the temperature dependence of Λ_0 is decreasing due to the decreasing temperature dependence of ε_s, the Boltzmann factor becomes the dominant factor and enhances the region II behavior. As a result, there is an increased distinction between region I and II at higher temperatures. It appears that the behavior of Λ with $c^{1/2}$ is controlled by two competing factors: (1) the decrease in Λ_0 and (2) the increase in $\exp[-E_a/RT]$. In TbaTf 1-alcohol solutions, Λ_0 is the dominant factor in region I, and in region II,

the Boltzmann factor (or the E_a) dominates. The minimum in Λ with concentration would then represent the transition from the dominance of one factor to the next. It is, however, the combined effect of both factors that yield the distinct regions observed in Λ with concentration.

The transition from non-Arrhenius to Arrhenius behavior also corresponds to a difference in the temperature dependence of the dielectric constant, which is contained in the exponential prefactor and therefore the molal exponential prefactor. The combined isothermal data of Λ_0 of the three temperatures in **Fig. 3.11** demonstrate the reduction of the temperature dependence of ε_s by merging at higher concentrations. For concentrations with a reduced temperature dependence in ε_s, the values of Λ_0 will become closer in magnitude. The values of Λ_0 for concentrated solutions will also be less than Λ_0 for concentrations with a strong temperature dependence in ε_s. As a result, a stronger temperature dependence in ε_s will yield more non-Arrhenius like behavior, as shown with the 0.00042 m solutions of 1-hexanol and 1-decanol in **Fig. 3.5** and **Fig. 3.6**, respectively. Adding a significant amount of TbaTf (*i.e.*, 0.1 m) to the 1-alcohols causes a reduction in the temperature dependence of the dielectric constant, which is the source of the reduced temperature dependence of the exponential prefactor. As the dielectric constant changes less with temperature, the curvature in a plot of $\ln(\sigma)$ versus $1/T$ will decrease, resulting in Arrhenius-like behavior.

3.7 Comparison to previous work: E_a of TbaTf 1-alcohol solutions

Petrowsky and Frech [17] showed that the average E_a calculated from the CAF for TbaTf 1-alcohol solutions increases with concentration from approximately 32.6 to 39.5 kJ mol^{-1} over the concentration range 4.30×10^{-5} to 0.0055 M^a for short to moderate chain length alcohols. [17] This concentration range corresponds to the decrease in Λ (region I). For the concentrations corresponding to the transition from region I to II the average E_a values level off to approximately 39 kJ mol^{-1} at 0.0055 M, which does not match the initial values around 52 kJ mol^{-1} calculated here for the 0.00042 – 0.005 m concentrations, which are also all located in region I. This difference is due to the selection of the family members used for the scaling procedure. We have shown that if much shorter alkyl chain family members are chosen (*e.g.*, methyl–butyl), the average E_a will be less. [51,54] The 1-alcohol members used in the previous study included ethanol, 1-propanol, 1-butanol, and 1-hexanol, which resulted in E_a values approximately 10 kJ mol^{-1} less than the long chain alcohols studied here. The E_a for 0.005 m was recalculated using the same 1-alcohol members from the previous study, and was found to be 40 ± 1 kJ mol^{-1}, which is consistent with the values reported. [17] It can be concluded that to see the increase in E_a with concentration for the long chain alcohols, the concentrations must be much more dilute and farther into region I than the concentrations presented here. However, it is not possible to measure the conductivity at such dilute concentrations with the longer alkyl chain members used in this

---

^{a}Here, M represents moles of solute per liter of solution. For dilute solutions, the density of the solution is approximately the density of the solvent so the use of molal units was unnecessary.

study because the longer chains have lower conductivity values which are unacceptably close to the detection limits of the instrument used in this work. It can be inferred that if measurements were possible, the same trends previously reported for short chain alcohols would be seen here: a leveling off of the E_a followed by a decrease with decreasing concentration. It can also be inferred that the decrease of Λ in region I is due in part to this increase in E_a previously seen. However, the short chain 1-alcohols have dielectric constants above 10, therefore distinct region I – II behavior is unlikely to be observed. Given that exponential prefactors were only calculated for 25°C, I am unable to discuss the concentration dependence of $\sigma_0(T)$, and its contribution to $\Lambda(c)$, but I do hypothesize that the decrease seen in Λ is due to contributions from both the E_a and Λ_0 as explained in § 3.6.

3.8   Summary and Conclusion

Temperature dependent conductivities and dielectric constants were collected for a family of TbaTf 1-alcohols over a broad concentration range. The CAF was applied to all systems and E_a values were determined from both CAF and simple Arrhenius plots (**Table 3.1**, page 44). Exponential prefactors were calculated for all concentrations and shown to all lie on a single master curve when plotted versus the solution dielectric constant.

It is clear that arguments based on ionic association do not adequately describe the behavior of the molal conductivity with concentration for low dielectric constant electrolytes (shown in **Fig. 2.1** on page 12) because the same behavior is seen using TbaTf as the salt, which exists as spectroscopically "free" ions, as supported by IR

57

spectra in **Fig. 3.1**. The decrease of Λ in region I and the increase in region II can, however, be described by the combined effect of the concentration dependence of both the E_a and the molal exponential prefactor, Λ_0, the latter having a dependence on the dielectric constant. It is therefore necessary to use the CAF to compensate for this dielectric constant dependence to calculate an appropriate E_a.

For the higher concentrations presented here, the temperature dependent conductivity exhibited Arrhenius-like behavior, and yielded simple Arrhenius E_a values that do not explain the observed increase in molal conductivity in region II as given in **Table 3.1**. The dielectric constant for these concentrations varies less with temperature than the lower concentrations, which results in a reduced temperature dependence of the exponential prefactor and therefore less curvature in the simple Arrhenius plot. It was also shown that the scaling procedure must still be performed for liquid electrolyte systems with a dielectric constant that varies even slightly with temperature.[49,51] The master curves shown in **Fig. 3.8** validate the assumption that the temperature dependence of σ_0 is due to the temperature dependence of ε_s for the concentrations spanning region II, even though the higher concentrations show Arrhenius-like behavior. The concentration dependence of the dielectric constant shown in **Fig. 3.2** on page 38 contributes to the concentration dependence in Λ_0 as will now be explained.

The CAF postulates that all of the temperature dependence of σ_0 is due to the temperature dependence of ε_s, or $\sigma_0(\varepsilon_s(T))$. The same is true for Λ_0, but extending this to the concentration dependence is not trivial. Λ_0 and the Boltzmann factor (*i.e.,* the E_a) have the opposite concentration dependence (**Fig. 3.11**), but appear to have a similar concentration-independent region. Further examination of the concentration
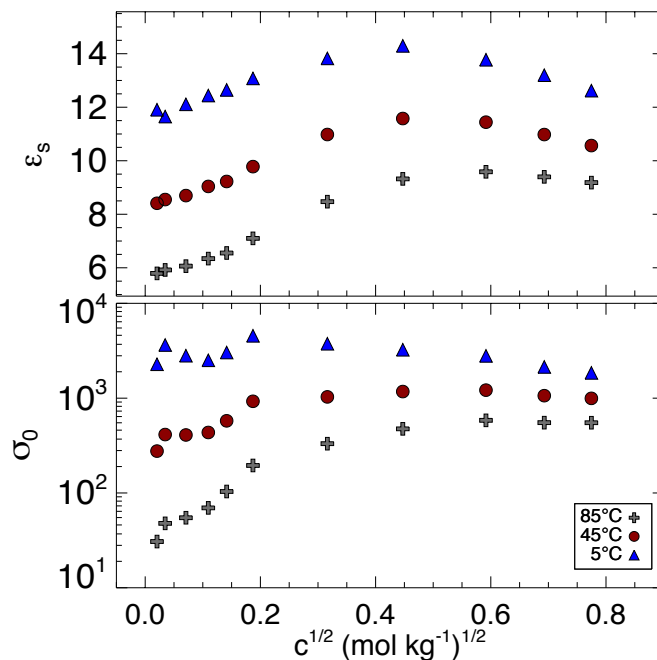
Figure 3.12: Dielectric constant (top) and exponential prefactor (bottom) versus square root of the concentration at 5, 45, and 85°C for TbaTf 1-octanol solutions.

dependence of Λ_0 requires the comparison of σ_0 and ε_s. **Fig. 3.12** shows the dielectric

constant (top) and exponential prefactor (bottom) versus $c^{1/2}$ for TbaTf 1-octanol solu-

tions at the same temperatures as **Fig. 3.11**. The dielectric constant behavior is similar

to that seen for 1-hexanol and 1-decanol in **Fig. 3.2** on page 38. The same concentration

range that corresponds to the concentration-independent region of Λ_0 in **Fig. 3.11** (0.1

– 0.2 m$^{1/2}$) shows a steady increase in dielectric constant with concentration. At these

same concentrations, there is a definite increase in σ_0. It can, therefore be concluded

that the concentration dependence of the prefactor is predominantly, if not entirely, due

to the concentration dependence of the dielectric constant. Adding this component into

the assumption of the CAF along with the observed concentration dependence of the

E_a yields a slightly corrected Arrhenius equation for ionic conductivity that introduces

a concentration dependence in both E_a and σ_0;

$$\sigma(T,c) = \sigma_0(\varepsilon_s(T,c)) \exp\left[\frac{-E_a(c)}{RT}\right]. \tag{3.1}$$

The concentration dependence of σ_0 can be easily linked to the concentration dependence of the dielectric constant (as shown in **Fig. 3.12**), but dividing by the total salt concentration, the concentration dependence of the exponential prefactor, *i.e.*, $\sigma_0(\varepsilon_s(T,c))/c$, becomes more complicated. Extending **eq. 3.1** to the molal conductivity (**eq. 2.5** on page 11), and specifically applying it to the concentration dependence of TbaTf in 1-alcohols yields:

$$\Lambda = \Lambda_0(\varepsilon_s(T,c),c)e^{\frac{-E_a(c)}{RT}} = F\left(\mu_i^+ + \mu_i^-\right). \tag{3.2}$$

The sum of the ionic mobilities are the only terms that can have a concentration and temperature dependence in the right hand side of the above equation. The left hand side has the concentration dependence separated into two contributions; Λ_0 and E_a. **Fig. 3.11** shows that both Λ_0 and the E_a have a concentration dependence which is linked through **eq. 3.2** by the concentration dependence of the ionic mobilites for TbaTf. The addition of TbaTf alters the magnitude of the dielectric constant and its temperature dependence, which in turn, affects the sum of the ionic mobilities, $(\mu^+ + \mu^-)$. It appears that $(\mu^+ + \mu^-)$ decreases in region I, becomes concentration independent through the minimum, and increases with concentration in region II. We suggest that $(\mu^+ + \mu^-)$ has both a temperature and concentration dependence that is governed by changes in the intermolecular interactions, which can be measured by the

dielectric constant and compensated for *via* the CAF. Changes in the solvent-solvent interactions, as well as ion-solvent interactions, are further complicated by hydrogen bonding in the systems studied here; both having a major effect on the concentration and temperature dependence of the dielectric constant. The physical interpretation of how the ions affect the dielectric constant of the solution on a local scale is still not well understood. Answering this question is more difficult with the data presented because of the presence of the hydrogen bonded network.

Chapter 4

Comparison of temperature-dependent diffusion coefficients in 1- and 3-alcohol solvents

4.1 Introduction

In Chapter 3, the CAF was applied to temperature-dependent conductivities of TbaTf 1-alcohol electrolytes over a broad concentration range. The 1-alcohol solvent family is considered an associated liquid with an extended hydrogen bonding network. It is likely that the extended structure plays a significant role in the behavior of the conductivity with concentration. The CAF has shown that the mechanism governing ionic conductivity is similar to that governing self-diffusion[16,51,54] as explained in §2.3 on page 32. The CAF has successfully described the temperature-dependent diffusion coefficients for a broad variety of pure solvent systems, including n-acetates, 2-ketones, 1-alcohols, n-thiols and nitriles[16,51] as well as salt-solutions with various cations.[55] The solvents studied thus far in which the temperature dependence of the self-diffusion coefficients have been analyzed by the CAF seem to fall into two broad classes: aprotic systems with an E_a of roughly 25 kJ mol^{-1}, and protic systems whose E_a values are in the range of 40-50 kJ mol^{-1}.[16,51,56] This suggests that the protic nature of the solvents creates a hydrogen-bonded network that requires more energy to surmount the energy barrier implicit in the transport mechanism.

To refine the differences within associated liquids, the CAF is applied to two different hydrogen-bonded solvent families: 1-alcohols and 3-alcohols. **Fig. 4.1** and **Fig. 4.2**
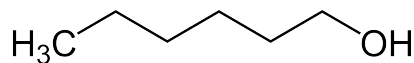
Figure 4.1: Chemical structure for 1-hexanol ($CH_3(CH_2)_5OH$).
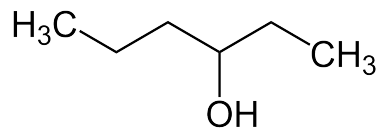
Figure 4.2: Chemical structure for 3-hexanol ($CH_3CH_2CHOH(CH_2)_2CH_3$).

show 1-hexanol and 3-hexanol, respectively. Comparing differences in selected solution properties between these two associating families will help identify some of the differences that structural properties have on mass transport in associated liquids, which can then be extended to charge transport. Many studies of variations in liquid structure have been done on the various isomers of alcohols.[57–66] It is well known that 1-alcohols can hydrogen bond to form extended linear chains.[60,67–69] Upon relocating the hydroxyl group from the terminal to an interior carbon, the formation of polymer-like linear networks is greatly hindered due to increased shielding of the hydroxyl group.[57,58,60,70,71]

By selecting 3-alcohol solvents as a comparison family to the 1-alcohol solvents, the hydrogen bonding network is reduced but not eliminated, while maintaining the same functional group. This comparison will give further insight into the nature of the hydrogen bonding network and its effect on mass transport without the added complexity of salt.[a] The solvent family members chosen for this work are in the 1-alcohol family: 1-hexanol, 1-heptanol, 1-octanol, 1-nonanol, and 1-decanol[b], and in the 3-alcohol family: 3-hexanol, 3-heptanol, 3-octanol, 3-nonanol, and 3-decanol. In this Chapter, the CAF is applied to temperature-dependent self-diffusion coefficients for 1- and 3-alcohols using temperature-dependent dielectric constants. The following claims

---

[a]The addition of salt to the 3-alcohols will be the topic of Chapter 5.

[b]To make the comparison as equal as possible 1-dodecanol, which was included in Chapter 3, is not included due to the difficulty in acquiring 3-dodecanol.

will be addressed:

- The extent of the hydrogen bonding network is different for the 1- and 3-alcohols and therefore affects the temperature-dependent diffusion coefficients.

- The dielectric constant is a measure of intermolecular interactions; therefore, the differences in the hydrogen bonding network between 1- and 3-alcohols will also be observed by differences in the dielectric constant.

- Differences observed in the results of the CAF for 1- and 3-alcohols are directly related to changes in the extent of the hydrogen bonding network and can be accounted for using the temperature dependent dielectric constant.

4.2 Temperature dependence of the diffusion coefficients of 1- and 3-alcohol solvents

The intermolecular forces on a single molecule result from a combination of several forces exerted by surrounding molecules. For associated liquids, these intermolecular interactions become more complicated due to the extended associating network, which will be shown to be temperature-dependent in the case of 1- and 3-alcohols. Temperature-dependent self-diffusion coefficients are a measure of how intermolecular interactions in a liquid change from system to system. As the temperature increases, diffusion coefficients also increase but at rates that depend to some degree on the extent of association in the liquid. For 1- and 3-alcohols, the rate of increase of the diffusion coefficients with temperature can be linked to differences in their respective

temperature-dependent hydrogen bonding networks.
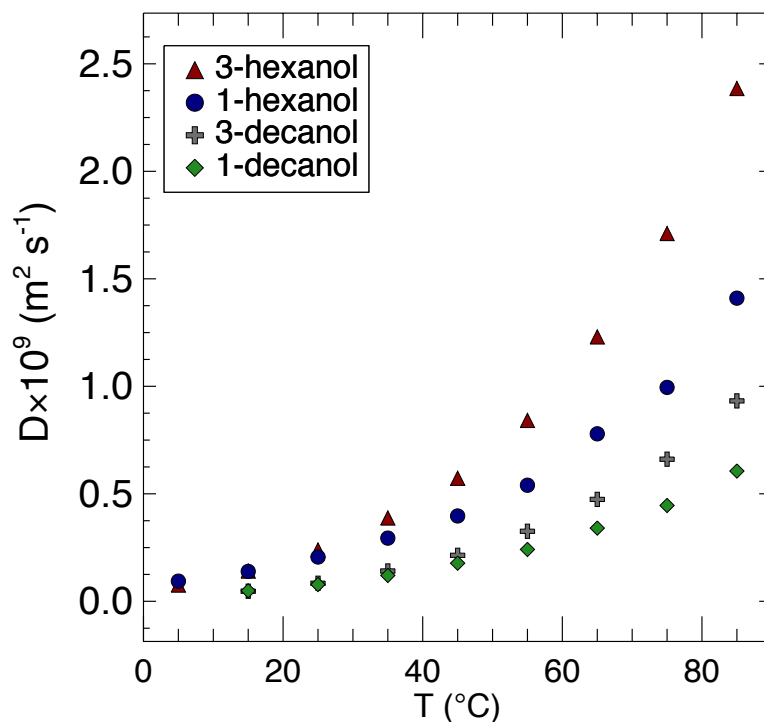
Figure 4.3: Diffusion coefficient versus temperature for 1-hexanol, 1-decanol, 3-hexanol and 3-decanol from 5–85°C.

Fig. 4.3 compares the self-diffusion coefficients as a function of temperature from 5 – 85°C for 3-hexanol and 1-hexanol, and from 15 – 85°C for 3-decanol and 1-decanol. The diffusion coefficient increases with temperature at a greater rate for 3-hexanol and 3-decanol compared to 1-hexanol and 1-decanol, respectively. There is little variation between the 1-hexanol and 3-hexanol at low temperature, but at 35°C the 3-hexanol diffusion coefficient begins to increases more rapidly than the 1-hexanol. At the higher temperatures, the intermolecular interactions in the 3-hexanol are weakened through a reduction of the hydrogen bonding network, resulting in a larger diffusion coefficient

than in 1-hexanol. This same trend is seen with the 1- and 3-decanol data above 45°C, but to a lesser extent.

4.3   Hydrogen bonding in 1- and 3-alcohol solvents

Fig. 4.4 shows temperature-dependent infrared spectra of the O-H stretching region ($3100 - 3600$ cm^{-1}) for 1- and 3- hexanol and decanol at several temperatures. The spectral region from approximately 3300 to 3380 cm^{-1} has been assigned to the O–H stretching frequency (ν(OH)) associated with the oxygen acting as both a proton donor and acceptor.[68,72] The breadth of the bands is due to multiple hydrogen-bonded O–H stretching populations, but shifts in the central band are a good indication of general changes in the strength and extent of the overall hydrogen bonding network.[73,74] A weakened O–H interaction will result in a shift of ν(OH) to higher frequency.[73]

As the temperature increases there is a shift in ν(OH) to higher frequency by roughly 31 cm^{-1} for both 1-hexanol and 1-decanol, showing that the reduction in the hydrogen bonding is comparable in these two solvents. A similar frequency shift was observed by Palombo *et al.*[59] and Paolantoni *et al.*[68] for 1-octanol over a similar temperature range. We can therefore assume that the same reduction of hydrogen bonding will be seen for 1-heptanol and 1-nonanol (*i.e.*, all members of the 3-alcohol family selected here) across the same temperature range. At low temperature, the bands for 3-hexanol and 3-decanol are not the same. The 3-hexanol band (3336 cm^{-1}) is at a lower frequency than the 3-decanol band, suggesting that extending the alkyl chain in the 3-alcohols reduces the hydrogen bonding at lower temperatures; this trend is not seen in the 1-alcohols. The temperature-dependent shift is not the same for 3-hexanol and 3-decanol.
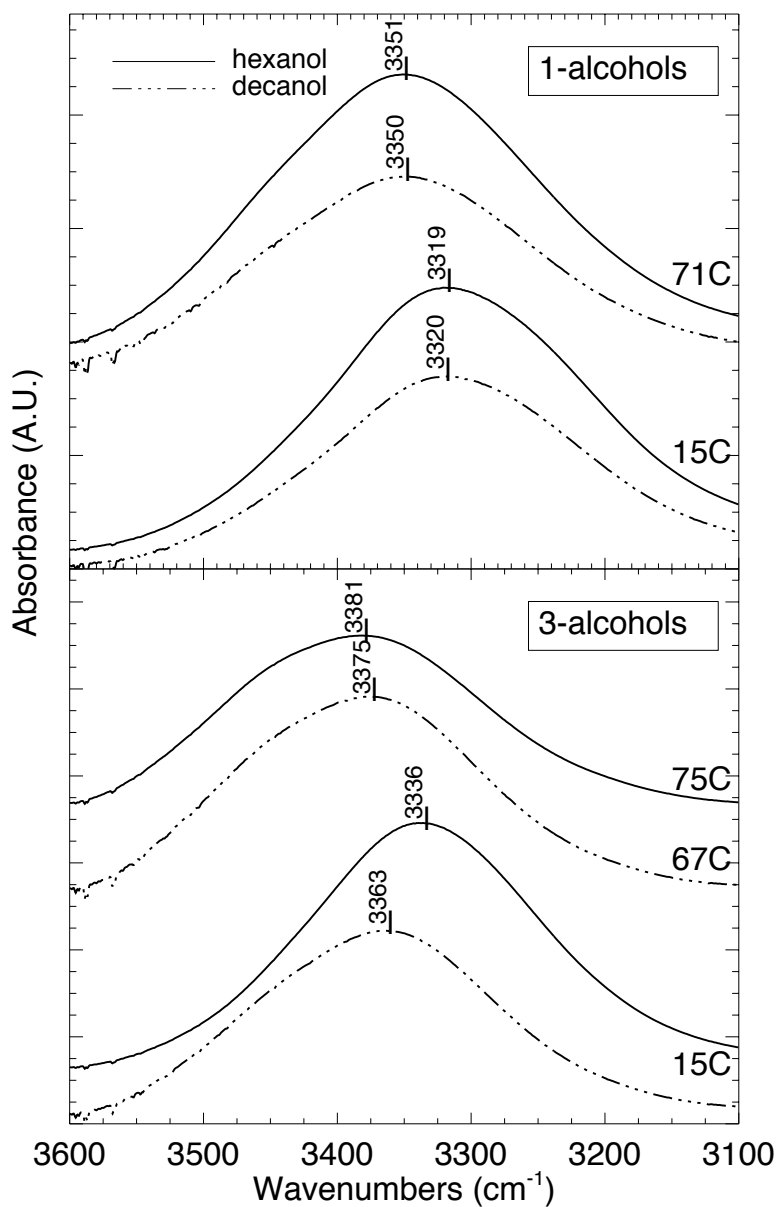
Figure 4.4: Infrared spectra of (top) 1-hexanol and 1-decanol at 15, and 71°C and (bottom) 3-hexanol and 3-decanol at 15°C and 67 (3-decanol) and 71°C (3-hexanol). Hexanol and decanol are marked with solid and dash-dot lines, respectively.

The change in frequency for 3-hexanol from 15 to 75°C is 45 cm^{-1}, while the shift in

frequency for 3-decanol is only 12 cm^{-1}. This supports the claim that the 3-alcohols

exhibit reduced hydrogen bonding with increasing temperature, but the length of the alkyl chain governs the extent of the reduction. Comparing the position of the $\nu(\text{OH})$ band for 1-decanol and 3-decanol at 15°C also shows the differences in the hydrogen bonding. The band for 1-decanol has a lower frequency (3320 cm^{-1}) than 3-decanol (3363 cm^{-1}). The location of the hydroxyl group at the third carbon in 3-decanol restricts the extent of hydrogen bonding. A smaller difference is seen between 1- and 3-hexanol.

It has been suggested that polymer-like hydrogen bonding networks are less favorable in alcohols that have a more centrally located hydroxyl group due to increased steric hinderance.[57,58,60,70,71] Campbell *et al.* found that upon diluting 1-octanol with a non-polar solvent the band at 3330 cm^{-1} shifts to 3340 cm^{-1} and becomes less intense, while a band assigned to the free O–H frequency (3650 cm^{-1}) becomes dominant, implying a reduced but not eliminated extended network.[57,63] The same measurements were taken with 3-octanol, and showed the free O–H band at 3650 cm^{-1} but no band at 3340 cm^{-1}, indicating that the interaction associated with extended hydrogen bonding is weaker in 3-octanol than in 1-octanol and therefore vanishes upon dilution.[57]

There is also a temperature dependence of the hydrogen bonding that is related to both the position of the hydroxyl group and the number of carbon atoms in the alkyl chain. Czarnecki and Orzechowski[58] determined that as the temperature increased, the rate of reduction of the hydrogen bonding network is greater for terminal hydroxyl groups than for more centrally located ones. These differences can also be seen in variations of the temperature dependence of the dielectric constant, which is known to play a major role in describing mass transport.[16,51]

4.4 Temperature dependence of the dielectric constants of 1- and 3-alcohol solvents
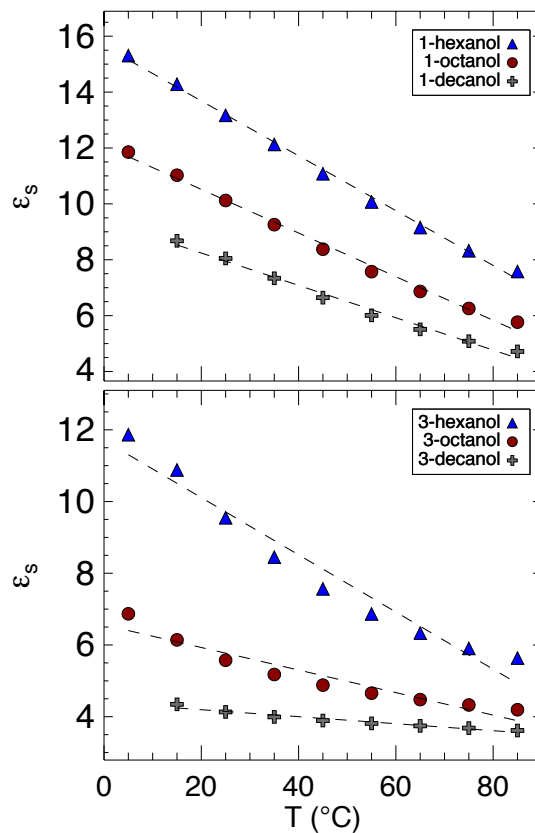
Figure 4.5: Dielectric constant versus temperature for (top) 1-hexanol, 1-octanol, and 1-decanol and (bottom) 3-hexanol, 3-octanol, and 3-decanol. The dashed lines are linear best fit lines.

Fig. 4.5 shows temperature-dependent dielectric constants for three members of the 1-alcohol family (top) and the 3-alcohol family (bottom) from 5 to 85°C. The dielectric constant of the 1-alcohols decreases linearly with temperature. The dashed lines show a linear best fit, with R^2 equal to 0.997, 0.993, and 0.988 for 1-hexanol, 1-octanol,

and 1-decanol, respectively. As the alkyl chain is extended, the linear dependence of the dielectric constant with temperature decreases only slightly for the 1-alcohols. The dielectric constants for 1-heptanol and 1-nonanol also show a linear decrease with temperature (data not shown).

The dielectric constants for the 3-alcohols, however, exhibit different behavior compared to the 1-alcohol family, as well as within their own solvent family, shown in the lower plot of **Fig. 4.5**. The shortest alkyl chain member (3-hexanol) has marked curvature from $5 - 85°C$, with the dashed linear best fit line demonstrating the deviation from linearity with an R^2 of 0.955. As the alkyl chain becomes longer the dielectric constant changes less with temperature. The linearity also reduces with R^2 values decreasing to 0.915 for 3-octanol and 0.911 for 3-decanol. The 3-decanol data appear to be almost independent of temperature for the range measured with a decrease from 4.3 to 3.6 for 15 and 85°C, respectively, but have the greatest curvature of the dielectric constants measured. The temperature dependent dielectric constants for 3-heptanol and 3-nonanol were also measured and fit in between their respective family members with curvature increasing as the alkyl chain increases (data not shown). The collinearity of ε_s with temperature in the 1-alcohols suggests that the temperature dependent properties of each 1-alcohol family member are similar, whereas the change of ε_s with temperature within the 3-alcohol family suggests that each member has a temperature dependence that is unique within the solvent family.

The values of ε_s are lower for the 3-alcohols than for the 1-alcohols, suggesting that hydrogen bonding is weaker in the 3-alcohols, based on evidence that more extended networks have higher dielectric constants.[75] The location of the hydroxyl group on

the third carbon introduces increased steric hindrance which reduces the extent of hydrogen bonding, as was shown in **Fig. 4.4**. Reducing the hydrogen bonding greatly affects the values of ε_s as well as its temperature dependence. Dielectric studies of formamide compared to dimethylformamide show that by exchanging the hydrogens of the nitrogen for methyl groups, (*i.e.*, 'turning off' the hydrogen bonding) results in a drastic decrease of the dielectric constant from 113 to 38.8.[75] The contrasting behavior of ε_s for the 1-alcohols and the 3-alcohols is not as dramatic as the change occurring in the amide systems upon methylation, but can still be linked to a reduction in the extended liquid structure through a weakened hydrogen bonding network.

Due to the limited temperature range of the equipment used throughout this work, the temperature range has an upper limit of 85°C. For the longer chain alcohols (both 1- and 3-) the boiling point is far above this temperature limit. Literature data were compiled for pure 1-, 2-, and 3-octanol for comparison to a more extensive temperature range than that measured here. **Fig. 4.6** shows ε_s versus temperature from this work for 1-octanol[a] (open circles) and 3-octanol[a] (open crosses), both connected by lines as a guide to the eye, with vertical dotted lines representing the measured temperature range. Literature data of ε_s are also plotted for 1-octanol[b] (blue circles)[64] and 3-octanol[c] (green crosses)[76] that extend the temperature range of the data measured here. The superscripts, a, b, and c correspond to the data labeling in **Fig. 4.6**. The 1-octanol data from this work are linear over the measured temperature range. The 1-octanol literature data (blue circles), however, show that as the temperature increases, ε_s begins to level off with a definite change in slope occurring around 125°C. For the 3-octanol data, the temperature range of this work shows marked curvature. The 3-octanol literature data
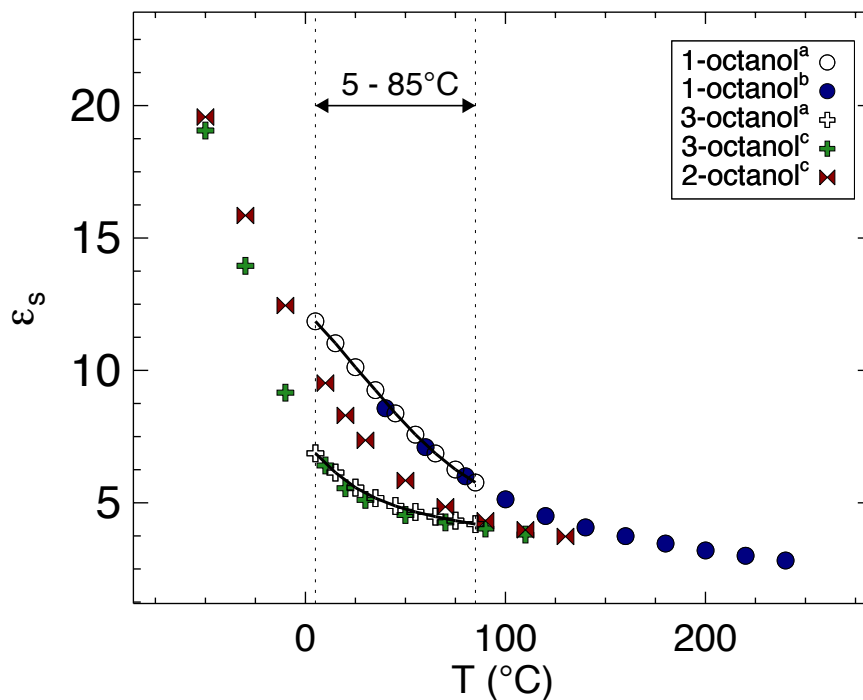
Figure 4.6: Dielectric constant versus temperature for 1-, 2-, and 3-octanol. [a]Data with open symbols are from this work connected by lines as a guide to the eye, with the vertical lines marking the temperature range. [b]High-temperature 1-octanol data (blue circles) taken from Dannhauser [64], [c]Low temperature 2-octanol (red bow-ties) and 3-octanol (green crosses) data taken from Wohlfahrt [76].

(green crosses) extends ε_s to lower temperatures, and shows a reduced curvature and a more linear trend with decreasing temperature below 0°C. Here, the change in slope is observed within the temperature range measured here, at approximately 35°C.

It has already been discussed that the differences observed in the temperature dependence of ε_s are due to changes in the hydrogen bonding. As the temperature increases, the extent of hydrogen bonding decreases.[73] The results of **Fig. 4.6** show that if the 1-alcohol ε_s data were measured at a higher temperature range, then the changes of the hydrogen bonding reflected in the 3-alcohol ε_s would also be observed. Likewise, if ε_s

of the 3-alcohols was measured over a lower temperature range, it is likely a linear rela-

tionship between ε_s and temperature would be seen. The temperature corresponding to

the change in slope of ε_s with temperature seems to increase with increasing hydrogen

bonding. For comparison, literature data for 2-octanol (red bow-ties) is also plotted

in **Fig. 4.6** and appears to fall in between the 1- and 3-octanol data. The change in

slope of ε_s with T is between the 1-octanol and 3-octanol change in slope location at

approximately 75°C. In can be concluded that for the semi-narrow temperature range

selected for this work (5 – 85°C) the differences in hydrogen bonding separate the 1-

and 3-alcohols into two different groups. These differences are developed further with

the temperature dependence of the Kirkwood g-factor discussed in the next section. If

a larger temperature range were possible, the ε_s data may appear to be more similar.

4.4.1 Application of the Kirkwood-Frölich model of $\varepsilon_s(T)$

We can further examine the differences between the 1-alcohols and 3-alcohols by use

of the Kirkwood-Frölich model for the dielectric constant, given in **eq. 4.1**.[77,78]

$$\frac{\varepsilon_s - 1}{\varepsilon_s + 2} - \frac{\varepsilon_\infty - 1}{\varepsilon_\infty + 2} = \frac{3\varepsilon_s(\varepsilon_\infty + 2)}{(2\varepsilon_s + \varepsilon_\infty)(\varepsilon_s + 2)} \frac{4\pi N}{9k_BT} g\mu_0^2 \tag{4.1}$$

Here ε_s is the static dielectric constant, ε_∞ is the high frequency permittivity found from

the square of the optical refractive index, N is the dipole density found by dividing the

liquid density by the molecular weight, μ_0 is the permanent dipole moment in vacuum,

g is the Kirkwood g-factor that is related to the extent of association of the liquid, k_B is

Boltzmann's constant, and T is temperature. For non-associating liquids, the g-factor

is unity.[78] It has been shown that there is both a temperature and alkyl chain length dependence in g.[60,62,65,66,79]

Fig. 4.7 shows the temperature dependence of $g\,\mu_0^2$ from **eq. 4.1** for pure 1-hexanol through 1-decanol (top) and pure 3-hexanol through 3-decanol (bottom). The dipole moment factors, $g\,\mu_0^2$, were calculated from **eq. 4.1** using measured values of ε_s and density[a] over the temperature range $5 - 85°$C. The refractive index values used are 1.43 for 1-alcohols,[80] and 1.42 for 3-alcohols.[80] For the 1-alcohol family, $g\,\mu_0^2$ decreases for all members in the same collinear fashion as ε_s. This suggests that the temperature dependence of g is the same for all members of the 1-alcohol family. This agrees with the IR spectra presented in **Fig. 4.4** that shows the hydrogen bonding to have the same temperature dependence for 1-hexanol and 1-decanol.

The bottom plot of **Fig. 4.7** shows a non-linear $g\,\mu_0^2$ with temperature for all members of the 3-alcohol family. The curvature is most apparent for the shorter chain members and decreases in the longer chain members with $g\,\mu_0^2$ in 3-decanol becoming independent of temperature above $45°$C. Each member of the 3-alcohol family has a temperature dependence in $g\,\mu_0^2$, but the temperature dependence changes from member to member because the strength and extent of association varies from member to member. This change was also seen in the marked difference in the spectra of 3-hexanol and 3-decanol in **Fig. 4.4** on page 67. The hydrogen bonding of 3-hexanol is stronger than that in 3-decanol at $15°$C with a higher $\nu(\text{OH})$ frequency. As the temperature increases, 3-hexanol has a large shift in frequency indicating weakened hydrogen bonding, while the $\nu(\text{OH})$ frequency of the 3-decanol increases much less. 3-hexanol has the greatest

---

[a]Experimental techniques for acquiring the density are given in Appendix A.5.
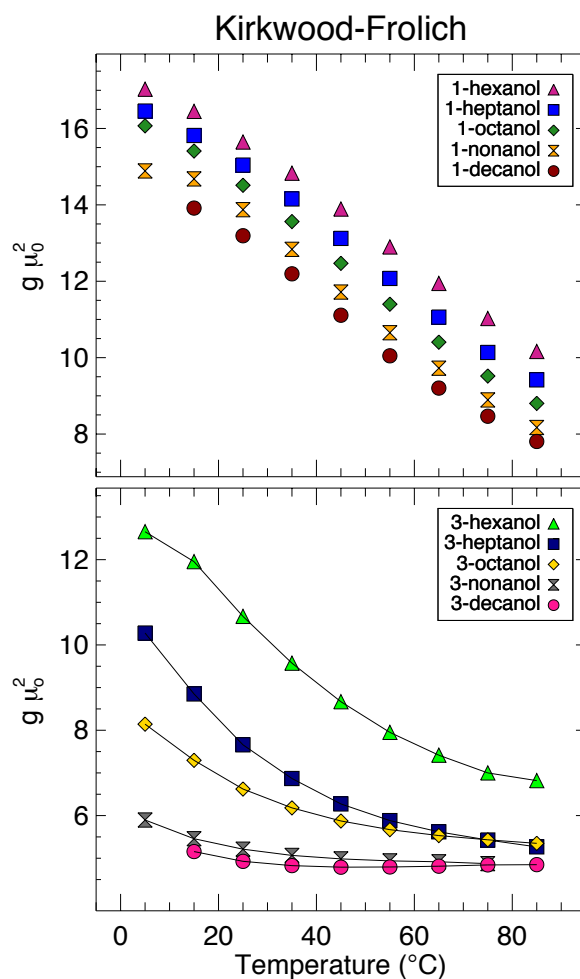
Figure 4.7: Kirkwood dipole factor, $g\,\mu_0^2$, versus temperature for (top) 1-alcohols as labelled and (bottom) 3-alcohols as labelled. The solid lines are given as guides to the eye.

difference in hydrogen bonding across the temperature range and subsequently has the greatest temperature dependence of $g\,\mu_0^2$. The O–H stretching band of 3-decanol shows a much smaller difference in hydrogen bonding across the temperatures ($\Delta\,\nu(\mathrm{OH})$ of 12 cm^{-1}), indicating little variation in $g\,\mu_0^2$ with temperature.

The behavior of $g\,\mu_0^2$ with temperature of both 1-alcohols and 3-alcohols follows the temperature dependence of ε_s with temperature. All previous CAF studies of the temperature dependence of ε_s have shown a linear dependence with temperature for aprotic solvents and 1-alcohols.[16,51] The 3-alcohol family is the first solvent family studied with the CAF that shows a non-linear temperature dependence in ε_s. This is explained by the temperature dependence in the $g\,\mu_0^2$ factor.

Johari and Dannhauser[66] determined ε_s and density values of several octanol isomers over the temperature range $15 - 90°$C. Using **eq. 4.1** they determined the temperature dependence of g for 2-octanol and 3-octanol, as well as other isomers of octanol.[66] Their data for 3-octanol follow the trend for 3-octanol shown in **Fig. 4.7**. What is more interesting is that their plot of g versus temperature for 2-octanol[66] resembles a combination of the $g\,\mu_0^2$ factors for 1- and 3-alcohols. The g-factor for 2-octanol is more linear with temperature than the 3-octanol, but not completely linear like the g-factor for 1-octanol. This behavior follows the trend of ε_s with temperature for 2-octanol shown in **Fig. 4.6**. It is possible that other isomers of the protic solvent families studied using the CAF will lead to a similar conclusion regarding the temperature dependence of both ε_s and $g\,\mu_0^2$.

4.4.2 Comparison of the Kirkwood g-factor to aprotic liquids

The temperature dependence of ε_s and the Kirkwood g-factor arise from changes in the liquid structure. However, it is with hesitation that any relationship be made between the absolute value of g for associated liquids and a specific molecular model due to variations that occur which depend on the method of calculation. For exam-

ple, g factors for 1-pentanol were found to vary from $2.75\,^{60}$ to $3.15\,^{61}$ at 25°C, and $3.43\,^{77}$ (at 20°C); g factors for 1-heptanol varied from $2.97\,^{61}$ to $3.4\,^{62}$ at 25°C. Regardless, the quantity $g\,\mu_0^2$ is a useful parameter in identifying qualitative changes in liquid structure. For solvents that are not associated, the temperature dependence of ε_s is due to $N(T)/T$ as given in **eq. 4.1** with g being unity. For comparison, **Fig. 4.8**
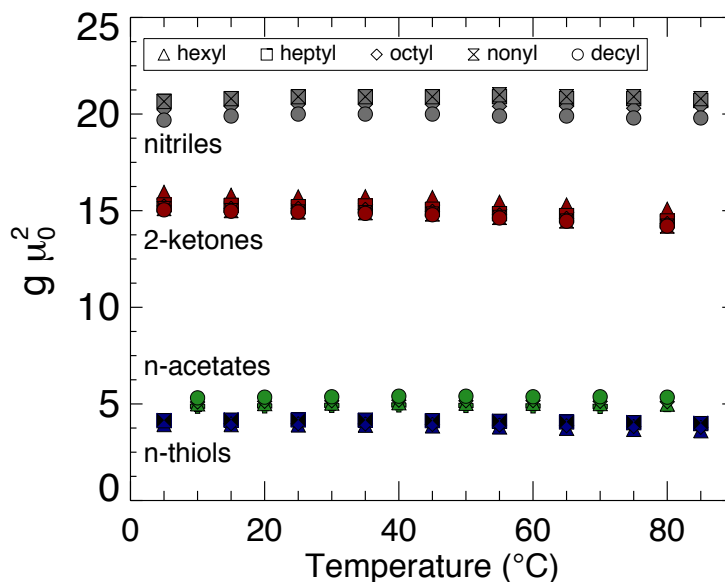
Figure 4.8: Kirkwood dipole factor, $g\mu_0^2$ (calculated from **eq. 4.1**) versus temperature for nitriles (grey), 2-ketones (red), n-acetates (green), and n-thiols (blue). The symbols correspond to the respective solvent family members.

shows $g\,\mu_0^2$ versus temperature for several different aprotic families that have negligible long–range association; nitriles (grey), 2-ketones (red), n-acetates (green), and n-thiols (blue). Each aprotic family consists of carbon chain members hexyl through decyl, with the symbols given in the figure matching accordingly. As the permanent dipole moment increases, so does the magnitude of $g\,\mu_0^2$, which is to be expected with the nitrile family having the highest $g\,\mu_0^2$ term. The nitriles, 2-ketones, n-acetates, and n-thiols also show

no temperature dependence in $g\,\mu_0^2$ because the temperature dependence of ε_s is due only to the dipole density and temperature, as has been shown previously.[56] The temperature dependence of the dielectric constant is a crucial component in describing the temperature-dependent diffusion coefficients. Fluctuations in the extended hydrogen bonding network in the 1- and 3-alcohol families produce an additional temperature dependence in $g\,\mu_0^2$. The additional temperature dependence due to $g\,\mu_0^2$ is still accounted for in the compensated Arrhenius formalism, as will now be discussed.

4.5 Applying the compensated Arrhenius formalism to diffusion coefficients of pure 1- and 3-alcohol solvents

4.5.1 CAF: E_a values of $D(T)$

The CAF is applied to the temperature dependent diffusion coefficients of both 1- and 3-alcohol families given in § 4.1. A detailed description of the scaling procedure was given in § 2.2, with application to diffusion coefficients described in § 2.3 beginning on page 32.

Fig. 4.9 shows the simple Arrhenius (filled circles, left axis) and compensated Arrhenius (open diamonds, right axis) plots for pure 1-octanol (top) and 3-octanol (bottom). Both 1-octanol and 3-octanol exhibit Arrhenius-like behavior without having applied the scaling procedure. It was discussed in § 3.5 that regardless of the linearity of the SAE plot a compensation must still be performed if there exists a temperature dependence of the dielectric constant.[16,51] This condition is true for both solvents as can be seen in the temperature dependence of ε_s in **Fig. 4.5** on page 69. Upon compensation,
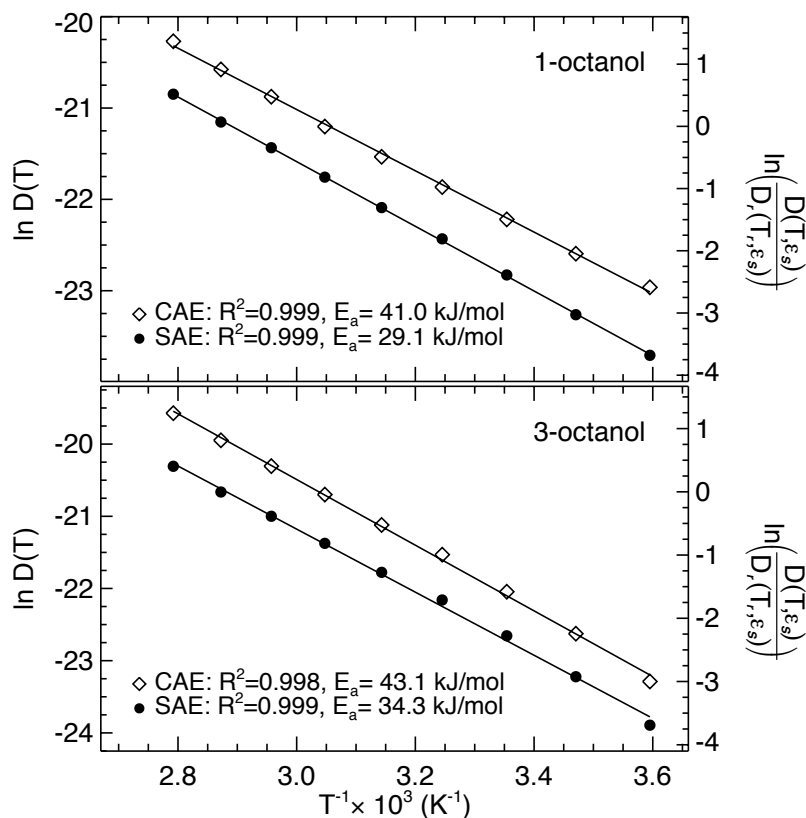
Figure 4.9: Simple Arrhenius plot (filled circles, lext axis) and Compensated Arrhenius plot (open diamonds, right axis) of diffusion coefficients for 1-octanol (top) and 3-octanol (bottom).

both 1-octanol and 3-octanol still show Arrhenius-like behavior, however, the values of E_a calculated from the SAE are very different than those from the CAE for both 1-octanol and 3-octanol. There is a greater difference in the SAE and CAE E_a for the 1-octanol than for the 3-octanol, which can be related back to the difference in the temperature dependence of the dielectric constant. The 1-octanol has more of a temperature dependence in the dielectric constant than the 3-octanol, which increases the temperature dependence in the exponential prefactor. As a result, there is a greater

temperature dependence not accounted for using the simple Arrhenius method resulting in a greater difference between the two E_a values.

The CAF was applied to all other diffusion coefficients for 1- and 3-alcohols (data not shown). **Table 4.1** gives E_a values averaged from the slope and intercept for 1- and 3-alcohols with the respective reference temperature used in the scaling procedure. The average E_a was found to be 42.3 ± 0.5 kJ mol^{-1} and 43.4 ± 0.3 kJ mol^{-1} for 1-alcohols and 3-alcohols, respectively. Previously, the average E_a for 1-alcohols was

family member	1-alcohol E_a (kJ mol^{-1})	T_r (°C)	3-alcohol E_a (kJ mol^{-1})	T_r (°C)
hexanol	42.3 ± 0.9	25	41.8 ± 0.2	15
heptanol	41.6 ± 0.5	35	43.6 ± 0.5	35
octanol	42.2 ± 0.5	45	42.7 ± 0.6	65
nonanol	42.5 ± 0.3	65	44.6 ± 0.8	75
decanol	43.0 ± 0.2	75	44.3 ± 0.9	85
Average	42.3 ± 0.5		43.4 ± 0.3	

Table 4.1: Energies of activation for pure 1-alcohols and 3-alcohols calculated based on the CAF using the listed T_r.

found to be 37 ± 1 kJ mol^{-1}.[16] The increase in E_a from the previous study corresponds to the selection of different 1-alcohol family members to comprise the family used in the scaling procedure. The previous study[16] used ethanol, propanol, 1-butanol, 1-hexanol, and 1-octanol, whereas this study used longer alkyl chain 1-alcohol family members. As discussed in § 3.7, if much shorter members are chosen, the average E_a values will be lower than if longer members are used,[51] consistent with this study.

The E_a values given in **Table 4.1** are within the experimental error for both 1- and 3-alcohols. In order for mass transport to occur, the diffusing molecule must have an energy that exceeds the activation energy. The 1- and 3-alcohols have similar E_a values,

suggesting that the energy barrier is similar for both solvents. The presence of hydrogen bonding increases the intermolecular interactions which results in a larger average E_a than those reported for aprotic solvents (approximately 25 kJ mol^{-1}).[51,54,56] The 1-alcohols and 3-alcohols share a similar functional group, but as shown with the dielectric constant and the hydrogen bonding differences (**Fig. 4.4**, page 67) the placement of the functional group governs the liquid structure of the system, which appears to affect mass transport.

4.5.2 CAF: exponential prefactors of $D(T)$

The values of the diffusion coefficients are greater for a 3-alcohol family member than the corresponding 1-alcohol family member (*e.g.*, D for 3-hexanol $> D$ for 1-hexanol), particularly at higher temperatures. The reason for this is found in the exponential prefactor, D_0, calculated as described in § 2.2.5 on page 30. The top plots of **Fig. 4.10** show the isothermal diffusion coefficients versus dielectric constant for 1-alcohols (left) and 3-alcohols (right). The isothermal diffusion coefficient data break apart into distinct temperature-dependent curves that increase with decreasing dielectric constant, corresponding to each family member. The curves are numbered according to the number of carbon atoms in the alkyl chain (*e.g.*, (6) corresponds to either 1- or 3-hexanol). The isothermal diffusion coefficients curves represent the reference diffusion coefficient curves. For example, the 45°C reference temperature is depicted by the red circles and was used in the compensation procedure for 1-octanol; the temperature-dependent curve labeled (8).

When the diffusion coefficients are divided by the Boltzmann factor using the average
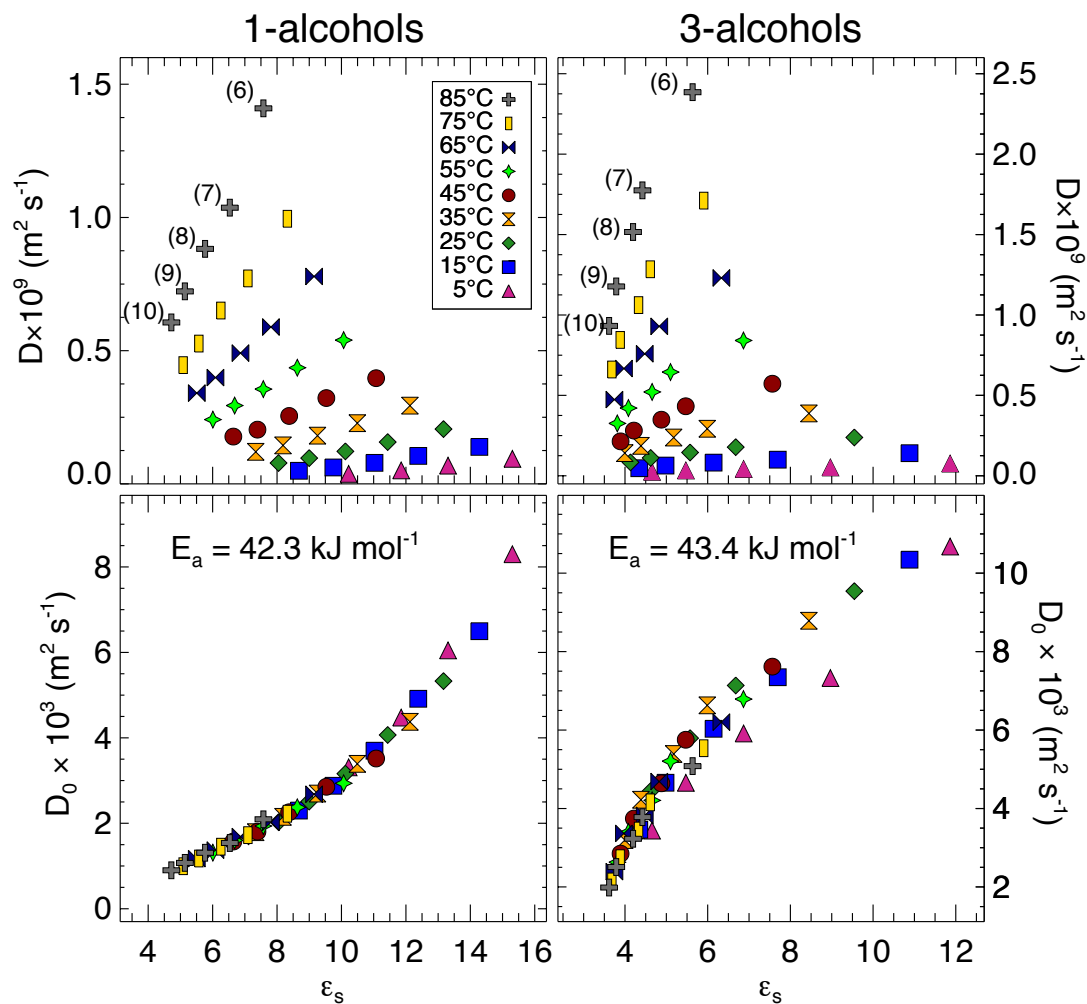
Figure 4.10: (Top) Isothermal diffusion coefficients versus dielectric constant for 1-alcohols (left) and 3-alcohols (right). The temperature dependent curves are labeled as (6) hexanol (7) heptanol (8) octanol (9) nonanol and (10) decanol for both 1- and 3-alcohols. (Bottom) Exponential prefactors, D_0, versus dielectric constant for 1-alcohols (left) and 3-alcohols (right). The symbols correspond to the temperatures as shown.

E_a, the exponential prefactor data collapse to form a single master curve, shown in the lower two plots of **Fig. 4.10**. The D_0 curve for the 1-alcohols follows a similar trend as seen for aprotic solvents.[51] The formation of a master curve confirms the key

assumptions in the compensated Arrhenius formalism; the temperature dependence of the exponential prefactor, D_0, is due to the temperature dependence of the dielectric constant. The exponential prefactors increase with increasing dielectric constant for both the 1- and 3-alcohols. However, the temperature dependence of the dielectric constant is different between the 1- and 3-alcohols, which causes the different shapes of the master curves for the 1- and 3-alcohols. This difference is better observed by considering the isothermal diffusion coefficients versus ε_s, shown replotted in **Fig. 4.11** for the 1-alcohol family (top) and the 3-alcohol family (bottom) at 35°C. The family members that comprise the reference curve are labelled accordingly in the figure. For the purposes of interpolating between data points, the isothermal plots are empirically fit to a function that best describes the data. Due to the different behavior of ε_s in the 1- and 3-alcohols, the empirical functions have different forms:

1-alcohols: $$D(\varepsilon_s) = A_1 + B_1 \times e^{(\varepsilon_s/C_1)} \tag{4.2a}$$

3-alcohols: $$D(\varepsilon_s) = A_3 - B_3 \times C_3^{\varepsilon_s} \tag{4.2b}$$

where A_1, B_1, C_1 and A_3, B_3, C_3, are unique to each reference curve. The 1-alcohol diffusion reference curve (**eq. 4.2**a) has an exponential growth functional dependence on the dielectric constant. The same exponential growth functional form is seen in the master curve formed from the exponential prefactors plotted versus the dielectric constant (**Fig. 4.10**). The 3-alcohol reference curve, however, follows a different functional dependence with ε_s, as shown in **eq. 4.2**b. The 3-alcohol family is the first solvent system studied with the CAF that has had a reference diffusion coefficient curve with this
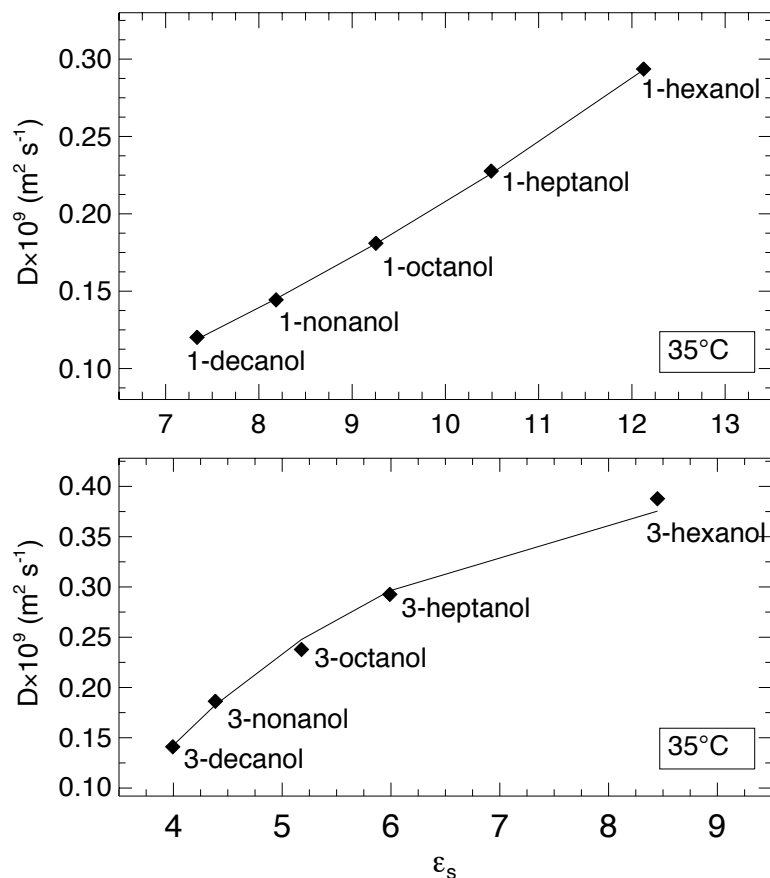
Figure 4.11: Isothermal diffusion coefficients versus dielectric constant at 35°C for 1-alcohols (top) and 3-alcohols(bottom). The plots are also considered diffusion reference curves with $T_r = 35°C$

type of functional dependence. The master curve for the 3-alcohols formed in **Fig. 4.10** follows this same functional dependence. For the 3-alcohols, the longer chain members have a different temperature dependence of ε_s than the shorter chain members, displayed in **Fig. 4.5**. This difference results in a reference diffusion coefficient curve (bottom of **Fig. 4.11**) that changes less with dielectric constant for the longer chain alcohols and changes more for the shorter chain alcohols compared to the 1-alcohol diffusion reference curve. The non-linear temperature dependence of the dielectric con-

stant within the 3-alcohol family originates in the varying temperature dependence of the $g\,\mu_0^2$ factor from **eq. 4.1** on page 73.

Onsager related the temperature dependence of the dielectric constant to $N(T)/T$, where the dipole density N is also temperature dependent. When the Kirkwood g-factor becomes unity, **eq. 4.1** reduces to the Onsager equation leaving the only temperature dependence in ε_s contained in the factor $N(T)/T$, as shown in **eq. 4.3**.[78]

$$\frac{\varepsilon_s - 1}{\varepsilon_s + 2} - \frac{\varepsilon_\infty - 1}{\varepsilon_\infty + 2} = \frac{3\varepsilon_s(\varepsilon_\infty + 2)}{(2\varepsilon_s + \varepsilon_\infty)(\varepsilon_s + 2)} \frac{4\pi N}{9k_B T}\mu_0^2 \qquad (4.3)$$

A plot of ε_s versus $N(T)/T$ yields a linear relationship for the aprotic solvents, establishing that the temperature dependence in ε_s is primarily due to the $N(T)/T$ factor. **Fig. 4.12** shows a similar plot of dielectric constant versus $N(T)/T$ for the 1-alcohols and 3-alcohols. Only hexanol, octanol, and decanol data of both the 1- and 3-alcohols are shown for clarity; the 1- and 3-heptanol and nonanol data are not shown but follow similar trends of their respective family members. The dashed lines represents linear fits to the 1-alcohol data and all have an R^2 value greater than 0.996.

The dielectric constants for the 1-alcohols all show a linear dependence with $N(T)/T$. Unlike the aprotic systems, the 1-alcohols do have an extra temperature dependence in ε_s due to $g\,\mu_0^2$ as shown in **Fig. 4.7**. This additional temperature dependence is the same for all members of the solvent family. Even with this added temperature dependence, however, the result is a master curve of D_0 versus ε_s that follows the same form as the aprotic solvents. The exponential prefactor data of the 1-alcohol family do not show any deviations (*i.e.*, scatter) in the master curve because ε_s and $g\,\mu_0^2$ are collinear
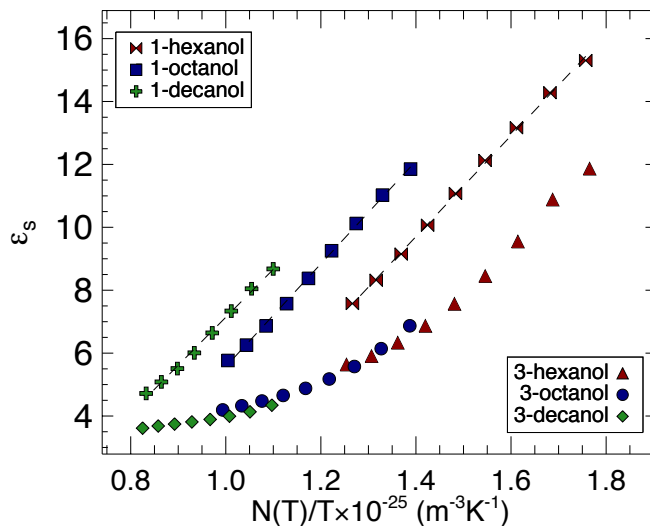
Figure 4.12: Dielectric constants versus dipole density, N divided by temperature for 1-hexanol, 1-octanol, 1-decanol, and 3-hexanol, 3-octanol, 3-decanol over the temperature range 5–85°C. Symbol identification is labeled in the figure, and the dashed lines are best-fit trend lines with $R^2 \geqslant 0.996$.

with temperature for each member of the 1-alcohol family.

The 3-alcohol dielectric constant data are not linear with $N(T)/T$ because of the additional non-linear temperature dependence in $g\,\mu_0^2$. In addition, each 3-alcohol family member has a different $g\,\mu_0^2$ dependence with temperature, yielding small deviations in the exponential prefactor dependence on the dielectric constant (*i.e.*, increased scatter in the master curve shown in **Fig. 4.10**). Deviations occur at the lower temperatures due to the increased temperature dependence of $g\,\mu_0^2$ shown in **Fig. 4.7** for the shorter chain members, *e.g.*, 3-hexanol, 3-heptanol, and 3-octanol. The exponential prefactors for 3-nonanol and 3-decanol have little to no deviation from the master curve because the majority of the temperature dependence of D_0 is due to $N(T)/T$, consistent with the aprotic systems.

4.6 CAF: using the dipole density factor, $N(T)/T$

The temperature dependence of D_0 is further developed by considering the inherent temperature dependence of ε_s that follows **eq. 4.1** for associated solvents and **eq. 4.3** for non-associated solvents. In the case of aprotic solvents, the temperature dependence of ε_s is due to $N(T)/T$, because the g-factor is independent of temperature (**Fig. 4.8**). A plot of D_0 versus ε_s forms a master curve because all of the temperature dependence of D_0 is due to ε_s. Examples of master curves for the aprotic systems previously shown in **Fig. 4.8** are given in the left plot of **Fig. 4.13**.[a] For these aprotic systems, all of the temperature dependence in ε_s is due to the dipole density and temperature so master curves are formed with little scatter. The right side of **Fig. 4.13** will be discussed over the next few paragraphs, but is given here for comparison to the left side of **Fig. 4.13**.

If all of the temperature dependence of ε_s is due to $N(T)/T$ then a plot of the isothermal diffusion data versus $N(T)/T$ should also construct a reference curve that can be used in the scaling procedure of the CAF, similar to the curves produced in **Fig. 4.11**.[56] This is true for the aprotic solvents presented here. The resulting scaling procedure (outlined using ε_s in § 2.2.2) is shown below using $N(T)/T$ in place of ε_s. The exponential prefactor has a temperature dependence due to $N(T)/T$ (**eq. 4.4**a). The scaling procedure cancels this out in **eq. 4.4**b because $D_0\left(\frac{N(T)}{T}\right) = D_0\left(\frac{N(T_r)}{T_r}\right)$ through the use of the reference curve. Taking the natural log of the scaled diffusion coefficients results in a CAE that is now based on the dipole density and temperature,

---

[a]As a side note, the left plot of **Fig. 4.13** gives an excellent display of the differences of the dielectric constant for the various aprotic solvents used. The acetates and thiols are to the low side of ε_s, while the ketones and nitriles are on the higher side. The resulting E_a values from the CAF (both scaling with ε_s, or $N(T)/T$) are all approximately 25 kJ mol^{-1}. This is a fine example of the differences between associating and non-associating liquids; the 1- and 3-alcohols both have a much higher E_a value than the aprotic systems, but cover a similar range of ε_s.
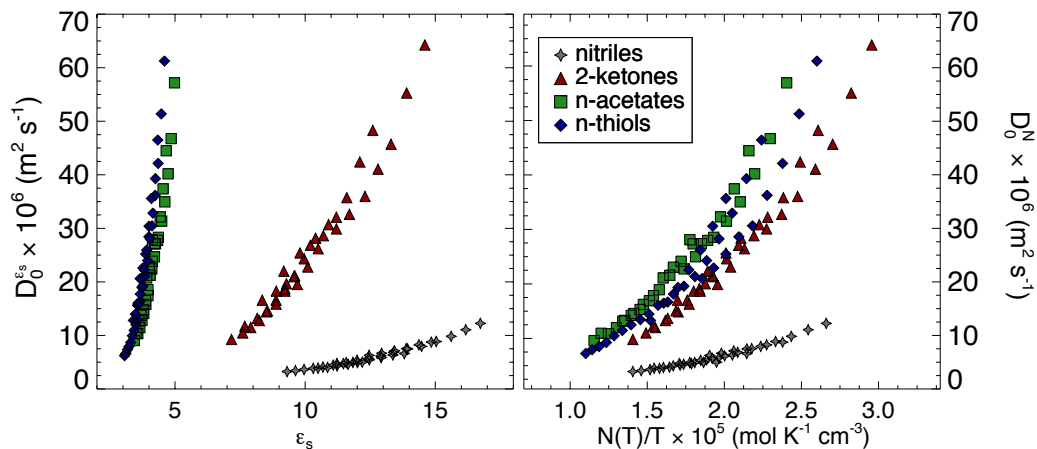
Figure 4.13: (Left) Diffusion exponential prefactors calculated using ε_s plotted versus ε_s over the range 5–85°C for the aprotic solvent families: nitriles (grey stars), 2-ketones (red triangles), n-acetates (green squares), and thiols (blue diamonds). (Right) Diffusion exponential prefactors calculated using $N(T)/T$ plotted versus $N(T)/T$.[56]

and not on ε_s.[56]

$$D\left(T, \frac{N(T)}{T}\right) = D_0\left(\frac{N(T)}{T}\right) \exp\left[\frac{-E_a}{RT}\right] \tag{4.4a}$$

$$\frac{D\left(T, \frac{N(T)}{T}\right) = D_0\left(\frac{N(T)}{T}\right) e^{-E_a/RT}}{D_r\left(T_r, \frac{N(T_r)}{T_r}\right) = D_0\left(\frac{N(T_r)}{T_r}\right) e^{-E_a/RT_r}} \tag{4.4b}$$

$$\ln\left(\frac{D\left(T, \frac{N(T)}{T}\right)}{D_r\left(T_r, \frac{N(T_r)}{T_r}\right)}\right) = \frac{-E_a}{RT} + \frac{E_a}{RT_r} \tag{4.4c}$$

The CAF scaling procedure just described is applied to the aprotic solvents: nitriles, 2-ketones, n-acetates and thiols.[56] For clarity, results from the CAF scaling out ε_s are labelled with a superscript "ε_s", and results from the CAF scaling out $N(T)/T$ are labelled with superscript "N". The resulting CAE plots are linear and the E_a^N are within 6% of the $E_a^{\varepsilon_s}$ values.[56] A plot of D_0^N versus $N(T)/T$ also results in a master curve for all of the systems shown in the right plot of **Fig. 4.13**. The primary difference between $D_0^{\varepsilon_s}$ and D_0^N is that ε_s contains the permanent dipole moment factor, μ_0^2, which

is different for the different aprotic solvents. By scaling to the dipole density factor, the master curves are normalized to a μ_0^2 value of unity, yielding master curves that are more similar than those produced by scaling with ε_s.

The additional temperature dependence contained in the g-factor for associating liquids, however, does not follow the trends observed with aprotic systems as just described. The same scaling procedure using $N(T)/T$ was performed for both 1- and 3-alcohol solvent families. **Fig. 4.14** shows the diffusion exponential prefactors D_0^N versus $N(T)/T$ for 1-alcohols (left plot) and 3-alcohols (right plot). A master curve is
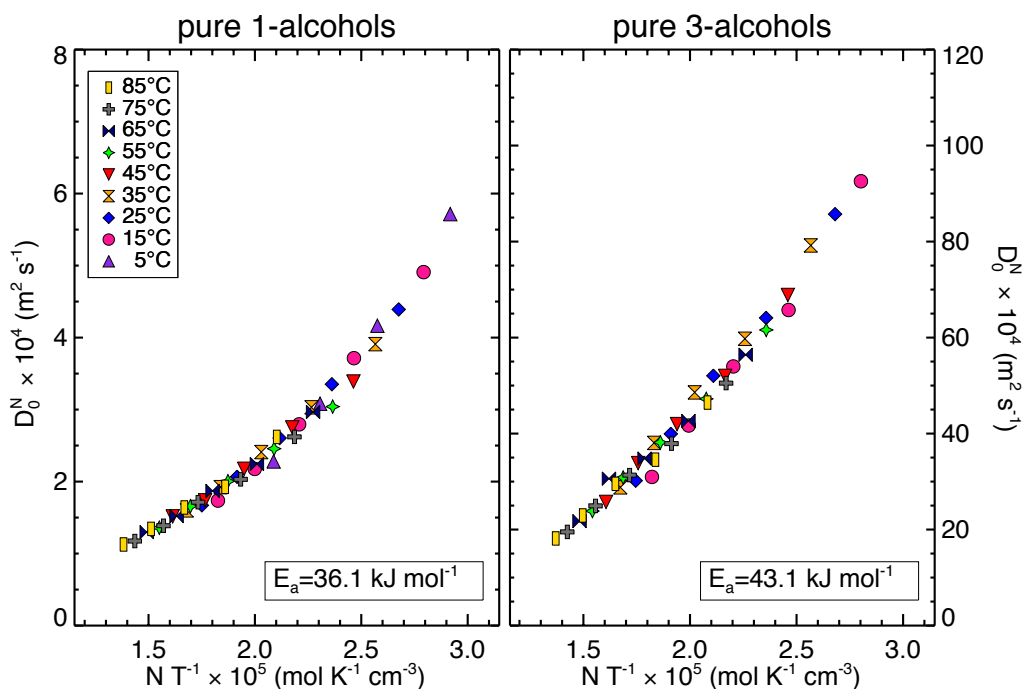
Figure 4.14: Diffusion exponential prefactors versus $N(T)/T$ (calculated by scaling with $N(T)/T$) over the range 5–85°C for the 1-alcohol solvent family (left) and the 3-alcohol solvent family (right).

formed for the 1-alcohols, however, the average E_a^N (36.1 $\pm$ 0.5 kJ mol^{-1}) is not the

same as the average $E_a^{\varepsilon_s}$ (42.3 ± 0.5 kJ mol^{-1}). The temperature dependence of the g-factor is the same for each member of the 1-alcohol family so the general functional form is the same for the master curve as it is in **Fig. 4.10**, however the values of D_0^N are an order of magnitude less than values of $D_0^{\varepsilon_s}$. The lower values of E_a^N and D_0^N show that scaling the diffusion coefficients to $N(T)/T$ scales out some of the temperature dependence, but not all of it. The remaining temperature dependence contained in the g-factor (shown in **Fig. 4.7**, page 75) has the same linear dependence for all members and therefore a master curve is still produced.

The right plot of **Fig. 4.14**, however, does not look similar to the master curve produced by $D_0^{\varepsilon_s}$ in **Fig. 4.10**. The value of E_a^N is the same as $E_a^{\varepsilon_s}$, and the values of D_0^N are only slightly less than $D_0^{\varepsilon_s}$.[a] The reason the master curves look different is because the temperature dependence contained in $N(T)$ is linear for the 3-alcohols, which results is a more uniform master curve. The temperature dependence contained in the g-factor is non-linear, and the extent of non-linearity is different for each member the 3-alcohol family as shown in **Fig. 4.7**. The result is a master curve formed by $D_0^{\varepsilon_s}$ with more scatter because ε_s contains the temperature dependence of both $N(T)/T$ and the g-factor. It is unclear why the E_a^N is the same as $E_a^{\varepsilon_s}$. The scaling procedure is designed to incorporate each member of the solvent family. The g-factor for 3-hexanol has a large temperature dependence, while the g-factor for 3-decanol has almost none. Therefore, the values of E_a could be similar because the values average to approximately 43 kJ mol^{-1}.

---

[a]Note the abscissa for **Fig. 4.10** is $D_0 \times 10^4$ and in **Fig. 4.14** it is $D_0 \times 10^3$

4.7 Summary and Conclusion

Temperature-dependent self-diffusion coefficients and dielectric constants are compared for two protic solvent families: 1-alcohols and 3-alcohols. The temperature dependence of ε_s for these systems differs due to differences in their respective hydrogen bonding networks. The non-linear temperature dependence of ε_s for the 3-alcohol family is due to variations in the temperature dependence of the Kirkwood factor, $g\,\mu_0^2$, which are most likely caused by changes in the hydrogen bonding network for each member as a result of the interior location of the hydroxyl group.

The compensated Arrhenius formalism is applied to both 1- and 3-alcohol systems. The formation of a master curve from a plot of D_0 versus ε_s (**Fig. 4.10**, page 82) validates the primary assumption of the CAF; the temperature dependence of D_0 is due to the temperature dependence of ε_s, which could be due to $N(T)/T$ or both $N(T)/T$ and $g\,\mu_0^2$. A master curve results for the 1-alcohol family that is similar to the exponential-like master curves that have been previously reported when using the CAF with $N(T)/T$ or ε_s.[15–17,49,51,52] The master curve formed from the 3-alcohol diffusion coefficient data is different from the 1-alcohol master curve when scaling with ε_s, but it still validates the assumption of the CAF. For the higher temperatures (lower ε_s) and longer chain 3-alcohols the temperature dependence of $g\,\mu_0^2$ vanishes and the temperature dependence of ε_s becomes due solely to $N(T)/T$, as seen with aprotic systems.[56] Therefore, deviations of D_0 from the master curve (**Fig. 4.10**) are expected to occur at low temperatures and shorter alkyl chain length due to the increased non-linear temperature dependence of $g\,\mu_0^2$ as shown in **Fig. 4.7**. When the temperature dependence

of $g\,\mu_0^2$ is removed, *i.e.* the diffusion coefficients are scaled using just $N(T)/T$, the scatter in the master curve is not observed which supports the claim that the source of the scatter in **Fig. 4.10** is due to $g(T)\,\mu_0^2$. However, if the temperature range of this study were expanded to a larger range, say -10 – 150°C,[a] then more scatter would be observed in the master curves as $g(T)\,\mu_0^2$ would have more of a variation due to changes in hydrogen bonding in both 1- and 3-alcohol systems.

E_a values for both 1- and 3-alcohols ($\approx$ 42 kJ mol^{-1}) are higher than E_a values determined for the aprotic systems studied ($\approx$ 25 kJ mol^{-1}).[51] The increased association between molecules for the alcohol systems increases the energy needed to disrupt the intermolecular interactions so that transport can occur, whereas the aprotic systems are considered non-associated resulting in a lower E_a. It is unclear why the E_a values for both alcohol systems are similar to each other, given the apparent difference in their respective hydrogen bonding interactions. The E_a is an average value reflecting the energy barrier of the activated mechanism for the entire family, which suggests that the 1- and 3-alcohols have similar intermolecular interactions. The differences between the systems, namely the hydrogen bonding, can be seen in the vibrational spectra (**Fig. 4.4**, page 67) and the diffusion coefficients, which are higher for the 3-alcohols, shown in **Fig. 4.3** on page 65. The CAF explains this difference through the values of the exponential prefactor, D_0, which are greater for the 3-alcohols, seen in **Fig. 4.10**.

Glasstone et al. [81] use Eyring's model of thermally activated diffusion and viscosity to relate the exponential prefactor for diffusion and viscosity to an entropy of activation. The similarity in the CAF and the activated process models of Eyring could result

[a]That is also assuming that the melting and boiling points of the solvents fits within this range

from a similarity in the exponential prefactor being related to the entropy of activation. Petrowsky and Frech [52] have shown that the CAF can be applied to dielectric relaxation, suggesting that the properties governing self-diffusion also play a major role in the mechanism controlling dielectric relaxation.

Shinomiya [61] used Eyring's models for dielectric relaxation and viscosity to determine activation parameters for several linear-alcohol families with different locations of the hydroxyl group. The entropy of activation was found to increase for both relaxation and viscosity as the hydroxyl group moved to the center of the chain. The entropy of activation for dielectric relaxation increased from 41.2 to 117 J mol^{-1}K^{-1} for 1-octanol and 3-octanol, respectively, and for viscosity it increased from 18.4 to 49.4 J mol^{-1}K^{-1}.[61] Vij et al. [62] measured dielectric relaxation times and showed a similar increase for the entropy of activation from 31.8 to 129.7J mol^{-1}K^{-1} for 1-heptanol and 3-heptanol, respectively. Our results of an increased D_0 for the 3-alcohols are consistent with the observed increase of the entropy of activation for dielectric relaxation and viscosity.[61,62] The extended hydrogen-bonded structure in the 3-alcohols is less than that in the 1-alcohols[59] as shown in **Fig. 4.4** (page 67) which could correspond to an increased number of available states in the 3-alcohols, and therefore a larger value for the exponential prefactor, which would explain the higher diffusion coefficients values.

Changes in the hydrogen bonding with temperature in 3-hexanol are not the same as 3-decanol, which are consistent with the changes in the temperature dependence of the dielectric constant and $g\,\mu_0^2$ factor. This behavior yields a diffusion reference curve and master curve that do not follow the 1-alcohol and aprotic systems. We therefore conclude that when applying the CAF, care must be taken when selecting the members

of a solvent family. It is best that the temperature-dependent properties have a similar dependence on temperature for all members. If not, discrepancies may arise as shown with the 3-alcohol family. Regardless, the E_a and D_0 values calculated for the 3-alcohol solvent family do describe the temperature-dependent diffusion coefficient data, with deviations being due to the added temperature dependence contained in ε_s via $g\,\mu_0^2$.

Chapter 5

Concentration dependence of the molal conductivity and dielectric constant of TbaTf 3-alcohol electrolytes

5.1 Introduction
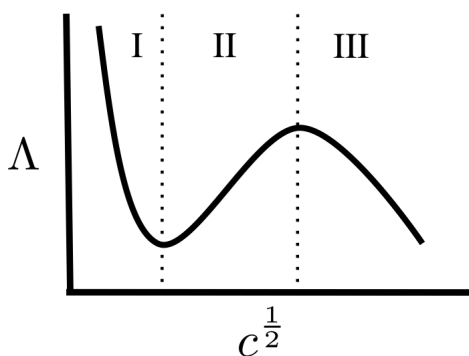
Figure 5.1: (Reprint of **Fig. 2.1**) Schematic of molal conductivity versus square root of the salt concentration depicting three different regions labelled I, II, & III for a low permittivity electrolyte.

The concentration dependence of the molal conductivity, Λ, is directly proportional to the sum of the ionic mobilities for TbaTf electrolytes, as shown in **eq. 2.5** on page 11. The increase in Λ with concentration (region II) is observed for solutions with a low dielectric constant ($\varepsilon_s \lesssim 10$), and illustrated by the schematic in **Fig. 5.1**. It was shown in Chapter 3 that for TbaTf 1-alcohol solutions, the increase in Λ in region II is due to the combined effect of the concentration dependence of the energy of activation, E_a, and the molal exponential prefactor, Λ_0 (defined as σ_0/c). The concentration dependence contained in σ_0 was determined to be primarily due to the concentration dependence of ε_s. There are then two contributions to the concentration dependence

in Λ_0: one contribution is from the dielectric constant, and the other is due directly to the concentration contained in the denominator, $i.e.$, $\Lambda_0 = \sigma_0(\varepsilon_s(c))/c$.

Solutions of TbaTf 3-alcohols also show region II behavior in Λ. The dielectric constant of the pure 3-alcohols, however, does not depend linearly on temperature as the 1-alcohol solvent family, as discussed in Chapter 4 (**Fig. 4.5**, page 69). Moving the hydroxyl group from the terminal carbon of the 1-alcohols to the third carbon in the 3-alcohols reduces the extent of hydrogen bonding, (**Fig. 4.4**, page 67) which affects the temperature dependence of ε_s. The difference in the behavior of ε_s with temperature for the 3-alcohols compared to the 1-alcohols had major effects on the results of the CAF for the temperature-dependent diffusion coefficients, as shown in **Fig. 4.10** (page 82). Given the differences observed in ε_s and $D(T)$, the results of the CAF for the temperature-dependent conductivities of TbaTf 3-alcohol solutions should yield different results than results for the 1-alcohol TbaTf solutions. The increase in region II, however, should still follow the conclusions reached in Chapter 3. It is the goal of this work to show:

- The increase of Λ with concentration in region II for TbaTf 3-alcohol solutions is due to two contributions: the concentration dependence of ε_s, which is contained in σ_0 and the concentration dependence of E_a.

- The addition of TbaTf to the 1- and 3-alcohols has a different effect on their respective hydrogen bonding networks, which plays a significant role in the concentration dependence of E_a and σ_0, and therefore the concentration dependence of Λ.

5.2 Concentration dependence of Λ in TbaTf 3-alcohol solutions

Fig. 5.2 shows Λ versus the square root of the concentration for TbaTf 3-hexanol solutions (top) and TbaTf 3-nonanol solutions (bottom) for 25, 45, and 65°C. The data are plotted against $c^{1/2}$ to better showcase the changes that occur at lower concentration. We make no claim of any quantitative relationship between Λ and $c^{1/2}$, but use it as a matter of convenience. The data for 3-hexanol show a distinct minimum at approximately 0.15 $m^{1/2}$ at 65°C. The minimum in Λ shifts to higher concentration as
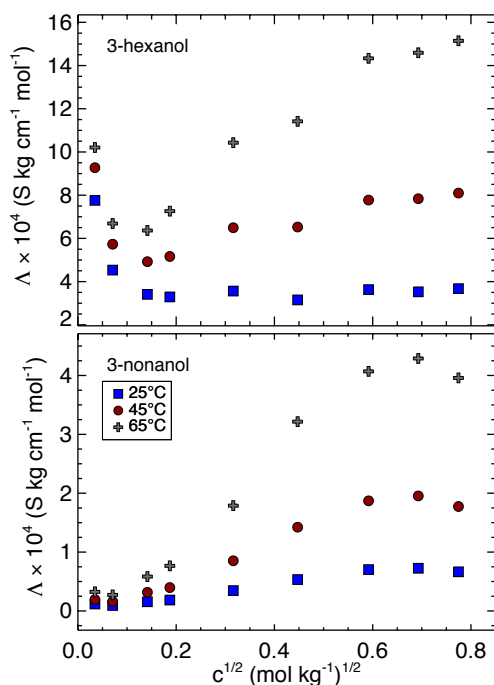
Figure 5.2: Molal conductivity versus square root of the concentration of TbaTf in 3-hexanol (top) and 3-nonanol (bottom) for 25, 45, and 65°C.
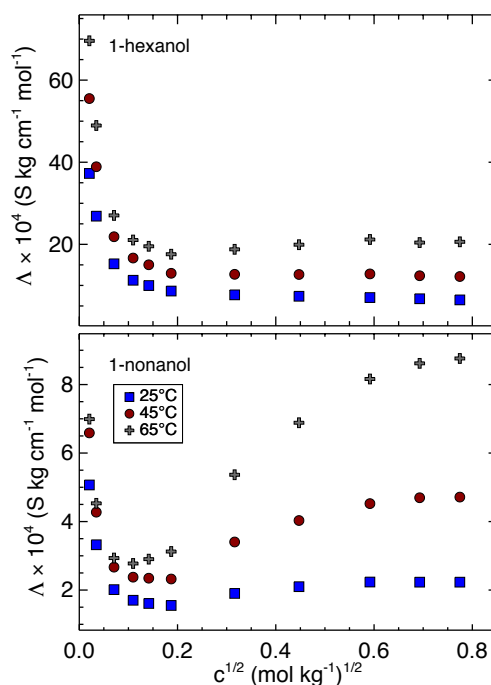
Figure 5.3: Molal conductivity versus square root of the concentration of TbaTf in 1-hexanol (top) and 1-nonanol (bottom) for 25, 45, and 65°C.

the temperature decreases. The increase in Λ in region II is more pronounced at higher temperatures. As the alkyl chain length of the 3-alcohols increases, the minimum in Λ shifts to lower concentration. The minimum of Λ for TbaTf 3-nonanol solutions is at the most dilute concentration measured. The maximum in Λ with concentration is also visible for the temperatures shown for TbaTf 3-nonanol solutions. For comparison, **Fig. 5.3** shows Λ versus $c^{1/2}$ for TbaTf 1-hexanol solutions (top) and 1-nonanol solutions (bottom) at the same temperatures as **Fig. 5.2**. The minimum of Λ also shifts to lower concentrations as the alkyl chain lengthens. The most pronounced difference between the 1-hexanol solutions and 1-nonanol solutions is that Λ does not increase with concentration in region II as much for the 1-hexanol, unlike the 3-alcohol solutions, which shows pronounced region II behavior for both 3-hexanol and 3-nonanol. At higher concentrations, Λ appears to level off for both 1-alcohol solutions at all temperatures.

The locations of the minimum and the maximum in Λ with $c^{1/2}$ change within the solvent family for both 1- and 3-alcohol solutions. The concentration dependence of the sum of the ionic mobilities is therefore also affected by the changes to the system properties that occur by the addition of a methylene group, *i.e.*, increasing the alkyl chain lowers ε_s and affects the sum of the ionic mobilities.

The behavior of Λ with concentration cannot be due to changes in ionic association as previously argued,[24,26,27] because TbaTf exists only as spectroscopically "free" ions as described in § 2.1.3 and § 3.1.1. **Fig.** 5.2 shows infrared vibrational spectra for the $\nu_s(\text{SO}_3)$ stretching region of the triflate anion for 0.48 m TbaTf 3-decanol at 35, 55, and 71°C. The spectrum for pure 3-decanol at 35°C is also given. It is clear by the presence
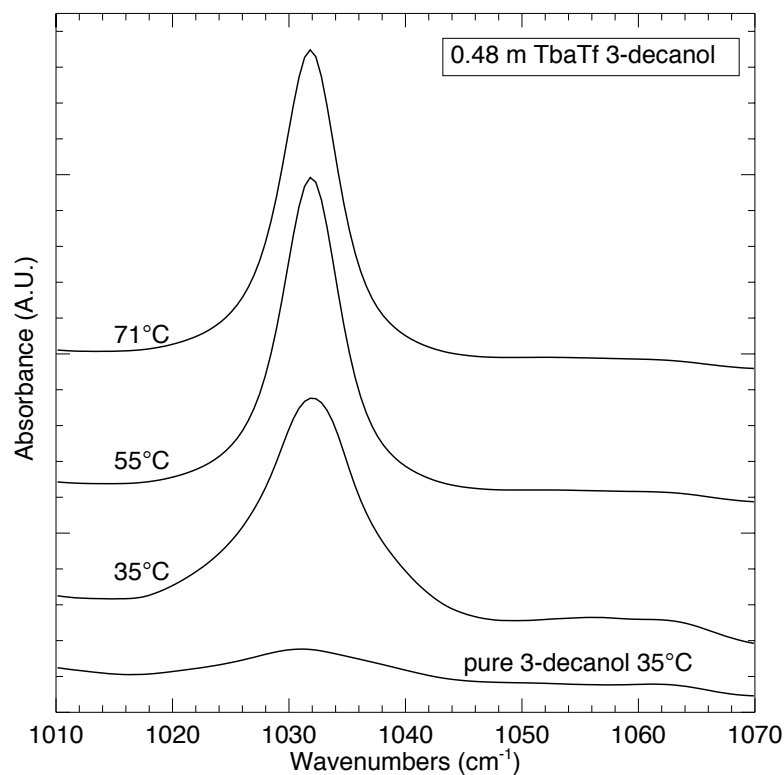
Figure 5.4: IR vibrational spectra for 0.48 m TbaTf 3-decanol at 35, 55, and 71°C, and pure 3-decanol at 35°C

of only a single band at 1032 cm^{-1} that only "free" ions of triflate exist and therefore no observable ionic association is occurring.[42] Ionic association is known to increase as the dielectric constant decreases.[8] The 3-decanol family member will have the lowest value of ε_s of the family. The dielectric constant also decreases as the temperature increases. Therefore, it can be assumed that if ionic association does not occur in 3-decanol at the 0.48 m TbaTf over the measured temperature range, it will not occur in a shorter alkyl chain family member or at lower concentrations over the same temperature range.

5.3 Concentration dependence of ε_s for TbaTf 3-alcohol solutions
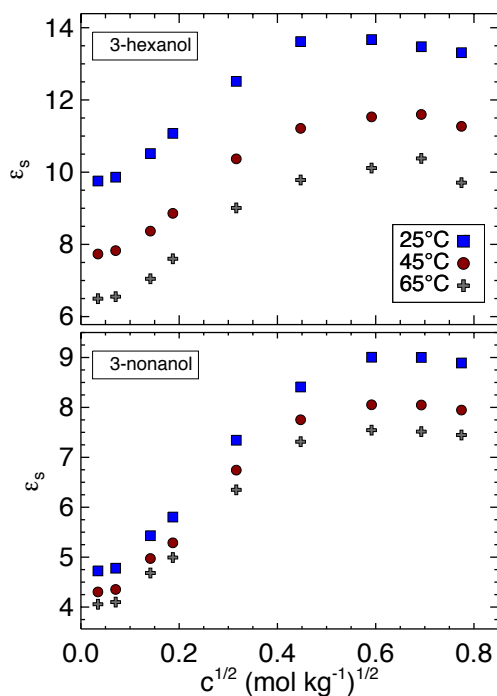
Figure 5.5: Dielectric constant versus square root of the concentration for TbaTf 3-hexanol (top) and TbaTf 3-nonanol (bottom) at 25, 45, and 65°C.
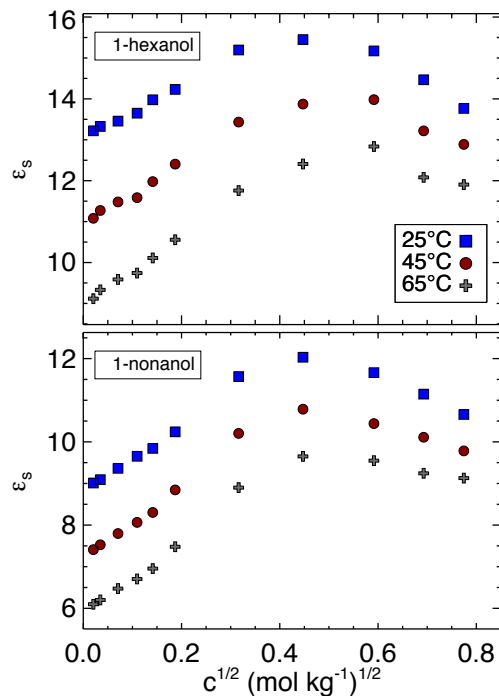
Figure 5.6: Dielectric constant versus square root of the concentration for TbaTf 3-hexanol (top) and TbaTf 3-nonanol (bottom) at 25, 45, and 65°C.

Changes in the dielectric constant are an excellent measure of changes in the intermolecular interactions. **Fig. 5.5** shows ε_s versus $c^{1/2}$ for 3-hexanol (top) and 3-nonanol (bottom) for 25, 45, and 65°C. As TbaTf is added to 3-hexanol the dielectric constant increases to a maximum and then begins to decrease. In the 3-nonanol solutions, ε_s appears to plateau at this maximum value for all three temperatures. The magnitude of ε_s is higher for 3-hexanol solutions than for the 3-nonanol solutions, which is consistent

with other solvent families studied; as the alkyl chain length increases, the value of the dielectric constant decreases. For comparison, **Fig. 5.6** shows the dielectric constant versus $c^{1/2}$ for TbaTf solutions of 1-hexanol (top) and 1-nonanol (bottom) at 25, 45, and 65°C. The dielectric constant for both 1-alcohol solutions follows a similar increase with increasing concentration, but reaches a maximum at a lower concentration than that of the 3-alcohol solutions, at approximately 0.45 m$^{1/2}$ compared to 0.65 m$^{1/2}$ TbaTf. After the maximum, ε_s decreases more for the 1-alcohol solutions than the 3-alcohol solutions. The differences in the concentration dependence of ε_s between the 1- and 3-alcohol solutions can be, in part, related to changes in the extent of association through the solutions, as will now be discussed.

5.4   Effect of TbaTf on hydrogen bonding in 1- and 3-alcohol solutions

In Chapter 4 (§ 4.3) it was shown that changes in the dielectric constant are, in part, associated with changes in the liquid structure, *i.e.*, changes in the hydrogen bonding. It is well known that the extent of hydrogen bonding is less in pure alcohol solvents with a hydroxyl group located on an interior carbon compared to a terminal carbon.[57,58,60,70,71] Adding TbaTf to pure 1-alcohol liquids disrupts the hydrogen bonding network differently than adding TbaTf to the 3-alcohol solvent families.

Fig. 5.7 shows infrared vibrational spectra of the $\nu(\text{OH})$ stretching region for pure and 0.48 m TbaTf 1-hexanol (top) and 3-hexanol (bottom) at 25°C. Adding TbaTf to 1-hexanol results in an increase in frequency of 21 cm^{-1}. A positive shift in frequency
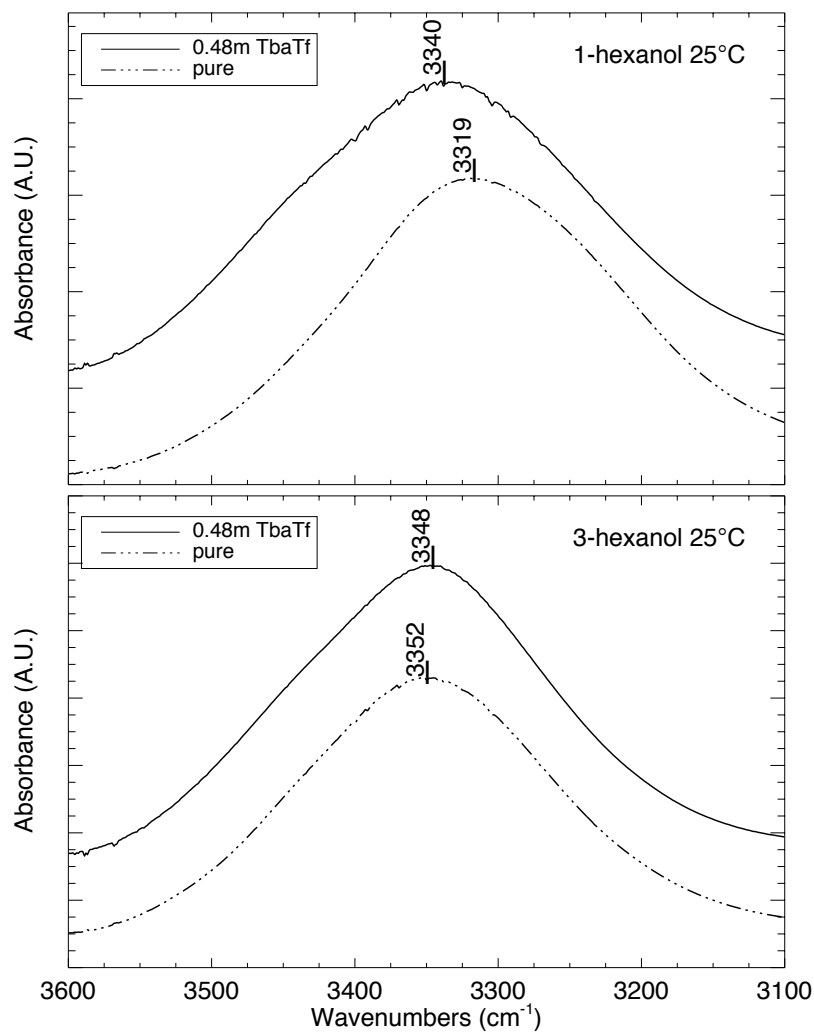
Figure 5.7: IR spectra of pure (dashed line) and 0.48 m (solid line) TbaTf 1-hexanol (top) and 3-hexanol (bottom) solutions at 25°C.

of $\nu(\text{OH})$ is attributed to a reduction of hydrogen bonding.[73] The concentrated 1-hexanol solution also shows an asymmetric broadening of the band at higher frequency compared to the pure solvent, which can be interpreted as an increase in a population of weaker hydrogen bonded species possibly due to the addition of salt. Adding TbaTf to 3-hexanol (lower plot) also shows this asymmetric broadening at higher frequency

(≈ 3450 cm^{-1}), however, the maximum of the ν(OH) band shows only a small decrease

of 4 cm^{-1}. Changes in hydrogen bonding are also seen when TbaTf is added to 1- and
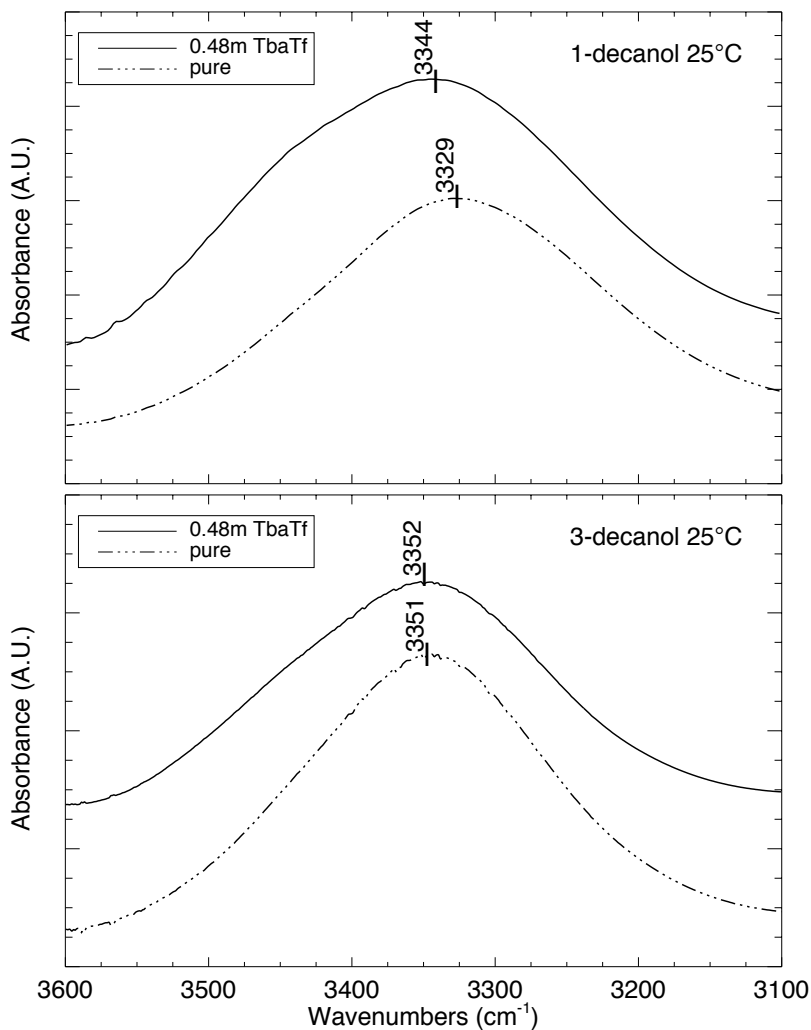
Figure 5.8: IR spectra of pure and 0.48 m TbaTf 1-decanol (top) and 3-decanol (bottom) solutions at 25°C.

3-decanol. **Fig. 5.8** is similar to **Fig. 5.7** showing the ν(OH) stretching region for pure

and 0.48 m TbaTf 1-decanol (top) and 3-decanol (bottom) solutions at 25°C. Adding

salt to pure 1-decanol increases the frequency of the band by 15 cm^{-1}. An asymmetric

broadening is also observed at higher frequency for concentrated 1-decanol, similar to the concentrated 1-hexanol in **Fig. 5.7**.

For comparison, **Table 5.1** gives the ν(OH) band frequencies shown in **Fig. 5.7** and **Fig. 5.8**. The difference between the ν(OH) bands of the pure 1-hexanol and 1-decanol solvents indicates that there is a reduction of the hydrogen bonding resulting from extending the alkyl chain. There is a negligible difference between the pure 3-hexanol and 3-decanol bands, suggesting that the shielding of the hydroxyl group alters the intermolecular interactions such that extending the alkyl chain has little effect on the hydrogen bonding. Adding TbaTf, however, affects the hydrogen bonding in the 1-alcohol solutions, but not the 3-alcohol solutions according to the spectra shown.

	ν(OH) (cm^{-1})	
solvent	pure	0.48 m TbaTf
1-hexanol	3319	3340
1-decanol	3329	3344
3-hexanol	3352	3348
3-decanol	3352	3352

Table 5.1: Summary of the frequencies of the dominant bands in the ν(OH) stretching region of the IR spectra of pure and 0.48 m TbaTf solutions of 1- and 3- hexanol and decanol given in **Fig. 5.7** and **Fig. 5.8**.

The bulky Tba^{+} cation can be considered charge protected[55,82] and therefore has a limited effect on the hydrogen bonding structure. Kay and Evans[7] speculate that larger monovalent anions can act as "structure-breakers" of the hydrogen bonding network of water. It is possible that the triflate anion is acting as a structure-breaker of the hydrogen bonded network of the 1-alcohols, but more data is required to make such a claim. The 3-alcohol solvents already have a reduced hydrogen bonding structure compared to the 1-alcohols due to the steric hinderance imposed by the interior loca-

tion of the hydroxyl group. This difference could reduce the effectiveness of the triflate anion acting as a structure-breaker in the 3-alcohols. The study by Kay and Evans [7], however, was based on changes in the Walden product and was thereby using hydrodynamic models to interpret their data. Regardless, the differences observed between the concentrated 1- and 3-alcohol IR spectra support the claim that the hydrogen bonding structure responds differently to the addition of salt in the two solvent families.

The difference in the shift of ν(OH) with the addition of TbaTf in 1- and 3-alcohol solvents is consistent with the differences observed in the concentration dependence of ε_s shown in **Fig. 5.5** and **Fig. 5.6**. At higher concentrations, ε_s decreases with concentration for the 1-alcohol solutions, whereas ε_s decreases almost negligibly in the 3-alcohol solutions. The decrease in ε_s with concentration indicates that the intermolecular interactions have changed to some degree. This is not the case for the higher concentration of the 3-alcohol solvents that show a negligible change both spectroscopically and in terms of ε_s.

The changes observed in the hydrogen bonding network for the 1- and 3-alcohol TbaTf solutions are by no means conclusive of how the hydrogen bonding affects either the conductivity or dielectric constant, but indicate that differences do exist between the two systems with the addition of salt. Temperature-dependent measurements of the ν(OH) frequency region should be compared to determine if the differences seen between the two systems can be related back to the dielectric constant, given there is a large difference in the temperature dependence of ε_s between the 1- and 3-alcohol TbaTf solutions. Further study into the effect of large symmetrical cations, and possible solvent-ion interactions of the anion in non-aqueous associated liquids is also needed.

In particular, use of the near infrared frequency regions would give valuable insight into the nature of the hydrogen bonding network by looking at overtone and combination bands.

5.5   Temperature dependence of ε_s in TbaTf 1- and 3-alcohol solutions

The location of the hydroxyl group in 1- and 3-alcohols plays a key role in determining the nature of the liquid structure. It also affects the temperature dependence of the dielectric constant, as previously discussed in § 4.4 on page 73 in terms of the Kirkwood-Frölich relation (**eq. 4.1**) of ε_s to $g\,\mu_0^2$. Adding salt also affects the temperature dependence of the dielectric constant of 1- and 3-alcohol solutions, but in different ways. **Fig. 5.9** compares temperature-dependent dielectric constants for three concentrations of TbaTf 1-hexanol and TbaTf 1-nonanol (left column) and TbaTf 3-hexanol and TbaTf 3-nonanol (right column). To aid in comparison, all of the scales of the ordinate are the same. The TbaTf 1-alcohol solutions all show a similar linear decrease with temperature. The increase of salt only shifts the magnitude of ε_s, but does not substantially affect the temperature dependence. The dielectric constants for the 3-alcohol solutions in **Fig. 5.9** (right) do not follow a linear trend with temperature. For the lowest concentration, the curvature of ε_s with temperature is more apparent for the 3-hexanol solution than the 3-nonanol solution. As the concentration increases, the magnitude of ε_s for both solutions increases, and the curvature for the 3-nonanol solutions becomes more pronounced.
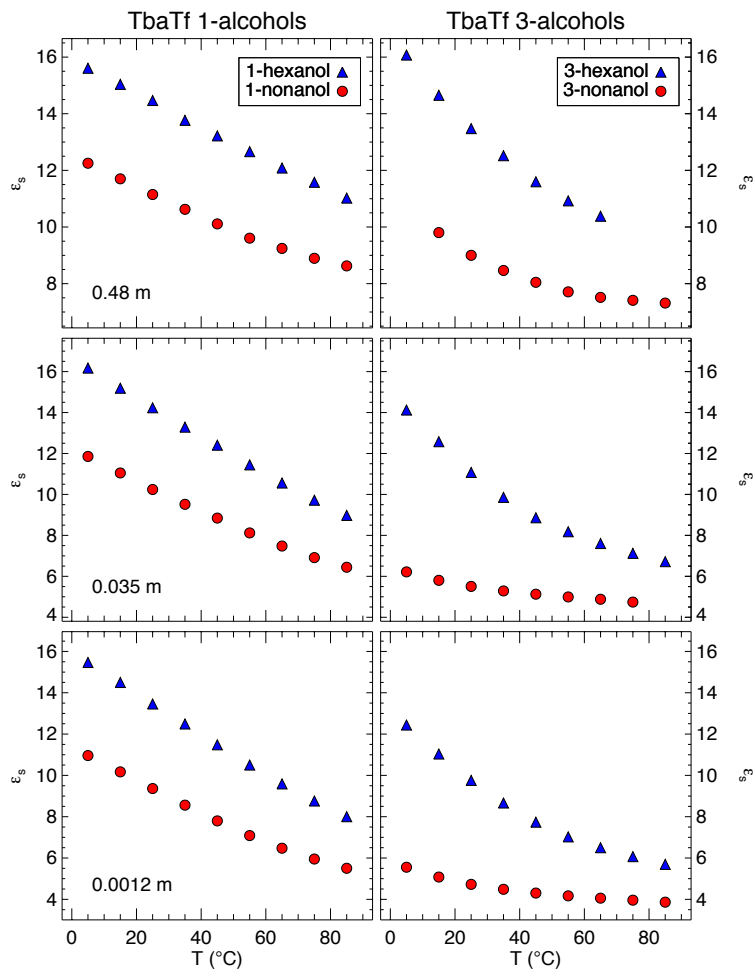
Figure 5.9: Dielectric constant versus temperature for 1-hexanol and 1-nonanol solutions (left) and 3-hexanol and 3-nonanol solutions (right) for 0.0012, 0.035, and 0.48 m TbaTf from $5 - 85°C$.

In § 4.4, the relationship between the non-linearity of ε_s and $g\,\mu_0^2$ with temperature of pure 3-alcohol solvents was discussed and compared to the linear behavior of ε_s and $g\,\mu_0^2$ of the 1-alcohol solvents. It was determined that an additional temperature dependence contained in the Kirkwood g-factor causes the temperature dependence of ε_s to differ within the 3-alcohol solvent family, *i.e.*, the slope of $g\,\mu_0^2$ with temperature are different for 3-hexanol and 3-nonanol. There is also a temperature dependence of

the g-factor in the 1-alcohol solvent family, however, this temperature dependence is collinear for all members of the 1-alcohol solvent family (*i.e.*, the slope of $g\,\mu_0^2$ with temperature is the same for all 1-alcohols members) resulting in no obvious difference between the temperature dependence of ε_s.

It is clear from the non-linear temperature dependence of ε_s that the additional temperature dependence due to $g\,\mu_0^2$ in the pure 3-alcohol solvent family members is still present in the electrolyte solutions, and may have a different concentration dependence than in the 1-alcohol solutions. Throughout this work, it has been stressed that the temperature dependence of the dielectric constant governs, to a large extent, the temperature dependence of the conductivity. The effect of introducing TbaTf on the temperature dependence of the conductivity will now be discussed.

5.6 Temperature dependence of σ in TbaTf 1- and 3-alcohol solutions

The dynamics of the pure 1-alcohol solvent family are different than the pure 3-alcohol solvent family as shown by the differences in the diffusion coefficients in **Fig. 4.3** on page 65. The diffusion coefficients for 3-alcohols are higher than the diffusion coefficients of the 1-alcohols. This is due, in part, to the reduced association (*i.e.*, the reduced hydrogen bonding network) of the 3-alcohols compared to the 1-alcohols. **Fig. 5.10** shows temperature-dependent conductivities for the same three concentrations as **Fig. 5.9** with the left column showing data for 1-hexanol and 1-nonanol TbaTf solutions, and the right column showing data for 3-hexanol and 3-nonanol TbaTf solu-
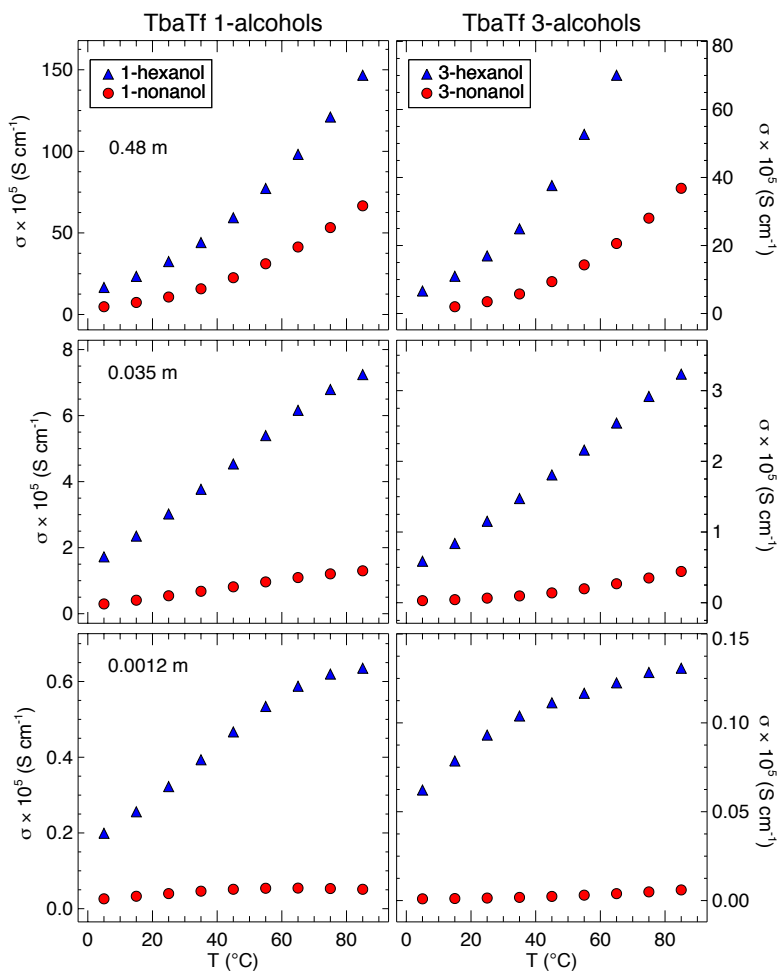
Figure 5.10: Conductivity versus temperature for 1-hexanol and 1-nonanol solutions (left) and 3-hexanol and 3-nonanol solutions (right) for 0.0012, 0.035, and 0.48 m TbaTf from $5 - 85°C$.

tions. The general behavior of σ with temperature is very similar for the two alcohol families. Note that the conductivity values are larger in magnitude (about double) for the 1-alcohol TbaTf solutions than the 3-alcohol solutions, unlike the diffusion coefficients. The 0.0012 m TbaTf solutions for both 1- and 3-alcohols show a similar dependence on temperature, with a slight curvature at higher temperatures occurring for 1- and 3-hexanol. The 0.0012 m TbaTf 3-nonanol solution does not exhibit the

convex shape at higher temperatures. As the concentration increases, the concavity of the conductivity curve shifts to a convex shape for the 1- and 3-hexanol and for the 1-nonanol solutions, while the 3-nonanol solution maintains its convex character with temperature. For both the 1- and 3-alcohol 0.48 m solutions, the temperature dependence of σ is more similar than for the lower concentrations.

The differences observed in the temperature dependence of the conductivity with concentration for the 1- and 3-alcohols can be explained, to a large extent, by differences seen in the energy of activation and exponential prefactor calculated from the CAF, which will be discussed in the following sections.

5.7 Applying the compensated Arrhenius formalism to the conductivity of TbaTf 3-alcohol solutions

5.7.1 CAF: E_a values of $\sigma(T)$

Following the procedure given in § 2.2, the CAF was applied to each 3-alcohol family member at each concentration. Due to the limited solubility and higher melting point of 3-decanol, it was not included in the 3-alcohol solvent family.[a]

Fig. 5.11 shows the simple Arrhenius equation (SAE, filled circles) and the CAE (open diamonds) plotted versus reciprocal temperature for four concentrations of TbaTf 3-hexanol. A similar plot is given for TbaTf 3-nonanol solutions in **Fig. 5.12**. The SAE plot of the 0.012 m TbaTf 3-hexanol shows the greatest deviation from linearity with an R^2 value of 0.920. The CAF corrects for this non-linearity as shown by the more linear

---

[a]For the 0.035 m TbaTf solutions, the difference of including 3-decanol and excluding it yielded no difference in the CAF E_a value.
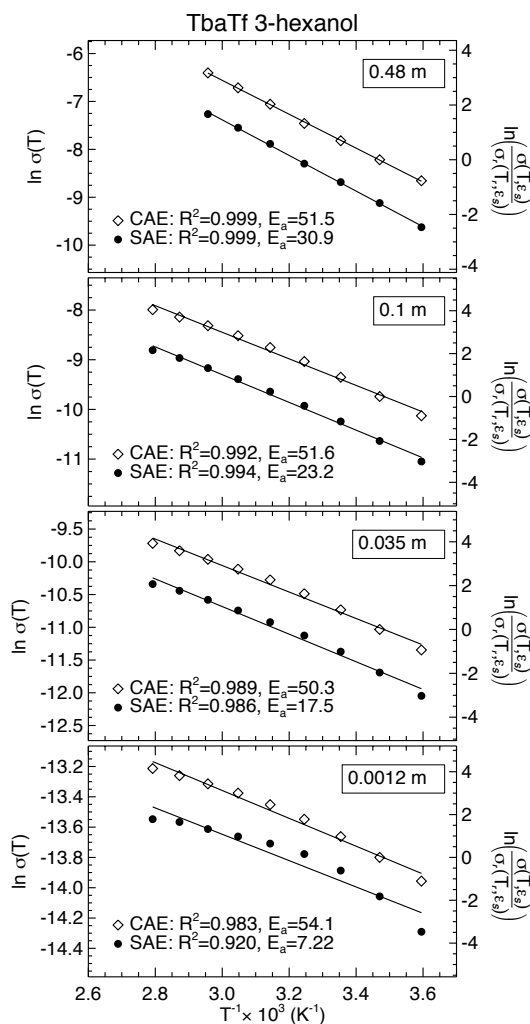
Figure 5.11: Simple Arrhenius plots (SAE, left axis, filled circles) and compensated Arrhenius plots (CAE, right axis, open diamonds) for four concentrations of TbaTf 3-hexanol. E_a values calculated from the corresponding model are given.
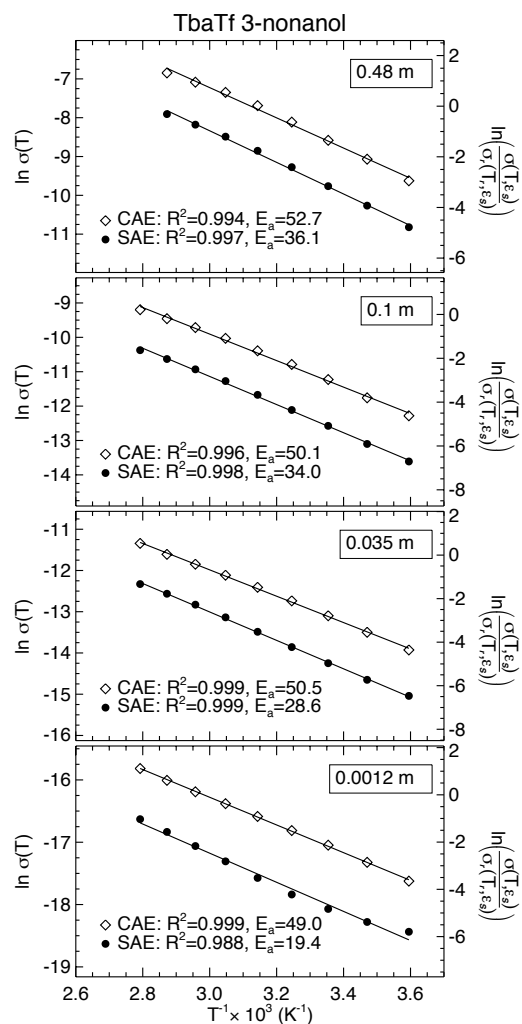
Figure 5.12: Simple Arrhenius plots (SAE, left axis, filled circles) and compensated Arrhenius plots (CAE, right axis, open diamonds) for four concentrations of TbaTf 3-nonanol. E_a values calculated from the corresponding model are given.

CAE plot of 0.0012 m TbaTf 3-hexanol with an increased R^2 value of 0.983. As the

concentration of TbaTf is increased, the CAE plots become more linear with reciprocal

temperature for the 3-hexanol solutions. CAE plots of other salt solutions are typically

more linear than those shown for the 3-hexanol solutions, with R^2 values of 0.99 or higher.[15,49,51,55] However, the non-linearity of the dielectric constant with temperature due to the additional temperature dependence within $g\,\mu_0^2$ of the pure solvent shown in **Fig. 4.7** on page 75 is most likely the cause for the deviation. This temperature dependence of $g\,\mu_0^2$ is dramatically reduced in pure 3-nonanol, and results in both a linear SAE and CAE plot at the lowest concentration (**Fig. 5.12**, lower plot).

As the concentration increases, both the SAE and CAE plots become more linear for the 3-hexanol solutions, as noted by the increasing R^2 values. The natural log of the conductivity and scaled conductivity for the 3-nonanol solutions maintain a linear trend with inverse temperature for all of the concentrations shown. The behavior of the other members of the 3-alcohol solvent family follow the trends seen with 3-nonanol at all concentrations for both the SAE and CAE plots.

The CAF was performed for each 3-alcohol family member at each concentration, and the resulting E_a values were averaged and are summarized in **Table 5.2**. For comparison, the average E_a for the corresponding concentration of TbaTf 1-alcohol solutions are also given in the table, and both 1- and 3-alcohol E_a values are plotted in **Fig. 5.13** versus concentration of TbaTf.

As the concentration of TbaTf increases, the E_a values for the 3-alcohol solutions decrease slightly and then increase slightly, covering a range of approximately 4 kJ mol^{-1}. The 1-alcohol TbaTf solutions, however, steadily decrease with increasing concentration by more than 10 kJ mol^{-1}, as discussed in § 3.4.1. Both 1- and 3-alcohol solutions show a very slight, but similar plateau in E_a at approximately $0.1 - 0.2$ m$^{1/2}$. This same concentration range is similar to the concentration range of the minimum

concentration m TbaTf (mol kg^{-1})	concentration$^{1/2}$ m$^{1/2}$ TbaTf (mol kg^{-1})$^{1/2}$	3-alcohols E_a (kJ mol^{-1})	1-alcohols E_a (kJ mol^{-1})
0.0012	0.03	51.5 ± 0.8	51.8 ± 0.5
0.005	0.07	51.0 ± 0.9	49.9 ± 0.3
0.02	0.14	50.5 ± 0.8	47.7 ± 0.4
0.035	0.19	50.7 ± 0.7	47.7 ± 0.2
0.1	0.32	51.4 ± 0.7	44.5 ± 0.2
0.2	0.45	51.3 ± 0.3	42.7 ± 0.3
0.35	0.59	52.5 ± 0.9	41.5 ± 0.1
0.48	0.69	52.3 ± 0.6	39.9 ± 0.2
0.6	0.77	53.7 ± 0.5	39.1 ± 0.1

Table 5.2: Average energies of activation for the 3-alcohol solvent family and 1-alcohol solvent family for concentrations of TbaTf calculated based on the CAF.
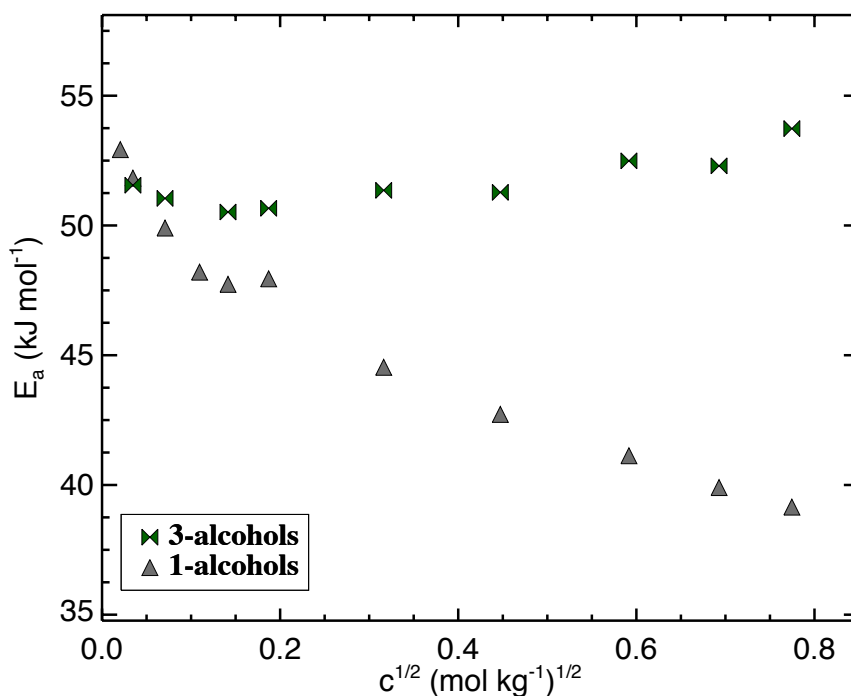
Figure 5.13: Average CAF E_a values for TbaTf 1-alcohol solutions (grey triangles) and TbaTf 3-alcohols solutions (green bow-ties). Data are given in **Table 5.2**.

observed in Λ for both solvent families. As the concentration increases, however, the two solvent families show very different behavior in E_a. The decrease of the E_a values for the 1-alcohol TbaTf solutions is large enough to be representative of physical

changes within the system. We speculate that the slight increase in E_a in the 3-alcohol solutions, however, is close to the error of the measurements and is possibly artificial. It is therefore concluded that, in comparison to the 1-alcohol solvent family, the E_a for the 3-alcohol solvent family is approximately independent of concentration.

5.7.2 CAF: Arrhenius versus non-Arrhenius behavior in TbaTf 3-alcohols

The 1-alcohol TbaTf solutions from § 3.4.1 in **Fig. 3.5** and **Fig. 3.6** on page 43 show non-linear behavior when the natural log of the conductivity is plotted against reciprocal temperature at low concentrations. As the concentration of TbaTf increases, the SAE plots become more linear. This trend is seen for each member of the 1-alcohol family. The 3-alcohol family members, however, do not show a similar trend. The non-linear SAE plots are seen with the short alkyl chain members (*e.g.*, 3-hexanol and 3-heptanol) but not for the longer chain 3-alcohol family members (**Fig. 5.11** and **Fig. 5.12**). The unscaled and scaled conductivities for the lowest concentration in **Fig. 5.12** have a linear dependence, whereas the lowest concentration in **Fig. 5.11** does not. This is because the curvature in a SAE plot originates from the temperature dependence contained in the exponential prefactor. This temperature dependence is due to the temperature dependence of ε_s, which is greater in 3-hexanol, and almost non-existent in 3-nonanol at the lower concentrations, as shown in **Fig. 5.9**. Therefore, the deviation from linearity for the SAE will be seen more for the 3-hexanol.

This is not the same for the 1-alcohol TbaTf solutions because the dependence of ε_s on temperature is collinear within the family. The same temperature dependence

of ε_s is seen in both 1-hexanol and 1-decanol (*i.e.*, the slope of ε_s with temperature is the same). As the alkyl chain is extended, the magnitude of ε_s decreases, but the temperature dependence remains the same. Therefore, the effect of the temperature dependence will be greater in 1-decanol which has a lower ε_s value, but maintains the same temperature dependence as 1-hexanol (same $\frac{\Delta\varepsilon_s}{\Delta T}$). This is why there is more curvature in the SAE plot for the 1-decanol compared to the 1-hexanol in **Fig. 3.5** and **Fig. 3.6** on page 43. Since the slope of ε_s with temperature changes from family member to family member in the TbaTf 3-alcohol solutions, a different degree of curvature is seen in the SAE plots for the lowest concentration solutions (**Fig. 5.11** and **Fig. 5.12**).

It is clear that there is a concentration dependence in the conductivity for both 1- and 3-alcohol systems. The dominant source of that concentration dependence, however, is different for the two systems. The concentration dependence of E_a in the 1-alcohol solutions is an obvious contributor to the increase in Λ with concentration. But the semi-constant E_a values with concentration for the TbaTf 3-alcohol solutions do not explain the increase Λ in region II (**Fig. 5.2**). To explain this increase, we must consider the concentration dependence of the exponential prefactor, σ_0, which is addressed in the next section.

5.7.3   CAF: exponential prefactor of $\sigma(T)$

The exponential prefactor, σ_0, is calculated by dividing $\sigma(T)$ by the Boltzmann factor, $\exp[-E_a/RT]$ using the average E_a calculated via the CAF, as discussed in detail in § 2.2.5. First, **Fig. 5.14** shows the isothermal conductivities for three concentrations of TbaTf 3-alcohol solutions plotted versus the isothermal dielectric constants. The
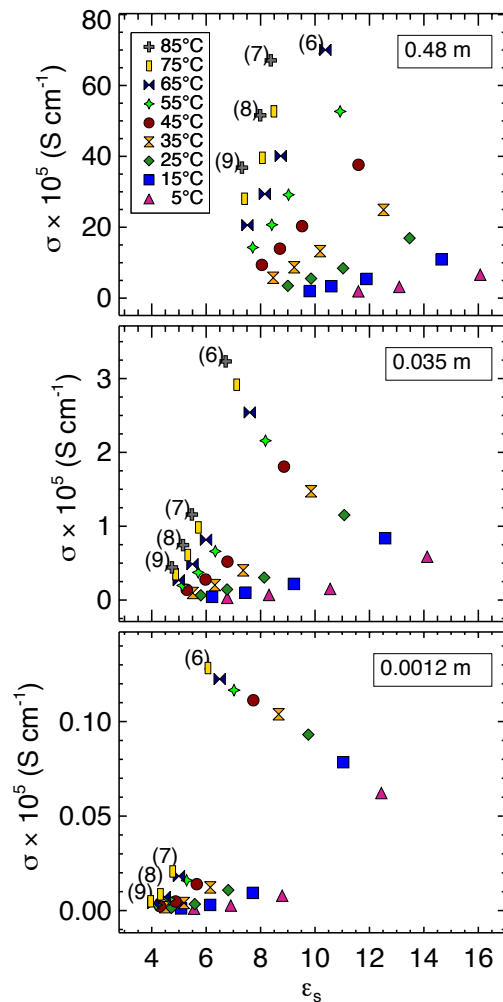
Figure 5.14: Isothermal conductivities versus dielectric constant for TbaTf solutions of 3-hexanol (6) 3-heptanol (7), 3-octanol (8), and 3-nonanol (9) from 5 – 85°C at 0.48 m (top) 0.035 m (middle) and 0.0012 m (bottom).
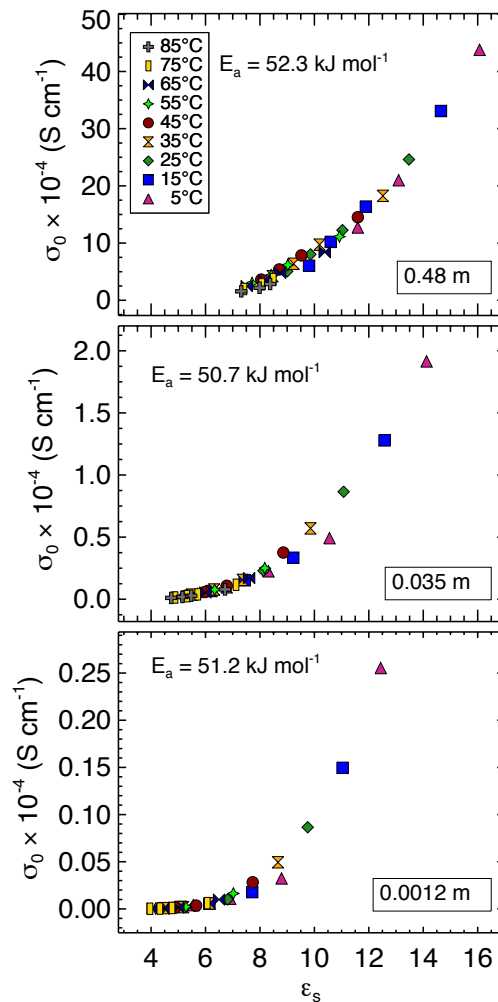
Figure 5.15: Conductivity exponential prefactors versus dielectric constant for the data in **Fig. 5.14**. Average CAF E_a are given in the figure.

isothermal conductivities separate into distinct temperature-dependent curves representing the individual 3-alcohol family members. The curves are labelled according to the number of carbons in their alkyl chain, *e.g.*, (6) represents 3-hexanol, *etc.* The obvious offset of the 3-hexanol temperature-dependent conductivity data in the lower plot

is due to the increased difference in the dielectric constant with temperature compared to the longer alkyl chain members as previously discussed in section § 5.5. This offset is reduced as the concentration increases, following the trend of both the temperature-dependent dielectric constant and temperature-dependent conductivity in **Fig. 5.9** and **Fig. 5.10**, respectively. As the concentration increases, the qualitative behavior of both properties with temperature become more similar.

The values of σ in **Fig. 5.14** are divided by the Boltzmann factor using the average E_a, and the resulting exponential prefactor is plotted versus dielectric constant in **Fig. 5.15**. The σ_0 values fall on a single master curve for all concentrations of TbaTf. The formation of a master curve validates the assumption that the temperature dependence of σ_0 is due to the temperature dependence of the dielectric constant. As the salt concentration increases, the range of σ_0 increases by two orders of magnitude over the concentration range covered. This concentration dependence will be discussed in more detail in the next section.

The exponential prefactors for the diffusion coefficients of the pure 3-alcohol solutions showed deviations from the master curve at lower temperatures (**Fig. 4.10** on page 82). As explained in § 4.5.2, this was due to the additional temperature dependence of $g\,\mu_0^2$, which was larger for the short-chain members and smaller for the long-chain members. The conductivity exponential prefactors, however, do not show these deviations, which suggests that the addition of salt alters the additional temperature dependence in $g\,\mu_0^2$. The value of the g-factor has been attributed to association in the liquid structure.[78] The addition of salt affects the temperature dependence of $g\,\mu_0^2$, as can be seen in the differences in the temperature dependence of the dielectric constant,

but the extent of the effect is unknown and is not discernible from the data presented here. Temperature-dependent density measurements of the concentrated solutions must be taken in order to better address this observation.

Another striking difference between the conductivity and diffusion coefficients of the 3-alcohol solvent family is the behavior of the diffusion master curves in **Fig. 4.10** on page 82 compared to the conductivity master curves in **Fig. 5.15**. The master curve created from the diffusion coefficient exponential prefactors follows a different functional form than the master curves created using the conductivity exponential prefactors. This is due to the nature of the reference curves, which are the isothermal diffusion or conductivity data plotted versus the dielectric constant as discussed in § 2.2.2. The conductivity reference curves, shown in **Fig. 5.14** follow the same exponential functional form shown for the 1-alcohol solvent family, as well as the conductivity reference curves seen for every system that has been analyzed with the CAF,[15–17,49–51] whereas, the diffusion reference curves follow an asymptotic function. The origin of the functional dependence of the reference diffusion coefficients and master curves for the pure 3-alcohol solvent family is unclear. The addition of TbaTf changes the behavior of the reference curves and master curves for conductivity of the 3-alcohols to the behavior of a "normal" solvent family, for lack of a better term. The extreme difference in the temperature dependence of $g\,\mu_0^2$ within the 3-alcohol solvent family, coupled with changes in the liquid structure upon the introduction of salt, could be the source of the differences observed, but further study is necessary to validate this claim. In particular, measuring the temperature dependence of the dipole density over a range of concentrations would give insight into the nature of the temperature dependence of $g\,\mu_0^2$ with concentration.

5.8 Concentration dependence of the molal exponential prefactor and Boltzmann factor

As previously discussed in § 3.6, the concentration dependence of the conductivity stems from two contributions: the concentration dependence in E_a and the concentration dependence in σ_0. Relating these concentration contributions to the behavior of Λ with concentration (*i.e.*, region II behavior) requires consideration of the molal exponential prefactor, Λ_0. It is calculated by dividing the exponential prefactor by the total salt concentration, σ_0/c. As described in § 3.6, and reprinted here in **eq. 5.1**, Λ has multiple concentration contributions.

$$\Lambda(T, c) = \left(\frac{\sigma_0(\varepsilon_s(T, c))}{c} \right) \exp\left[\frac{-E_a(c)}{RT} \right]. \tag{5.1}$$

The increase in Λ with concentration is seen for systems with a dielectric constant that is relatively low ($\epsilon_s \lesssim 10$). As shown in **Fig. 5.2** and **Fig. 5.3**, both 1- and 3-alcohol TbaTf solutions fall into this category. The increase in Λ in region II, however, is different for 1-alcohol solutions than 3-alcohol solutions. **Fig. 5.16** compares Λ, Λ_0, and the Boltzmann factor, $\exp[E_a/RT]$, for 1-octanol TbaTf solutions (left) and 3-octanol TbaTf solutions (right) at 5, 45, and 85°C. Note the scales on the ordinate for Λ for 1- and 3-octanol are not the same, whereas to aid in comparison the scales for Λ_0 are the same as are the scales for $\exp[-E_a/RT]$.

The minimum in Λ is more pronounced for the 1-octanol solutions than the 3-octanol solutions, but the increase in region II follows qualitatively similar behavior. The mini-
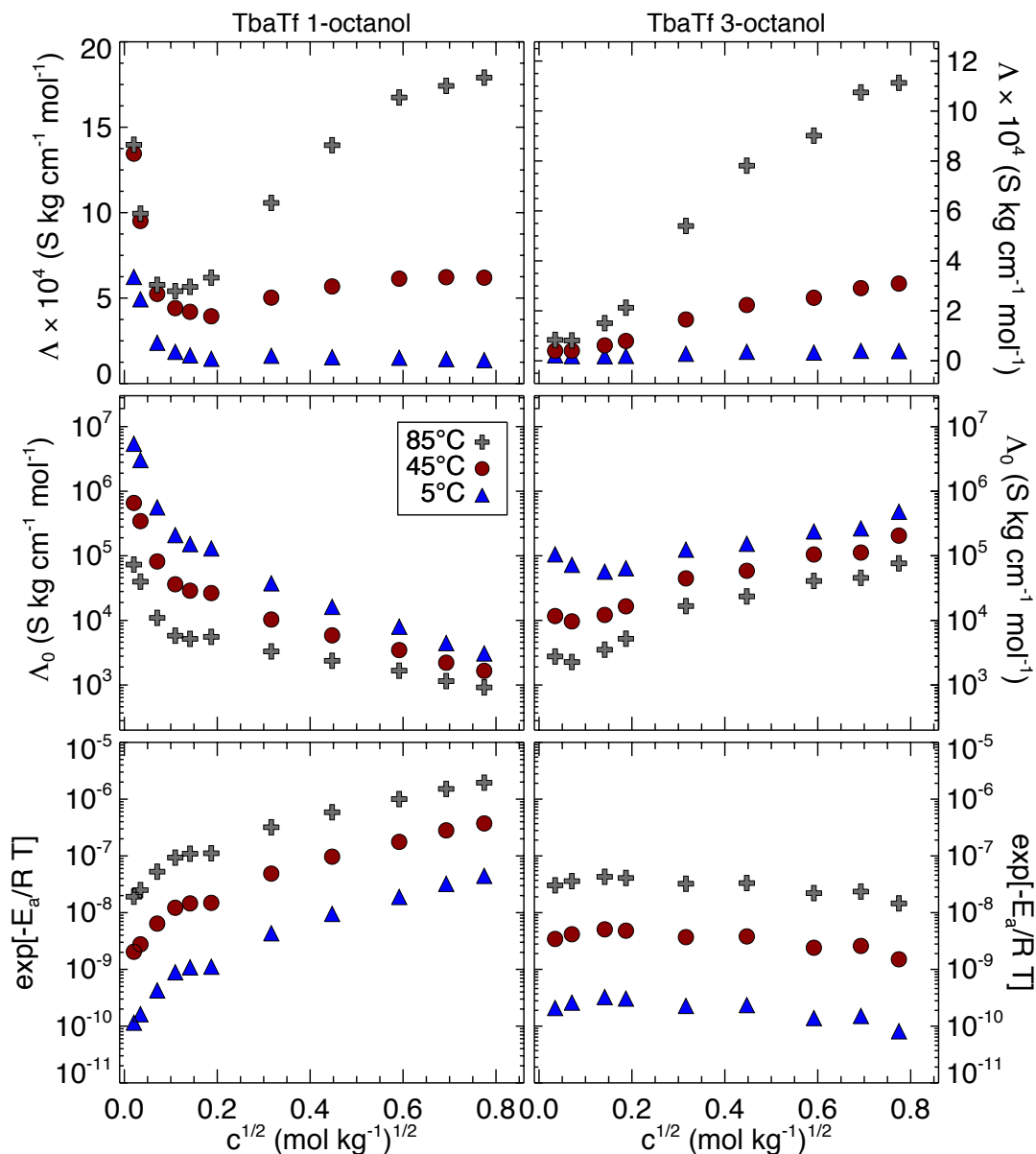
Figure 5.16: (Top) Molal conductivity, (middle) molal exponential prefactor, and (bottom) Boltzmann factor versus concentration for 1-octanol TbaTf solutions (left) and 3-octanol TbaTf solutions (right) at 5, 45, and 85°C.

mum in Λ for 3-octanol may occur at or below the lowest concentration measured. The

minimum was observed for the 3-hexanol TbaTf solutions, as shown in **Fig. 5.2**, but

not for the 3-nonanol solutions, which coincides with the trend that the minimum shifts to lower concentrations as the dielectric constant decreases.

The primary concern of this comparison, however, is the increase in Λ in region II. As previously discussed in § 3.6, the increase in region II for 1-octanol is due to the combined effect of the decrease in E_a and the decrease in Λ_0 with increasing concentration. The minimum of Λ occurs in the range of concentrations that exhibit a short-lived concentration independence.

The increase in region II for 3-octanol, on the other hand, is driven primarily by an *increase* in Λ_0 with concentration. The values of Λ_0 at low concentration show a minimum that coincides with the minimum observed in Λ. The increase in Λ_0 spans almost two orders of magnitude for the highest temperature, corresponding to a greater increase in Λ with concentration than the lower temperatures. The E_a values are relatively constant with concentration (**Table 5.2**) which is shown by the Boltzmann factor in the lower right plot of **Fig. 5.16**. The dominant variation in the Boltzmann factor is due to the temperature dependence contained in the denominator of the exponent, which also enhances the behavior of Λ with concentration at the higher temperatures.

The 3-alcohol solvent family members are associating liquids, but not to the extent as the 1-alcohol solvent family. Adding salt does not spectroscopically affect the association in the 3-alcohol solutions as it does in the 1-alcohol solutions, based on the minimal shifts in the $\nu(\text{OH})$ stretching frequency shown in **Fig. 5.7** and **Fig. 5.8**. If the E_a values represent the energy needed to relax the local structure such that charge transport can occur, then the local environment of the solvent-solvent interactions of a dilute 3-alcohol solution would be similar to that of a concentrated 3-alcohol solution. The relatively

constant E_a could therefore be an indication that adding TbaTf to 3-alcohols does not affect any extended hydrogen bonding structure that might exist. The decrease in E_a seen in the 1-alcohol solutions would then be a result of the reduction in the extent of association that occurs at high concentrations. This picture is probably only valid for charge protected cations that do not strongly coordinate to the heteroatom or other anions. If a strongly coordinating cation were involved, there would probably need to be an additional concentration dependent component contained in E_a to represent the stronger ion-solvent interactions as well as the added ion-ion interactions which TbaTf does not have.

§ 4.7 expressed the possibility that the differences between the diffusion exponential prefactors for pure 1- and 3-alcohols could be due to differences in the entropy of activation. Entropies of activation from dielectric relaxation data and viscosity data were found to be much higher for the 3-alcohol solvents than the 1-alcohol solvents.[61,62] If the diffusion prefactor is related to the entropy of activation of the system then the conductivity prefactor may also be related to the entropy of activation of the system. This is reasonable since it has been shown that the prefactors for diffusion and conductivity are related through their respective dependence on the dielectric constant.[82] The larger values for Λ_0 for the 3-alcohol solutions compared to the 1-alcohol solutions are consistent with this claim. An increase in the entropy of activation of the system would correspond to a larger number of system states being accessible for the transition state. Defining what constitutes a system "state" for the 3-alcohol solutions is not possible with the data presented here. Further study of the concentration dependence of Λ_0 is necessary. In particular, changing the cation and anion in systems that show a shift in

the ν(OH) infrared stretching frequency could rule out if an entropic increase is due to the effect of such a large cation or is inherent to the limited association of the 3-alcohols.

5.9 Summary and Conclusion

The molal conductivity for 1- and 3-alcohol solutions show a similar concentration dependent behavior but the source of the concentration dependence is very different. The 1-alcohol solutions show the increase in region II from a combination of a decreasing molal prefactor *and* a decreasing E_a. The 3-alcohol solutions, however, have a relatively constant E_a but an increasing molal exponential prefactor. **Eq. 5.2** simplifies the concentration dependent components contained in **eq. 5.1** to two concentration dependent terms:

$$\Lambda(T, c, \varepsilon_s) = \Lambda_0(\varepsilon_s(T, c), c)e^{\frac{-E_a(c)}{RT}} \quad (5.2)$$

Extending this to the sum of the ionic mobilties yields:

$$\Lambda(T, c, \varepsilon_s) = \Lambda_0(\varepsilon_s(T, c), c)e^{\frac{-E_a(c)}{RT}} = F\left(\mu_{Tba^+} + \mu_{Tf^-}\right). \quad (5.3)$$

It is well known that the sum of the ionic mobilities has both a concentration and a temperature dependence. Therefore, the source of the concentration and temperature dependence of the sum of the ionic mobilities can be related to the concentration and temperature dependence of the dielectric constant and E_a through the assumptions made by the CAF:

$$\Lambda(T, c, \varepsilon_s) = \Lambda_0(\varepsilon_s(T, c), c)e^{\frac{-E_a(c)}{RT}} = F\left[\mu_{Tba^+}(c, T) + \mu_{Tf^-}(c, T)\right]. \quad (5.4)$$

where the mobilities have a concentration dependence that originates in the concentration dependence of E_a, and ε_s, and a temperature dependence that originates in the Boltzmann factor and ε_s. The qualitative behavior of ε_s with concentration is similar for both 1- and 3-alcohol TbaTf solutions at low concentrations but different at higher concentrations, as compared in **Fig. 5.5** and **Fig. 5.6**. The 1-alcohol solutions show ε_s to decrease at higher concentrations, whereas the 3-alcohol solutions show constant behavior with increasing concentration at the higher concentrations. The differences in the concentration dependence of the E_a, however, are observed at even the most dilute solutions, which implies that there is a more subtle difference in the concentration dependence of ε_s than is evident from the qualitative behavior at low concentrations. Given that the concentration dependent term on the right hand side of **eq. 5.4** is shared between the mobility of both the cation and the anion suggests that the concentration dependences of E_a and ε_s are not separable. The concentration dependence of the sum of the mobilities, therefore, reflects the complex relationship between the dielectric constant and changes in the intermolecular interactions and the liquid structure, both of which are made more complicated by the presence, however slight, of hydrogen bonding.

Chapter 6

Concentration dependence of molal conductivity and dielectric constant for TbaTf 2-ketone electrolytes

6.1 Introduction

Chapters 3 and 5 used the CAF to describe the unusual behavior of the molal conductivity with concentration (*i.e.*, the increase in Λ defined as region II). It was determined that the increase is due to two concentration dependent contributions: the concentration dependence of the molal exponential prefactor, $\Lambda_0(\varepsilon_s(c), c)$,[a] and the concentration dependence of the energy of activation, $E_a(c)$; as illustrated in **eq. 6.1**.

$$\Lambda(T, c) = \Lambda_0(\varepsilon_s(T, c), c) \, \exp\left[\frac{-E_a(c)}{RT}\right]. \qquad (6.1)$$

For simple monovalent electrolyte systems, which is the case for all systems presented throughout this work, **eq. 6.1** can be related to the sum of the ionic mobilities of the cation and anion as described in § 2.1.1 and given in **eq. 6.2**. Furthermore, the relationship between Λ and the mobilities can be extended to include a temperature and concentration dependence on the right hand side of the equation as described in § 5.9.

$$\Lambda(T, c) = \Lambda_0(\varepsilon_s(T, c)) \, \exp\left[\frac{-E_a(c)}{RT}\right] = F\left[\mu_+(T, c) + \mu_-(T, c)\right]. \qquad (6.2)$$

---

[a]Where $\Lambda_0 = \sigma_0(\varepsilon_s(T, c))/c$, with part of the concentration dependence being due to the dielectric constant.

The systems studied in Chapters 3 and 5 (TbaTf 1- and 3-alcohol solutions), however, exhibit an extended hydrogen bonding structure that complicates the interpretation of the results. For the 1-alcohol solutions, both the E_a and Λ_0 decreased with increasing concentration. In the 3-alcohol solutions Λ_0 increased with concentration, while the E_a remained relatively constant. The differences observed were attributed to the differences in the hydrogen bonding structure with the addition of salt, and therefore no conclusive relationship could be made between the inherent concentration dependences of Λ_0 and E_a and the sum of the ionic mobilities.

A more straightforward investigation into the increase in Λ with concentration is afforded by the use of the 2-ketone solvent family. The 2-ketone solvent family is a non-associating solvent family, unlike the solvent families studied in the previous chapters, and the members cover a dielectric constant range that offers a unique opportunity in which to investigate region II behavior. It is well known that the increase of Λ in region II is observed for solutions with a low dielectric constant, ($\varepsilon_s \lesssim 10$). The members of the 2-ketone family used here extend above and below this approximate dielectric constant cutoff. A direct comparison can then be made between solvents with the same functional group that show region II behavior to those that do not show region II behavior. **Fig. 6.1** shows Λ versus square root of the concentration of TbaTf for 2-heptanone (top), 2-decanone (middle), and 2-tridecanone (bottom) at 35 and 75°C. The behavior of Λ with concentration for 2-heptanone is consistent with solvents that have a high dielectric constant; only a decrease in Λ is observed for all temperatures measured. The 2-decanone Λ data show region II behavior (Λ increases after the minimum is reached) at 75°C, but not at 35°C. The data for 2-tridecanone show distinct region
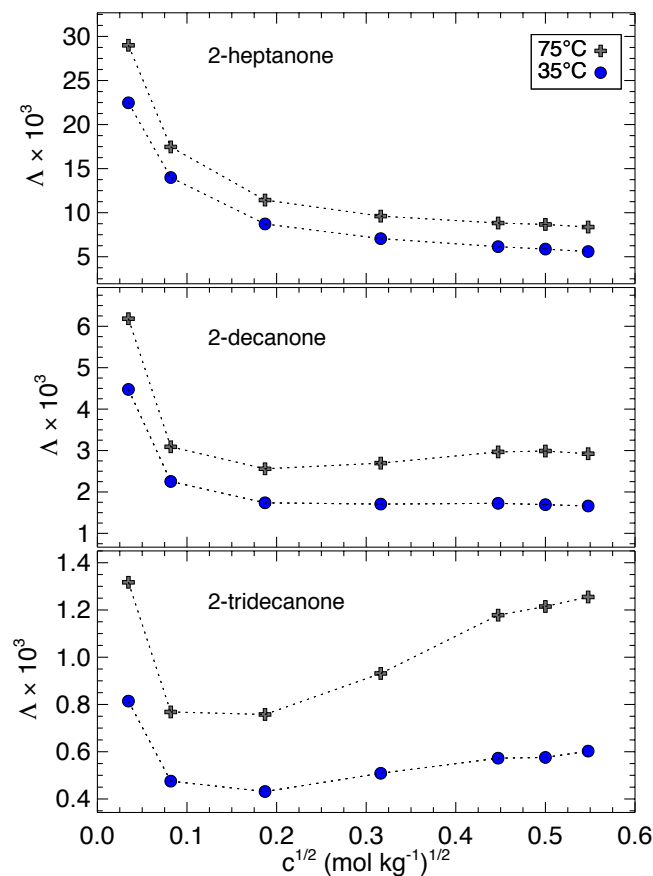
Figure 6.1: Molal conductivity versus square root of the concentration of TbaTf for 2-heptanone (top) 2-decanone (middle) and 2-tridecanone (bottom) for 35 and 75°C. Units for Λ are S kg cm^{-1} mol^{-1}. Dashed lines are drawn as a guide to the eye.

II behavior for all temperatures measured. Previous arguments for the behavior of Λ with concentration include changes in ionic association, which were discussed in detail previously (§ 2.1.1, page 10). These arguments are made invalid by selecting TbaTf as the salt which inhibits the formation of contact ion pairs, as discussed in §2.1.3

The 2-ketone solvents offer valuable insight in describing the concentration dependence of Λ, *i.e.*, the increase of Λ with concentration in region II. For clarity, the members of the 2-ketone family are divided into two groups: Group I includes 2-ketone

members that do not exhibit region II behavior (2-heptanone, 2-octanone, 2-nonanone, 2-decanone) and Group II includes 2-ketone members that exhibit region II behavior (2-decanone, 2-undecanone, 2-dodecanone, and 2-tridecanone). 2-decanone is included in both groups because it shows both behaviors, as demonstrated in **Fig. 6.1**. The CAF is applied to the temperature-dependent conductivities of TbaTf Group I 2-ketone solutions and TbaTf Group II 2-ketone solutions that cover a broad concentration range. The E_a and molal prefactors are determined for each group and compared. To establish a baseline for comparison of the pure solvents, the CAF is also applied to temperature-dependent self diffusion coefficients for both groups.

The work presented in this chapter will show:

- The concentration dependence of the dielectric constant plays an integral part in describing Λ with concentration. However, the magnitude of the dielectric constant is a poor criterion for predicting region II behavior in Λ, which has been used previously throughout the literature.[8,10,29,39,50] Rather, it is the concentration dependence of ε_s that dictates the behavior of region II.

- The concentration dependence of Λ, namely the increase in region II, is a complicated relationship between the concentration dependence of E_a and the concentration dependence of ε_s and can not be separated into individual components.

6.2   Concentration dependence of the dielectric constant

An indicator that the increase in Λ with concentration in region II will be observed has been the magnitude of the dielectric constant; solutions with values below approx-

imately 10 show the behavior, and solutions with values above 10 do not show the behavior.[8,10,29,39,50] The dielectric constant, however, has a concentration dependence that will either increase or decrease with concentration depending on the nature of both the salt and solvent used. It has been shown that for solvents with high dielectric constants, most notably aqueous solutions, the dielectric constant decreases with increasing salt concentration.[32,33] For solvents with lower dielectric constants, the dielectric constant increases with concentration to a maximum and then decreases.[35,38] A more detailed discussion of the concentration dependence of ε_s is given in § 2.1.2 on page 14.

The values of ε_s of the TbaTf 2-ketone solutions presented here all follow a similar concentration dependence. **Fig. 6.2** shows the concentration dependence of dielectric constant for 2-heptanone (top), 2-decanone (middle) for 15, 35, 55, and 75°C and 2-tridecanone (bottom) for 35, 55, and 75°C. The dielectric constant displays two trends with concentration as shown in **Fig. 6.2**: an increase with salt concentration (longer chain members) or an increase to a maximum and then a decrease as shown for 2-heptanone. This maximum is also seen in 2-octanone and 2-nonanone at higher temperatures (data not shown). As the alkyl-chain length increases, this maximum in dielectric constant is not seen in 2-decanone or 2-tridecanone. It is possible that the maximum exists at concentrations higher than those studied here, however, 0.3 m is the highest concentration attainable for the 2-tridecanone solution due to the solubility limit with TbaTf.[a] The introduction of salt at such high concentrations has a different effect on the dielectric constant for the short-chain ketones compared to the long-chain

---

[a]A concentration of 0.48 m TbaTf was attempted using 2-tridecanone, but the salt would not dissolve
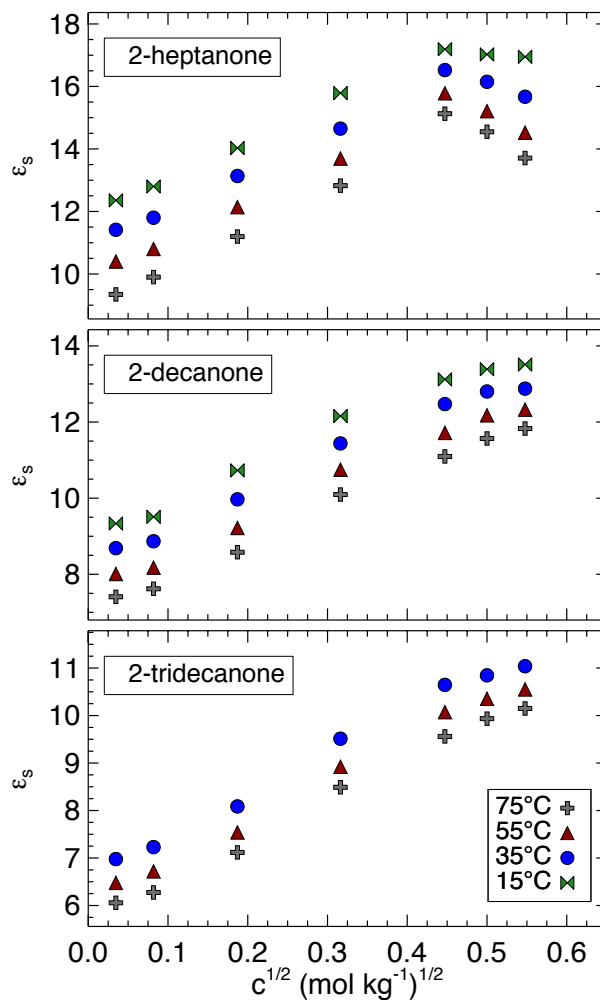
Figure 6.2: Dielectric constant versus concentration of TbaTf for 2-heptanone (top) 2-decanone (middle) and 2-tridecanone (bottom) for 15, 35, 55, and 75°C.

ketones. For the concentration range covered in this study, the Group I ketones display a maximum in the dielectric constant versus concentration curve for the lower temperatures and Group II ketones do not show a maximum in the dielectric constant with concentration.

The relationship between observing region II behavior and the absolute value of the dielectric constant is not as straightforward as a single value determining region II be-

havior. The 75°C values of ε_s in **Fig. 6.2** show that the 2-heptanone solutions span a range of approximately 9 – 15, but do not demonstrate region II behavior in **Fig. 6.1**, even though the solutions have a value of ε_s below 10 at low concentrations. The values of ε_s for 2-decanone at 75°C span a range of approximately 7 – 11.5 and does demonstrate region II behavior in **Fig. 6.1**. An interesting note is that the initial increase of ε_s with concentration is observed from 0.025 to 0.45 $m^{1/2}$ for both 2-heptanone and 2-decanone at 75°C. This concentration range corresponds to the concentration range for 2-decanone that region II is observed in **Fig. 6.1**. It is, of course, not observed for 2-heptanone. Upon comparison of the molal conductivity data of **Fig. 6.1** and the dielectric constant data in **Fig. 6.2**, it is not possible to identify a single correlation between the concentration dependence of ε_s and the onset of region II behavior. Therefore, the CAF is applied to the temperature dependent molal conductivity for both groups to determine the concentration dependence of the energy of activation and the molal exponential prefactor.

6.3 Applying the compensated Arrhenius formalism to the conductivity of TbaTf 2-ketone solutions

6.3.1 CAF: E_a values of $\Lambda(T)$

The CAF is applied to the temperature-dependent molal conductivity of each member of Group I and Group II at each concentration. Here, the CAF is applied directly to $\Lambda(T)$, rather than the specific conductivity, $\sigma(T)$, as described in § 2.2. Employing Λ rather than σ results in no difference in the values of E_a, but the comparison of the

concentration dependence of Λ to Λ_0 is made more straightforward. The modified CAE is

$$\ln\left(\frac{\Lambda(T)}{\Lambda_r(T_r)}\right) = \frac{-E_a}{RT} + \frac{E_a}{RT_r},\tag{6.3}$$

where Λ_r is the reference molal conductivity, T_r is the reference temperature, and E_a is the energy of activation. **Fig. 6.3** shows the isothermal molal conductivities versus dielectric constant for 0.0067 m (left) and 0.25 m (right) TbaTf 2-heptanone through 2-tridecanone from $5 - 85°$C, and is used in the scaling procedure for the CAF. The isothermal curves separate into the individual temperature-dependent Λ curves for each family members, labelled according the the number of carbons in the alkyl chain. The isothermal reference molal conductivity curves for both concentrations shown have a similar exponential growth functional form, *e.g.*, the $65°$C Λ_r curves (black bow-ties) in both plots have the same functional form. There is no obvious disconnect between the members of Group I and the members of Group II. The Λ values for the 0.25 m solutions are higher than the values for 0.0067 m solutions. The dielectric constant changes less with temperature at the higher concentrations, which results in higher slopes of the temperature-dependent molal conductivity curves at higher concentrations.

CAE plots are given in **Fig. 6.4** for the temperature-dependent molal conductivities for three concentrations of TbaTf in 2-octanone[a] (open diamonds) and 2-dodecanone[b] (filled circles). The E_a calculated for the specific 2-ketone is given in the figure. The CAE plots in **Fig. 6.4** all show a linear dependence with inverse temperature, as ex-

---

[a]The Λ reference curves used in the scaling procedure are composed of only Group I members; 2-heptanone through 2-decanone.

[b]The Λ reference curves used in the scaling procedure are composed of only Group II members; 2-decanone through 2-tridecanone.
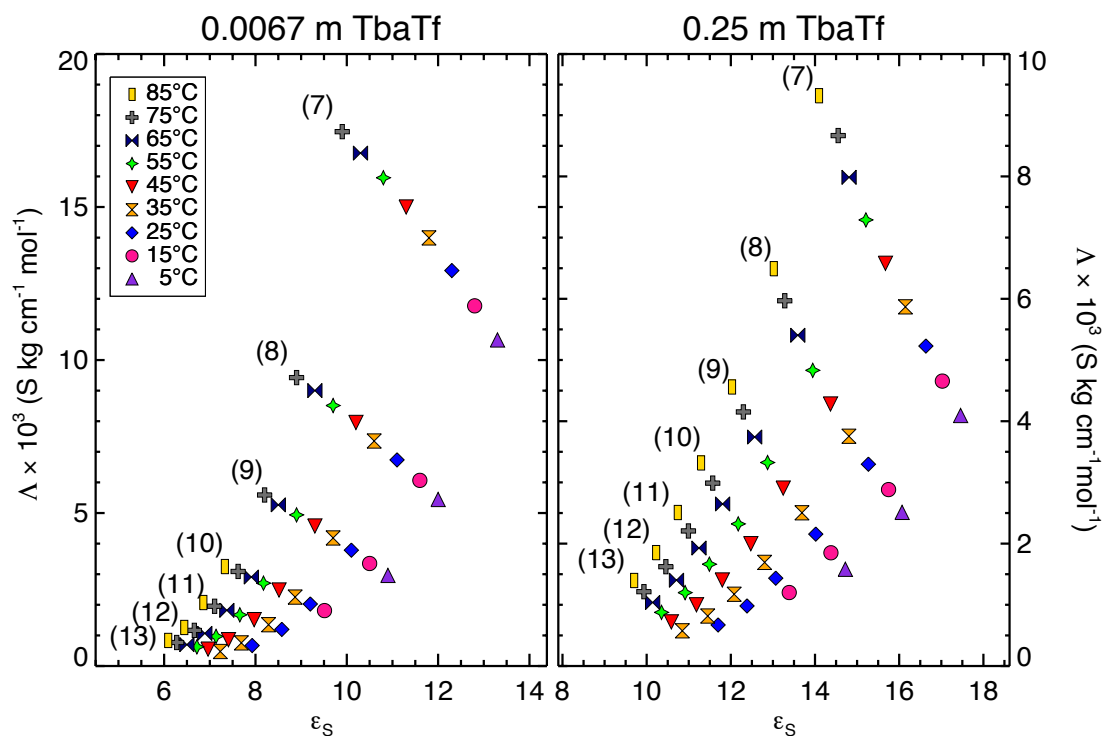
Figure 6.3: Isothermal conductivity *vs.* dielectric constant for 2-heptanone (7), 2-octanone (8), 2-nonanone (9), 2-decanone (10), 2-undecanone (11), 2-dodecanone (12), and 2-tridecanone (13) from 5 – 85°C for 0.0067 m TbaTf (left) and 0.25 m TbaTf (right).

pected from previous results of the scaling procedure. Comparing 2-octanone to 2-dodecanone within each concentration shows that there is an obvious difference in the slope of the line and consequently the E_a value, as indicated in the plots. These data suggest that the E_a depends on salt concentration for both Group I and Group II. To examine this apparent trend more carefully, the CAF was also applied to each 2-ketone family member using all members (2-heptanone through 2-tridecanone) in the scaling procedure, *i.e.* combining Group I and Group II and labeling this group as "All". The resulting E_a values are averaged and tabulated in **Table 6.1** according to whether the
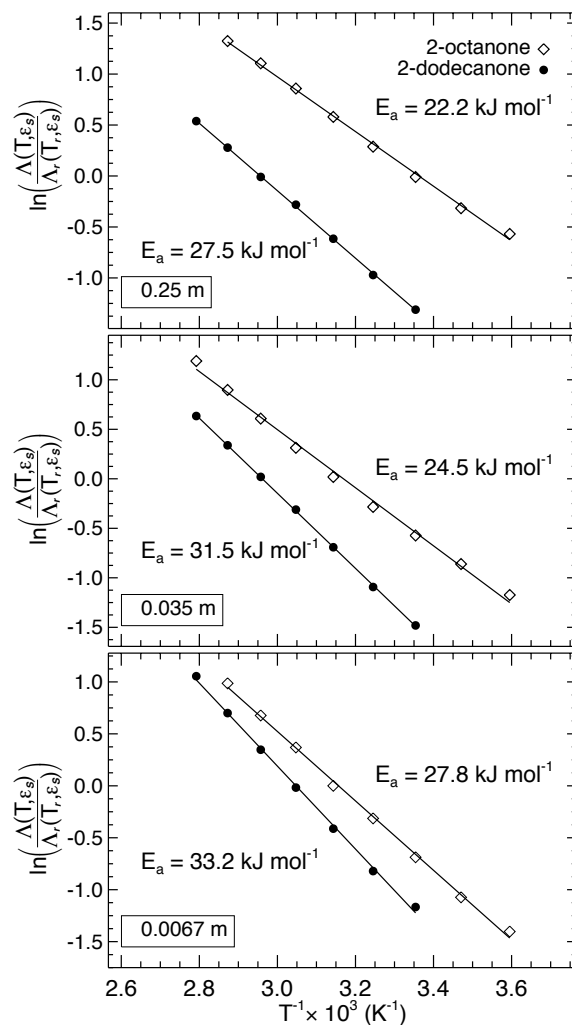
Figure 6.4: Compensated Arrhenius plots for molal conductivity of 2-octanone (open diamonds) and 2-dodecanone (filled circles) for 0.25 m (top), 0.035 m (middle) and 0.0067 m (bottom) TbaTf concentrations.

member belongs to Group I, Group II, or "All". The average E_a values of the two groups show a different concentration dependence, as evident in **eq. 6.1**. The "All" group also shows a concentration dependence that is similar to Group I. To better illustrate the differences between the concentration dependence of the E_a between the three groups, **Fig. 6.5** plots the values together for Group I (red circles), Group II (blue diamonds)

and Group "All" (grey crosses).

	Group I	**Group II**	**All**
TbaTf	E_a	E_a	E_a
(mol kg^{-1})	(kJ mol^{-1})	(kJ mol^{-1})	(kJ mol^{-1})
0.0012	28.7 ± 0.9	35.7 ± 0.6	30.0 ± 0.3
0.0067	27.5 ± 0.3	34.1 ± 0.3	29.7 ± 0.2
0.035	24.6 ± 0.3	30.2 ± 0.2	27.6 ± 0.2
0.1	22.3 ± 0.2	30.5 ± 0.2	25.6 ± 0.2
0.2	21.2 ± 0.2	30.2 ± 0.2	22.9 ± 0.2
0.25	22.1 ± 0.2	27.8 ± 0.2	24.1 ± 0.1
0.3	24.7 ± 0.2	26.2 ± 0.5	25.5 ± 0.2

Table 6.1: Average energies of activation for Group I 2-ketones (2-heptanone – 2-decanone), Group II 2-ketones (2-decanone – 2-tridecanone), and "All" 2-ketones for concentrations of TbaTf calculated based on the CAF. Data are plotted versus concentration in **Fig. 6.5**
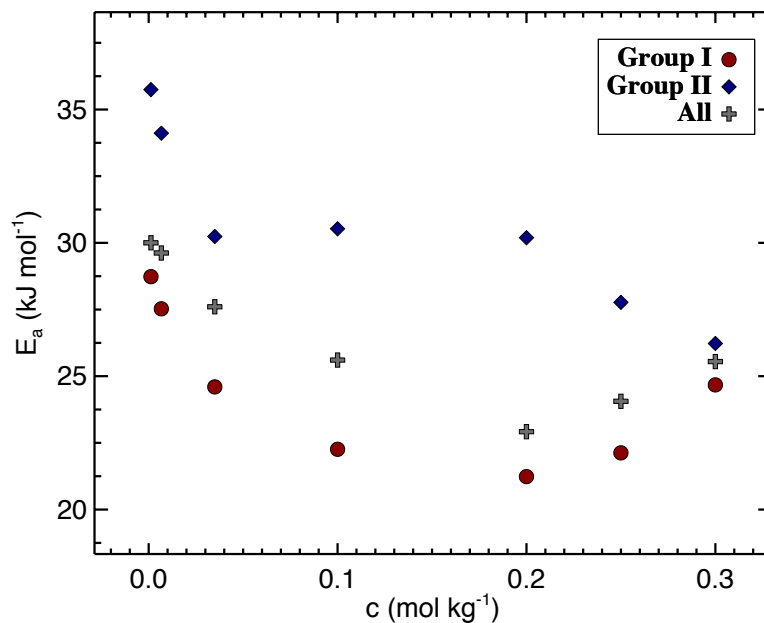
Figure 6.5: Compensated Arrhenius plots for conductivity for 2-octanone (open diamonds) and 2-dodecanone (filled circles) for 0.25 m (top), 0.035 m (middle) and 0.0067 m (bottom) TbaTf concentrations.

The E_a values calculated from the CAF show a different concentration dependent behavior for each of the two groups. For Group I, the E_a values are lower at the most

dilute concentration, approximately 7 kJ mol^{-1}. As the concentration increases, Group I E_a values decrease to a minimum and then increase. The values for Group II initially decrease, but level off from 0.035 - 0.2 m, and then decrease again. The trend in E_a with concentration for the group containing all members follows more closely the trend of Group I E_a values. This is due to the nature of the scaling procedure, in particular, the use of the reference conductivity curve to cancel out the exponential prefactor. The reference conductivity curve is constructed by a plot of the isothermal conductivity versus dielectric constant from each family member. The functional form of the curve follows an exponential growth function, with the short chain members making up the larger values of both the dielectric constant and the conductivity. These values are more heavily weighted in their contribution to the reference curve. Consequently, the concentration dependence inherently contained in the shorter members will shift the average values of the E_a towards the dependence followed by Group I, as shown in **Fig. 6.5**.

It can, therefore, be assumed that the differences observed between the E_a values for Group I and Group II are representative of differences in the concentration dependent behaviors of the two groups. If not, then both Groups would exhibit the same concentration dependent behavior as the values for the group containing all members. This idea will be further explored with the diffusion coefficients in § 6.5.

6.3.2 CAF: exponential prefactor of $\Lambda(T)$

Once the average E_a is calculated, the exponential prefactor, Λ_0, can be calculated by dividing $\Lambda(T)$ by the Boltzmann factor, exp[-E_a/RT], as explained in § 2.2.5. A

plot of Λ_0 versus ε_s (**Fig. 6.6**) results in a master curve for both Group I and Group II for all concentrations measured, as well as the group containing "all" members. The formation of a master curve supports the primary assumption of the CAF: the temperature dependence of the exponential prefactor is due to the temperature dependence of the dielectric constant. For all three groups here, this assumption is true. However, the extent that the scaling procedure compensates for the temperature dependence of ε_s varies among the groups. The result is a series of E_a values that are not equivalent. The difference observed in the E_a values for each group can be seen in the master curves formed in **Fig. 6.6**, and the E_a values are listed in **Table 6.1**.

There is a definite concentration dependence in the master curves for all three groups, in that the magnitude of Λ_0 decreases with increasing concentration. The dielectric constant range also varies for the three groups, as expected from **Fig. 6.2**. The functional form of the master curve for the group containing all members, however, follows more closely the trend for the Group I members, than Group II members. This is due to the nature of the scaling procedure previously discussed regarding the similarity of the E_a values between Group I and Group "All". Again, if there were no difference between the concentration dependence of the Group I members and Group II members, then the master curves would overlap from having equivalent E_a values. This is not the case, which suggests that there are physical differences in the concentration dependences of charge transport for both groups and they should be treated separately.
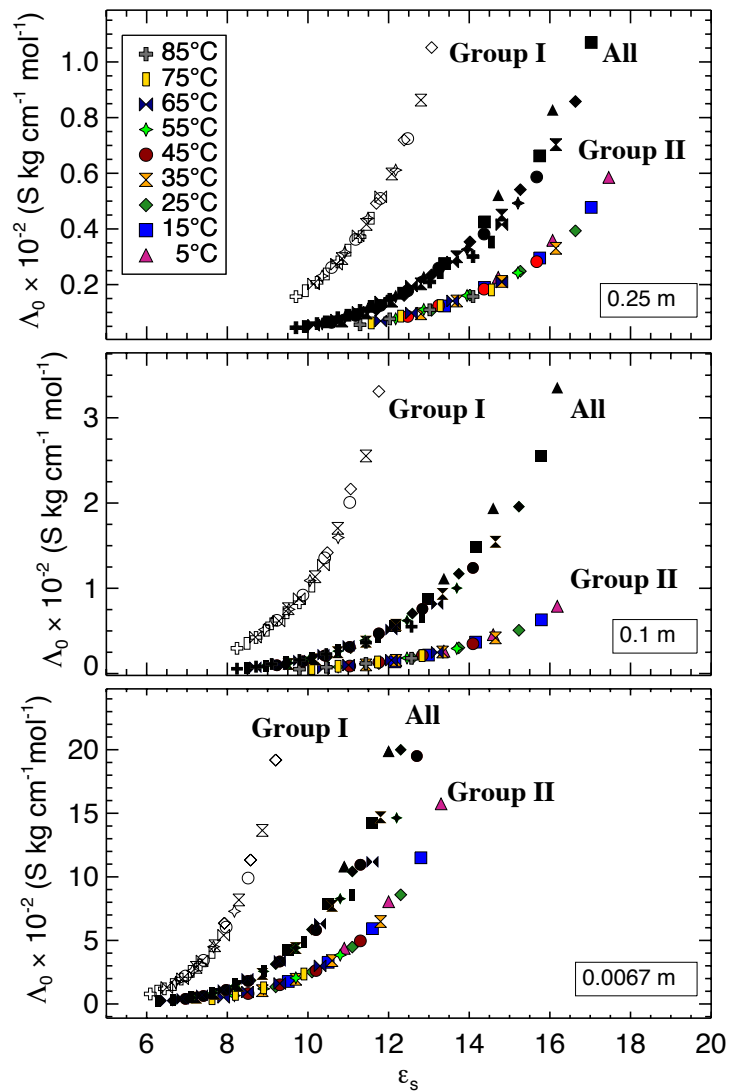
Figure 6.6: Molal exponential prefactors versus dielectric constants for three concentrations of TbaTf: Group I 2-ketones (black, open symbols), Group II 2-ketones (colored, filled symbols), and "All" members (black, filled symbols). The symbols correspond to the temperatures as shown. Average E_a values used to calculate Λ_0 can be found in table **Table 6.1**

6.4 Concentration dependence of the molal exponential prefactor and Boltzmann factor

To better compare the differences in the concentration dependent behaviors of Group I and Group II, **Fig. 6.7** plots the molal exponential prefactor (top) and Boltzmann factor (bottom) versus $c^{1/2}$ for 2-octanone and 2-dodecanone at 15, 55, and 75°C. To aid in the comparison between the two groups, the ordinates for Λ_0 are the same, as are the ordinates for $\exp[-E_a/RT]$.

The concentration dependence of the molal exponential prefactors and Boltzmann terms for 2-octanone are representative of Group I members, and likewise the 2-dodecanone data are representative of Group II members. The molal exponential prefactor for Group I members show a gradual decrease with concentration until 0.2 m and then an increase. The Boltzmann factors show the opposite behavior; the values increase gradually with concentration until approximately 0.45 $m^{1/2}$ and then decrease. The initial decrease of Λ_0 for Group II, however, is more sharp and decreases until approximately 0.19 $m^{1/2}$, which corresponds to the concentration region that the minimum in Λ is observed. From 0.19 to 0.45 $m^{1/2}$, Λ_0 increases slightly with concentration. This concentration range corresponds to the increase seen in Λ (region II). Across this same concentration range, Λ_0 is decreasing for Group I, which corresponds to the decrease observed in Λ (**Fig. 6.1**). From 0.45 to 0.54 $m^{1/2}$, the values of Λ_0 for Group II decrease, while Group I shows the opposite behavior. The Boltzmann factor also shows marked differences with concentration between the two groups.

Comparing the concentration dependent behavior of Λ between Group I and Group
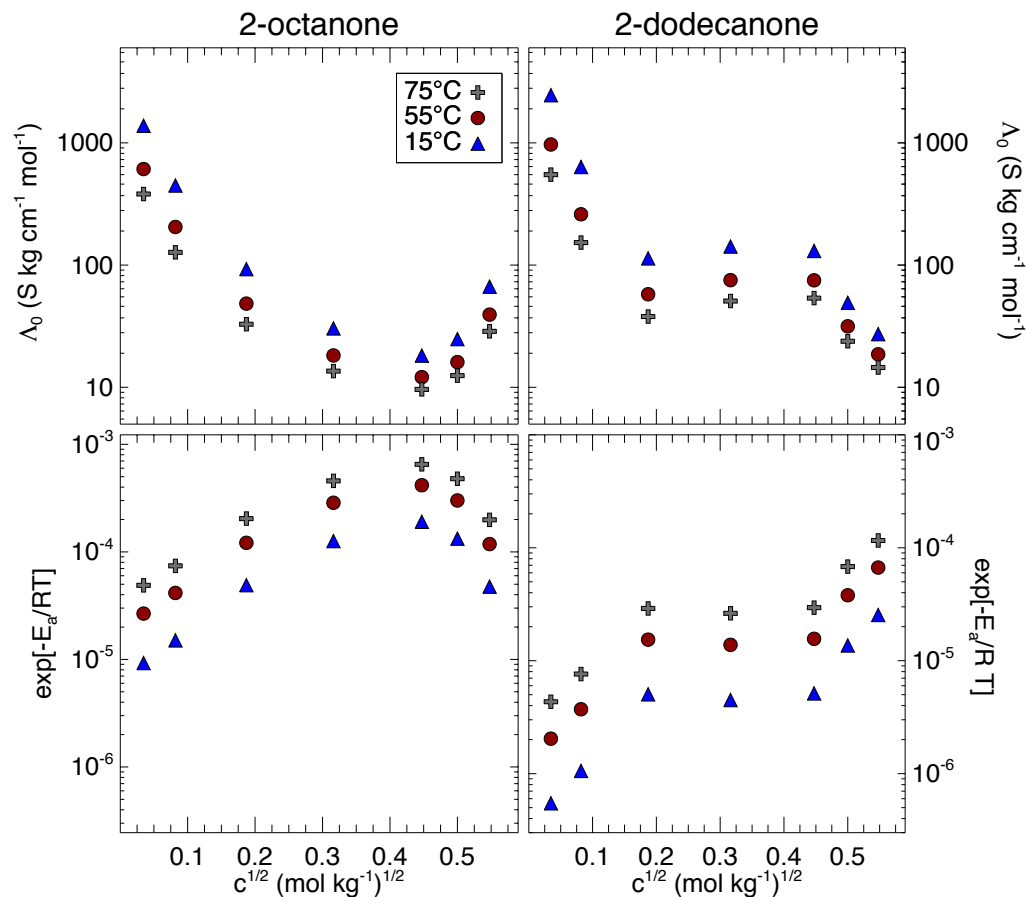
Figure 6.7: (Top) Molal exponential prefactor and (bottom) Boltzmann factor versus $c^{1/2}$ 2-octanone (left column) and 2-dodecanone (right column) at 15, 55, and 75°C.

II 2-ketones indicates that the concentration dependence of the mobilities of the cation and anion are different within the two groups. The similarity of the functional group further suggests that the differences observed in Λ originate in the differences in the lengths of the alkyl chains and their effect on the intermolecular interactions of the system. The dielectric constant is related to the number of dipoles in the system. By increasing the alkyl chain, the dipole density is decreasing thus decreasing the dielectric

constant. This reduced dipole density, and the increased number of non-polar regions within the system may contribute to the larger value of E_a observed for Group II members. To better understand the differences between the two groups of the pure solvents, the temperature-dependent diffusion coefficients will now be considered.

6.5   Diffusion coefficients of Group I and Group II 2-ketones

Temperature-dependent diffusion coefficients were collected for all members of the 2-ketones from 5 – 85°C. **Fig. 6.8** shows isothermal diffusion coefficients versus dielectric constant for 2-heptanone through 2-tridecanone from 5 – 85°C. The isothermal data separate to form temperature-dependent curves depicting each family member labelled according to the number of carbons in the alkyl chain. The isothermal diffusion coefficients increase with dielectric constant as the alkyl-chain decreases. Likewise, as the alkyl-chain decreases, the diffusion coefficient increases, creating an exponential-like functional form. Due to an increase in the melting temperature with increasing alkyl-chain length, the longer 2-ketone family members have a smaller temperature range. This difference, however, is taken into account with the scaling procedure.

The distinction between Group I and Group II is not clear in **Fig. 6.8**. The differences between the two groups originates from **Fig. 6.1** on page 127 with Group II having an increase in Λ with concentration marked as region II. The behavior of the diffusion coefficient with dielectric constant for the two groups is similar in **Fig. 6.8** suggesting that the differences in charge transport arise with the addition of salt and are negligible when considering only mass transport of the pure solvent.
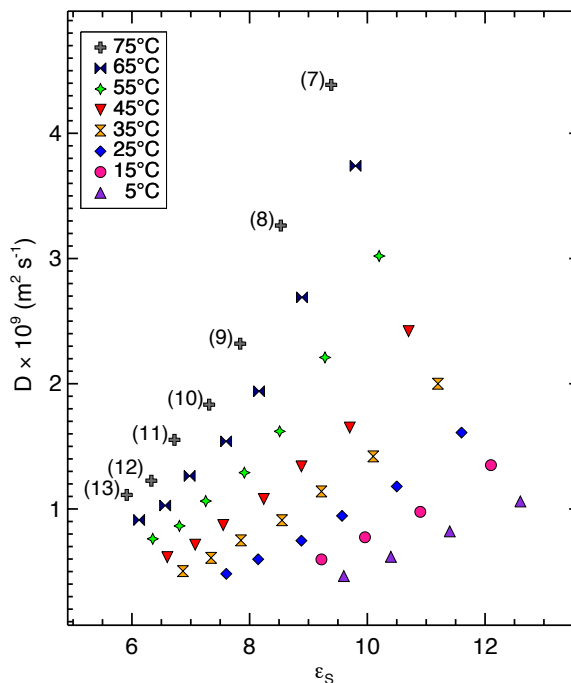
Figure 6.8: Isothermal diffusion coefficients dielectric constant for 2-heptanone (7), 2-octanone (8), 2-nonanone (9), 2-decanone (10), 2-undecanone (11), 2-dodecanone (12), and 2-tridecanone (13) from $5 - 85°C$.

6.6 Applying the compensated Arrhenius formalism to the diffusion coefficients of pure 2-ketones

6.6.1 CAF: E_a values of $D(T)$

Using **Fig. 6.8** for the scaling procedure detailed in § 2.3, the CAF is applied to the temperature-dependent diffusion coefficients of each group and E_a values are calculated for each member. The resulting CAE plots for 2-heptanone (Group I) and 2-dodecanone (Group II) are given in **Fig. 6.9**. Both sets of scaled diffusion coefficient data have approximately the same slope with inverse temperature which results in values of E_a that are very similar. The E_a values are calculated for each family member and
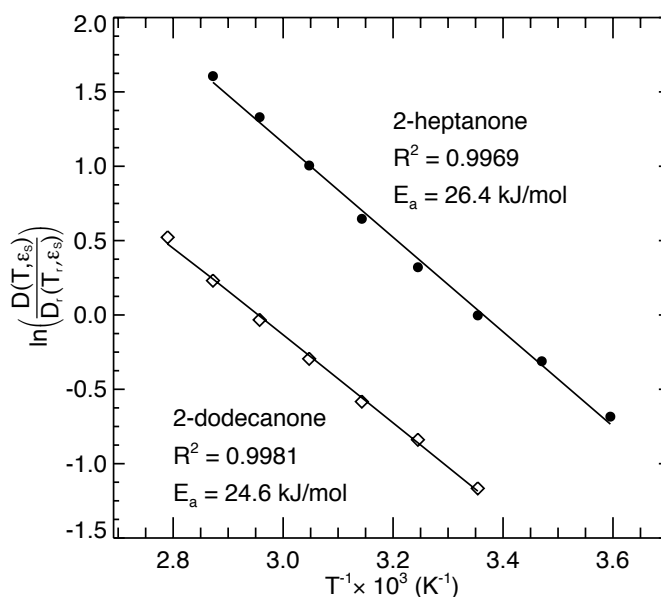
Figure 6.9: Compensated Arrhenius plot of diffusion coefficients for 2-heptanone (filled circles) with a T_r of 25°C and 2-dodecanone (open diamonds) with a T_r of 65°C.

are tabulated in **Table 6.2** along with the corresponding reference temperature used in the scaling procedure. Selection of the appropriate reference temperature has been explained in detail in §2.2.3 on page 24. The average E_a values from Group I and Group II are within 0.7 kJ mol^{-1} of each other. Since 2-decanone shows characteristics of both groups for Λ versus concentration, it is included in both groups. Comparing the E_a values for 2-decanone show that there is a slight increase of 2.3 kJ mol^{-1} using the Group I family members compared to the Group II family members. We have previously shown that if much shorter alkyl-chain family members are used in the scaling procedure, *e.g.*, 2-propanone and 2-butanone, then the E_a values calculated for the diffusion coefficients are approximately 10 kJ mol^{-1} less than the longer alkyl-chain family members.[51] This is not the case with the E_a values presented here for Group I and Group II: the average

E_a values are approximately the same and any deviations are within the error associated

with the CAF.

	E_a (kJ mol^{-1})	T_r(°C)
member	**Group I**	
2-heptanone	26.4 ± 0.7	15
2-octanone	25.2 ± 0.9	25
2-nonanone	25.9 ± 0.6	55
2-decanone	26.4 ± 0.6	75
Average	26.0 ± 0.4	
member	**Group II**	
2-decanone	24.1 ± 0.5	25
2-undecanone	26.7 ± 0.9	35
2-dodecanone	24.6 ± 0.5	65
2-tridecanone	25.7 ± 0.3	75
Average	25.3 ± 0.3	

Table 6.2: Diffusion coefficient energies of activation and corresponding reference temperatures for Group I 2-ketones and Group II 2-ketones using the compensated Arrhenius formalism.

The similarity of the E_a values for Group I and Group II suggests that there is

little difference in mass transport of the pure solvent as the length of the alkyl-chain

increases. The heteroatom plays a significant role in determining the nature of the

intermolecular interactions that occur in the different members studied, and it appears

that very similar interactions occur in both groups of the 2-ketone family.

6.6.2 CAF: exponential prefactor of $D(T)$

Another important quantity is the exponential prefactor, D_0. It is calculated following the procedure outlined in § 2.2.5. Plotting D_0 versus the dielectric constant

results in a single master curve if the assumptions of the CAF hold; that the temper-

ature dependence of the exponential prefactor is due to the temperature dependence

of the dielectric constant.[15,16,83] **Fig. 6.10** shows D_0 versus ε_s for both Group I and
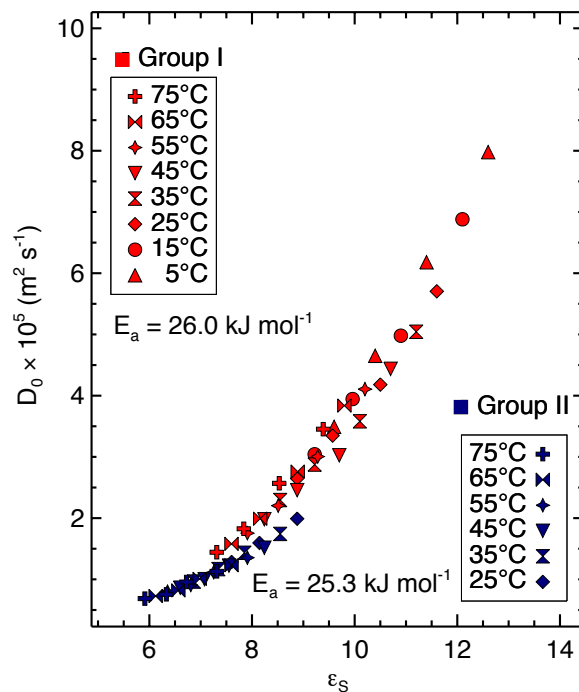
Figure 6.10: Diffusion exponential prefactors versus dielectric constant for Group I 2-ketones (red symbols) and Group II 2-ketones (blue symbols) using the average E_a values given in the figure.

Group II 2-ketone families. Each group forms a master curve for D_0 versus ε_s, with the master curve created by Group I in red and the master curve created by Group II in blue. The two master curves combine to form a semi-continuous master curve with only a slight deviation where the two curves do not completely overlap. The offset that is observed is due to the small difference in E_a which is considered to be within the error of the CAF. The formation of a continuous master curve from both Group I and Group II suggests that the dependence of D_0 on the dielectric constant is the same for both groups. To further interpret the differences between the diffusion coefficients for Group I and Group II the scaling procedure is performed including all 2-ketone family members, 2-heptanone through 2-tridecanone, and a single average E_a value is deter-
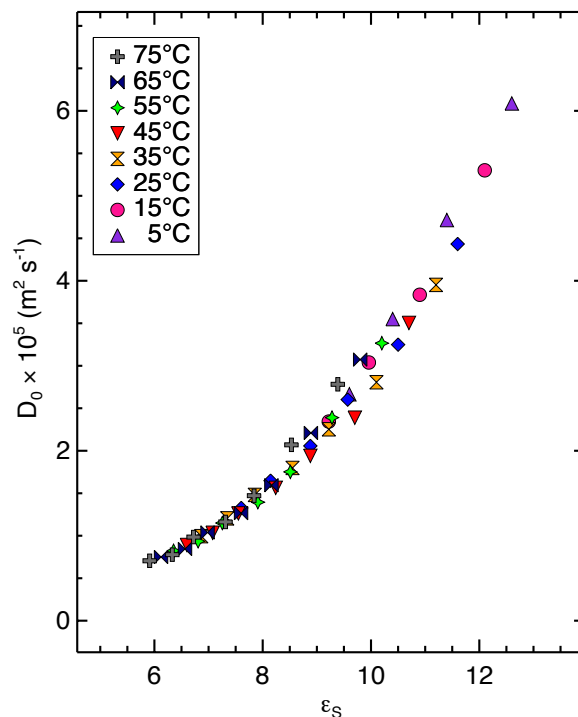
Figure 6.11: D_0 versus dielectric constant for all 2-ketone family members using an average E_a of 25.3 ± 0.3 kJ mol^{-1}.

mined. The average E_a was found to be 25.3 ± 0.3 kJ mol^{-1}, which is equivalent to 25.3 ± 0.3 (Group II) and within the error of 26.0 ± 0.4 (Group I1). The exponential prefactors are determined from the average E_a of 25.3 ± 0.3 kJ mol^{-1}, and the resulting plot of D_0 versus dielectric constant (**Fig. 6.11**) shows a master curve very similar to the combined master curves of **Fig. 6.10**. This further supports that there is little difference between the two groups of pure 2-ketones in terms of mass transport.

Based on the work of Eyring, the dependence of the exponential prefactor on ε_s for simple Arrhenius models have been linked to changes in the entropy of activation in the system.[81] The similarities between the two groups of 2-ketones could result from the entropy of activation of the system being very similar between the two groups. There

is no salt present to disrupt the intermolecular interactions, which suggests that the addition of a methylene groups does not disrupt the entropy of the system as would the addition of salt.

6.7   Summary and Conclusion

The increase in Λ with concentration (region II) is observed for TbaTf solutions with long chain 2-ketones (Group II), but not solutions with short chain 2-ketones (Group I). Comparing the diffusion coefficients shows that there is no discernible difference between the two groups in terms of mass transport, as shown with the similarity of the E_a calculated using the CAF. Upon the addition of salt, however, the differences become more apparent as shown in **Fig. 6.5**. Further differences can be seen by comparing the concentration dependences of Λ_0 and $\exp[-Ea/RT]$ in **Fig. 6.7** on page 140.

It can be assumed that the concentration dependence of Λ_0 is due to the concentration dependence of the dielectric constant (**eq. 6.1**), which is then extended to the concentration dependence of the ionic mobilities (**eq. 6.2**) and reprinted below:

$$\Lambda(T,c) = \Lambda_0(\varepsilon_s(T,c)) \, \exp\left[\frac{-E_a(c)}{RT}\right] = F\,\left[\mu_+(T,c) + \mu_-(T,c)\right]. \qquad \textbf{(6.4)}$$

From these relationships, the differences seen in Λ with concentration for Group I and Group II 2-ketones is due to the complex nature of the concentration dependence contained in Λ_0 and E_a, as well as the temperature dependence within ε_s and the Boltzmann factor. The concentration dependence in Λ_0 is primarily due to the concentration dependence of the dielectric constant. It is well known that the increase in Λ with

concentration (region II) is only seen for systems with a low dielectric constant ($\varepsilon_s \lesssim$ 10). It has been demonstrated that two systems, 2-octanone and 2-dodecanone, have dielectric constants that only differ by ≈ 2 dielectric constant units, and the range of dielectric constant covered by 2-octanone and 2-dodecanone is $8-16$ and $7-14$, respectively. Both of these ranges of ε_s span the accepted "10" value, but 2-octanone does not exhibit an increase in Λ with concentration while 2-dodecanone does. The behavior of ε_s with concentration for 2-octanone, however, is similar to that of 2-heptanone shown in **Fig. 6.2** (page 130), which shows ε_s decreasing at the higher concentrations. It is reasonable to conclude that the magnitude of ε_s is not a direct indication of observing the increase in Λ, but it is the inherent concentration dependence of ε_s that occurs for low values of ε_s contained in Λ_0 that dictates the increase in Λ with concentration.

The concentration and temperature dependence is further complicated by the relationship between ε_s and choice of salt and solvent. For Group II 2-ketone members, ε_s only increases with concentration for the concentrations presented here and shows no observable decrease at higher concentrations, unlike the shorter chain 2-ketones. The specific role that different types of intermolecular interactions play in the concentration and temperature dependence of ε_s is still not well understood, and further investigation is necessary. The temperature dependence of the dielectric constant, however, is a good measure of the changes that occur in the intermolecular interactions of the system and is a necessary component of the CAF in describing temperature-dependent mass and charge transport.

The other concentration dependence of Λ is contained in E_a. The difference in E_a seen between Group I and Group II indicates that E_a is not just associated with the type

of functional group, as suggested previously,[15,56] but is a complicated parameter that takes into account multiple intermolecular interactions of solvent–solvent, ion-solvent, and most likely in the case of other salts, ion-ion. These interactions vary with several factors including: the functional group, the alkyl-chain, and the number of ions present.

The individual concentration dependence contained within both Λ_0 and E_a are coupled in the shared concentration dependence contained in the sum of the ionic mobilities. The temperature dependence is also shared among the two factors, and affects the ionic mobilities but the extent of the effect is still not well understood. We therefore conclude that in order to characterize the increase of Λ with concentration, or lack thereof, then both the concentration dependence of Λ_0 *and* the concentration dependence of E_a must be taken into account.

Chapter 7

Concluding Remarks

The original purpose of this work was to answer the relatively simple question: *Why does the molal conductivity, Λ, increase with concentration in the region labelled "II,"* depicted by the schematic in **Fig. 7.1**. The answer is a straightforward statement that is extremely complicated: "it depends."
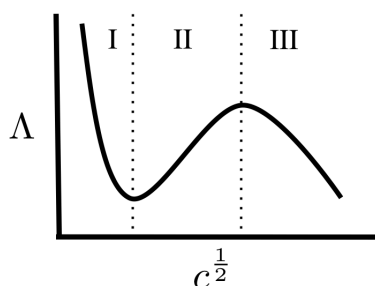
Figure 7.1: Schematic of molal conductivity, Λ with square root of the concentration, with labelled regions I, II, and III.

The increase in Λ depends on several factors that depend on the system, *i.e.*, the choice of salt and solvent. With the present work, I can only give results based on the effect of the solvent, but I speculate that the choice of salt also has a strong effect on charge transport that is not straightforward. The effect of the solvent on charge transport can be reduced to an equation that relates the temperature and concentration dependence of Λ to both the dielectric constant and the energy of activation of the solution, and then to the concentration and temperature dependence of the sum of the

ionic mobilities:

$$\Lambda(T, c) = \Lambda_0(\varepsilon_s(T, c), c) \exp\left[\frac{-E_a(c)}{RT}\right] = F(\mu_+ + \mu_-) = F[\mu_+(T, c) + \mu_-(T, c)] \quad (7.1)$$

First, consider the concentration dependence in the energy of activation. The electrolytes of this work can be considered "ideal" given TbaTf is a non-associating salt with a charge protected cation. The behavior of E_a with concentration is a general measure of the solvent-solvent interactions in the systems. **Fig. 7.2** shows the average E_a from the CAF for all systems presented in this work: TbaTf in 1- alcohols, 3-alcohols, short chain 2-ketones (Group I) and long chain 2-ketones (Group II).
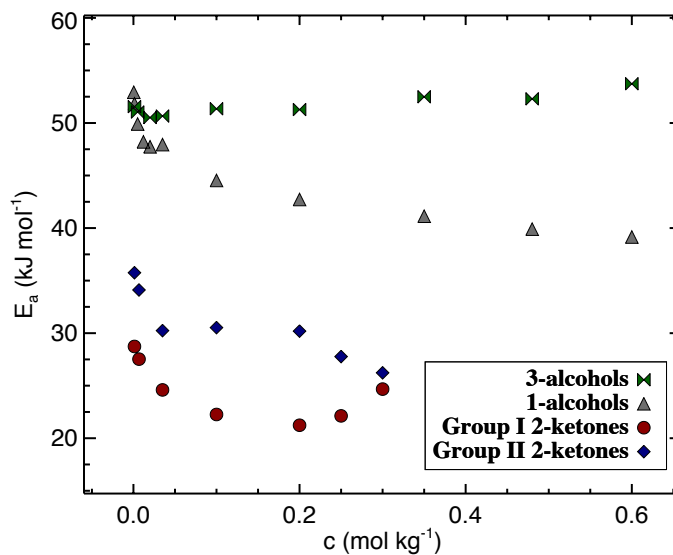
Figure 7.2: Energy of activation calculated from the CAF versus concentration for TbaTf solutions of 1-alcohols (grey triangles), 3-alcohols (green bow-ties), Group I 2-ketones (red circles), and Group II 2-ketones(blue diamonds).

As explained throughout this dissertation, the behavior of Λ in region II is not straightforward, and can not be reduced to the general statement that a decrease in E_a with concentration results in an increase in Λ. Three of the four solution groups

shown in **Fig. 7.2** show the increase of Λ in region II, but the E_a values of each group show very different qualitative trends with concentration. The associated solvents have a higher E_a than the non-associating solvents. Comparing the 1- and 3-alcohol solutions, it is clear that the E_a values of the 1-alcohol solutions have a much stronger dependence on concentration than the E_a values of the 3-alcohol solutions. The 2-ketone solution groups, which only differ by the number of carbons in the alkyl chain, show two different concentration dependences of E_a. The different behaviors of E_a with concentration can be linked to the different concentration dependent behaviors of ε_s, which are contained in Λ_0 in **eq. 7.1**. The concentration dependence of ε_s depends on the extent of association of the solvent, the interaction between the salt and solvent, as well as the temperature, and possibly other factors that have yet to be identified. What can be concluded is that the concentration dependence of Λ, namely the increase in region II, is a complicated relationship between the concentration dependence of E_a and the concentration dependence of ε_s and can not be separated into individual components. To understand the nature of charge transport in liquids, in particular the concentration dependence, the dielectric constant must be taken into account and the CAF must be used to determine both the E_a and exponential prefactor.

In summary, this dissertation has shown:

- The increase in Λ with concentration in region II is not only due to changes in ionic association.

- The increase in ε_s with concentration is not only due to changes in ionic association.

- The CAF is a valuable tool for determining molecular level properties of both mass and charge transport that continues to explain differences seen in the temperature-dependence of conductivity and self-diffusion data.

- The CAF must be applied to the temperature-dependent conductivity regardless of the linearity of the simple Arrhenius plot in order to determine an "appropriate" energy of activation.

- Differences observed in the results of the CAF for the diffusion coefficients of 1- and 3-alcohol solvents are directly related to changes in the extent of the hydrogen bonding network and can be accounted for using the temperature dependent dielectric constant.

- The addition of TbaTf to the 1- and 3-alcohols has a different effect on their respective hydrogen bonding networks, which plays a significant role in the concentration dependence of E_a and σ_0.

- The concentration dependence of the dielectric constant plays an integral part in describing Λ with concentration, and the magnitude of the dielectric constant is a poor criterion for predicting region II behavior in Λ.

- The concentration dependence of Λ, namely the increase in region II, is a complicated relationship between the concentration dependence of E_a and the concentration dependence of ε_s and can not be separated into individual components.

~~The End~~

The Beginning

References

[1] Gahran, A. *Survey says most U.S. cell phone owners have smartphones; so what?*; CNN, 2012, url: http://www.cnn.com.

[2] *Apple Press Information*; Apple. Inc., 2012 - url: http://www.apple.com.

[3] *Alternative Fuel Data Center*; U.S. Department of Energy: Office of Energy Efficiency and Renewable Energy, 2012; url: http://www.afdc.energy.gov/.

[4] Scrosati, B. *Nature Nanotechnology* **2007**, *2*, 598–599.

[5] Erlich, G. In *Battery Technology Handbook*, 3rd ed.; Linden, D., Reddy, T. B., Eds.; McGraw-Hill: New York, 2002.

[6] Jacobi, W. In *Battery Technology Handbook*, 2nd ed.; Kiehne, H. A., Ed.; Marcel Dekker: New York, 2003.

[7] Kay, R. L.; Evans, D. F. *The Journal of Physical Chemistry* **1966**, *70*, 2325–2335.

[8] Bockris, J.; Reddy, A. *Modern Electrochemistry*, 2nd ed.; Plenum Press: New York, 1998; Vol. 1.

[9] Cameron, G. G.; Ingram, M. D.; Sorrie, G. A. *Journal of Electroanalytical Chemistry and Interfacial Electrochemistry* **1986**, *198*, 205–7.

[10] Albinsson, I.; Mellander, B.-E.; Stevens, J. R. *The Journal of Chemical Physics* **1992**, *96*, 681–690.

[11] Fuoss, R. M. *Proceedings of the National Academy of Sciences* **1959**, *45*, 807–813.

[12] Longsworth, L. G.; MacInnes, D. A. *The Journal of Physical Chemistry* **1939**, *43*, 239–246.

[13] Mendolia, M. S.; Farrington, G. C. *Chemistry of Materials* **1993**, *5*, 174–181.

[14] Weingärtner, H.; Nadolny, H. G.; Käshammer, S. *The Journal of Physical Chemistry B* **1999**, *103*, 4738–4743.

[15] Petrowsky, M.; Frech, R. *The Journal of Physical Chemistry B* **2009**, *113*, 5996–6000.

[16] Petrowsky, M.; Frech, R. *The Journal of Physical Chemistry B* **2010**, *114*, 8600–8605.

[17] Petrowsky, M.; Frech, R. *Electrochimica Acta* **2010**, *55*, 1285–1288.

[18] Bockris, J.; Reddy, A. *Modern Electrochemistry*, 2nd ed.; Plenum Press: New York, 1998; Vol. 1; Chapter 4.6 - 4.8.

[19] Williams, M. L.; Landel, R. F.; Ferry, J. D. *Journal of the American Chemical Society* **1955**, *77*, 3701–7.

[20] Fulcher, G. S. *Journal of the American Ceramic Society* **1925**, *8*, 339–55.

[21] Tammann, G.; Hesse, W. *Zeitschrift fuer Anorganische und Allgemeine Chemie* **1926**, *156*, 245–57.

[22] Vogel, H. *Physikalische Zeitschrift* **1921**, *22*, 645–6.

[23] Levine, I. *Physical Chemistry (Chapter 16)*, 5th ed.; McGraw-Hill: New York, 2002.

[24] Stygar, J.; Biernat, A.; Kwiatkowska, A.; Lewandowski, P.; Rusiecka, A.; Zalewska, A.; Wieczorek, W. *The Journal of Physical Chemistry B* **2004**, *108*, 4263–4267.

[25] Gray, F. M. *Journal of Polymer Science Part B: Polymer Physics* **1991**, *29*, 1441–1445.

[26] Cameron, G. G.; Ingram, M. D.; Sorrie, G. A. *Journal of the Chemical Society, Faraday Transactions 1: Physical Chemistry in Condensed Phases* **1987**, *83*, 3345–53.

[27] Cavell, E. A. S.; Knight, P. C. *Zeitschrift fuer Physikalische Chemie (Muenchen, Germany)* **1968**, *57*, 331–4.

[28] Bruce, P. G.; Vincent, C. A. *Journal of the Chemical Society, Faraday Transactions* **1993**, *89*, 3187–3203.

[29] Fuoss, R. M.; Kraus, C. A. *Journal of the American Chemical Society* **1933**, *55*, 2387–2399.

[30] Ferry, A.; Jacobsson, P.; Torell, L. M. *Electrochimica Acta* **1995**, *40*, 2369–73.

[31] Pehlivan, İ. B.; Georén, P.; Marsal, R.; Granqvist, C. G.; Niklasson, G. A. *Electrochimica Acta* **2011**, *57*, 201–206.

[32] Gulich, R.; Köhler, M.; Lunkenheimer, P.; Loidl, A. *Radiation and Environmental Biophysics* **2009**, *48*, 107–114.

[33] Van Beek, W. M.; Mandel, M. *Journal of the Chemical Society, Faraday Transactions 1: Physical Chemistry in Condensed Phases* **1978**, *74*, 2339–51.

[34] Gestblom, B.; Mehrotra, S.; Sjöblom, J. *Journal of Solution Chemistry* **1986**, *15*, 55–68.

[35] Gestblom, B.; Sjöblom, J. *Journal of Solution Chemistry* **1986**, *15*, 259–268.

[36] Gestblom, B.; Svorstoel, I.; Songstad, J. *Journal of Physical Chemistry* **1986**, *90*, 4684–6.

[37] Cachet, H.; Cyrot, A.; Fekir, M.; Lestrade, J. C. *Journal of Physical Chemistry* **1979**, *83*, 2419–29.

[38] Sigvartsen, T.; Gestblom, B.; Noreland, E.; Songstad, J. *Acta Chemica Scandinavica* **1989**, *43*, 103–15.

[39] Kraus, C. A.; Fuoss, R. M. *Journal of the American Chemical Society* **1933**, *55*, 21–36.

[40] Bacelon, P.; Corset, J.; Loze, C. *Journal of Solution Chemistry* **1983**, *12*, 13–22.

[41] Bacelon, P.; Corset, J.; Loze, C. *Journal of Solution Chemistry* **1983**, *12*, 23–31.

[42] Frech, R.; Huang, W.; Dissanayake, M. *Materials Research Society Symposia Proceedings* **1995**, *369*, 523–534.

[43] Frech, R.; Huang, W. *Journal of Solution Chemistry* **1994**, *23*, 469–481.

[44] Petrowsky, M.; Frech, R. *The Journal of Physical Chemistry B* **2008**, *112*, 8285–8290.

[45] Huang, W.; Frech, R.; Johansson, P.; Lindgren, J. *Electrochimica Acta* **1995**, *40*, 2147 – 2151.

[46] Miles, M.; Doyle, G.; Cooney, R.; Tobias, R. *Spectrochimica Acta Part A: Molecular Spectroscopy* **1969**, *25*, 1515 – 1526.

[47] Petrowsky, M.; Frech, R.; Suarez, S. N.; Jayakody, J. R. P.; Greenbaum, S. *Journal of Physical Chemistry B* **2006**, *110*, 23012–23021.

[48] Schantz, S.; Sandahl, J.; Bojesson, L.; Torell, L.; Stevens, J. *Solid State Ionics* **1988**, *28-30, Part 2*, 1047 – 1053.

[49] Fleshman, A. M.; Petrowsky, M.; Jernigen, J. D.; Bokalawela, R. S. P.; Johnson, M. B.; Frech, R. *Electrochimica Acta* **2011**, *57*, 147–152.

[50] Petrowsky, M. Ion Transport in Liquid Electrolytes. Ph.D. Dissertation, University of Oklahoma, 2008.

[51] Bopege, D. N.; Petrowsky, M.; Fleshman, A. M.; Frech, R.; Johnson, M. B. *The Journal of Physical Chemistry B* **2012**, *116*, 71–76.

[52] Petrowsky, M.; Frech, R. *The Journal of Physical Chemistry B* **2009**, *113*, 16118–16123.

[53] Bjerrum, N. *Niels Bjerrum's Selected Papers*; Einer Munksgaard: Copenhagen, 1949.

[54] Bopege, D. N.; Petrowsky, M.; Frech, R.; Johnson, M. B. *Journal of Solution Chemistry* **2012**, *accepted for publication*.

[55] Petrowsky, M.; Fleshman, A.; Frech, R. *The Journal of Physical Chemistry B* **2012**, *116*, 5760–5765.

[56] Petrowsky, M.; Fleshman, A.; Ismail, M.; Glatzhofer, D. T.; Bopege, D. N.; Frech, R. *The Journal of Physical Chemistry B* **2012**, *accepted for publication*.

[57] Campbell, C.; Brink, G.; Glasser, L. *Journal of Physical Chemistry* **1976**, *80*, 686–90.

[58] Czarnecki, M. A.; Orzechowski, K. *The Journal of Physical Chemistry A* **2003**, *107*, 1119–1126.

[59] Palombo, F.; Tassaing, T.; Danten, Y.; Besnard, M. *The Journal of Chemical Physics* **2006**, *125*, 094503.

[60] D'Aprano, A.; Donato, D. I.; Agrigento, V. *Journal of Solution Chemistry* **1981**, *10*, 673–680.

[61] Shinomiya, T. *Bulletin of the Chemical Society of Japan* **1989**, *62*, 908–914.

[62] Vij, J. K.; Scaife, W. G.; Calderwood, J. H. *Journal of Physics D: Applied Physics* **1981**, *14*, 733.

[63] Campbell, C.; Brink, G.; Glasser, L. *Journal of Physical Chemistry* **1975**, *79*, 660–5.

[64] Dannhauser, W. *The Journal of Chemical Physics* **1968**, *48*, 1911–1917.

[65] Johari, G. P.; Dannhauser, W. *The Journal of Physical Chemistry* **1968**, *72*, 3273–3276.

[66] Johari, G. P.; Dannhauser, W. *The Journal of Chemical Physics* **1968**, *48*, 5114–5122.

[67] Lehtola, J.; Hakala, M.; Hämäläinen, K. *The Journal of Physical Chemistry B* **2010**, *114*, 6426–6436.

[68] Paolantoni, M.; Sassi, P.; Morresi, A.; Cataliotti, R. S. *Chemical Physics* **2005**, *310*, 169–178.

[69] Vahvaselkä, K. S.; Serimaa, R.; Torkkeli, M. *Journal of Applied Crystallography* **1995**, *28*, 189–195.

[70] Sartor, G.; Hofer, K.; Johari, G. P. *The Journal of Physical Chemistry* **1996**, *100*, 6801–6807.

[71] Shinomiya, K.; Shinomiya, T. *Bulletin of the Chemical Society of Japan* **1990**, *63*, 1093–1097.

[72] Woutersen, S.; Emmerichs, U.; Bakker, H. J. *The Journal of Chemical Physics* **1997**, *107*, 1483–1490.

[73] Pimentel, G. C.; McClellan, A. L. *The Hydrogen Bond*; W.H. Freeman and Company, 1960.

[74] Jeffrey, G. A. *An Introduction to Hydrogen Bonding*; Oxford University Press, 1997.

[75] Meighan, R. M.; Cole, R. H. *The Journal of Physical Chemistry* **1964**, *68*, 503–508.

[76] Wohlfahrt, C. *Static Dielectric Constants of Pure Liquids and Binary Liquid Mixtures*; Pure Liquids: Data. Landolt-Bornstein. Group IV physical chemistry; Springer-Verlag: New York, 1991; Vol. 6.

[77] Oster, G.; Kirkwood, J. G. *The Journal of Chemical Physics* **1943**, *11*, 175–178.

[78] Smyth, C. P. *Dielectric behavior and structure: dielectric constant and loss, dipole moment, and molecular structure*; McGraw-Hill, 1955.

[79] Dannhauser, W.; Bahe, L. W.; Lin, R. Y.; Flueckinger, A. F. *The Journal of Chemical Physics* **1965**, *43*, 257–266.

[80] Yaws, C. L. *Yaws' Handbook of Thermodynamic and Physical Properties of Chemical Compounds*; Knovel, 2003.

[81] Glasstone, S.; Laidler, K. J.; Eyring, H. *The Theory of Rate Processes*, 1st ed.; McGraw-Hill Book Co.: New York City, 1941.

[82] Petrowsky, M.; Fleshman, A.; Bopege, D. N.; Frech, R. *The Journal of Physical Chemistry B* **2012**, *accepted for publication*.

[83] Grunwald, E.; Pan, K.-C. *The Journal of Physical Chemistry* **1976**, *80*, 2929–2931.

[84] Bykova, Z.; Klugman, I.; Sorkin, Y. *Izmeritel'naya Tekhnika* **1981**, *10*, 56–58.

[85] Agilent 16452A Liquid Test Fixture Operation and Service Manual. 2000.

[86] Chang, H.-C.; Jaffe, G. *Journal of Chemical Physics* **1952**, *20*, 1071–7.

[87] Johnson, J. F.; Cole, R. H. *Journal of the American Chemical Society* **1951**, *73*, 4536–40.

[88] Maruska, H.; Stevens, J. *Transactions on Electrical Insulation* **1988**, *23*, 197–200.

[89] Scheider, W. *Journal of Physical Chemistry* **1975**, *79*, 127–36.

[90] Grosse, C.; Tirado, M. *IEEE Transactions on Instrumentation and Measurement* **2001**, *50*, 1329 –1333.

[91] Van der Touw, F.; Mandel, M. *Transactions of the Faraday Society* **1971**, *67*, 1336–1342.

[92] Winsor, P.; Cole, R. H. *The Journal of Physical Chemistry* **1982**, *86*, 2486–2490.

[93] Stejskal, E. O.; Tanner, J. E. *The Journal of Chemical Physics* **1965**, *42*, 288–292.

[94] Price, W. S. *Concepts in Magnetic Resonance* **1997**, *9*, 299–336.

[95] Markwardt, C. B. In *Astronomical Data Analysis Software and Systems XVIII*; Bohlender, D. A., Durand, D., Dowler, P., Eds.; Astronomical Society of the Pacific Conference Series; 2009; Vol. 411; p 251.

Appendix A

Experimental Techniques

A.1   Sample Preparation

All glassware was cleaned with soap and water, rinsed three times with distilled water, and allowed to dry in a 160°C oven overnight. The same cleaning procedure was followed for all plastic components, but a 60°C oven was used for drying. All solvents and salts (99 % pure) were obtained from Sigma-Aldrich, Acros Organics, TCI America, or Alfa-Aesar and used as received. All chemicals were stored in and all samples were prepared in a glovebox ($\leq$ 1 ppm H_2O) under a nitrogen atmosphere. All liquid electrolytes were made at ambient glove box temperature (approximately 27 °C) by dissolving salt into solvent until the appropriate molal concentration (moles salt/kg solvent) were obtained. The electrolyte solution was then stirred for an average of 24 hours.

A.2   Impedance Spectroscopy

A.2.1   Sample holder for measuring conductivity and dielectric constant

The sample holder was an Agilent 16452A liquid test fixture, shown disassembled in **Fig. A.1** and assembled in **Fig. A.2**. Each piece was cleaned with soap and water, rinsed thoroughly with distilled water and dried in a 60°C oven overnight. The elec-
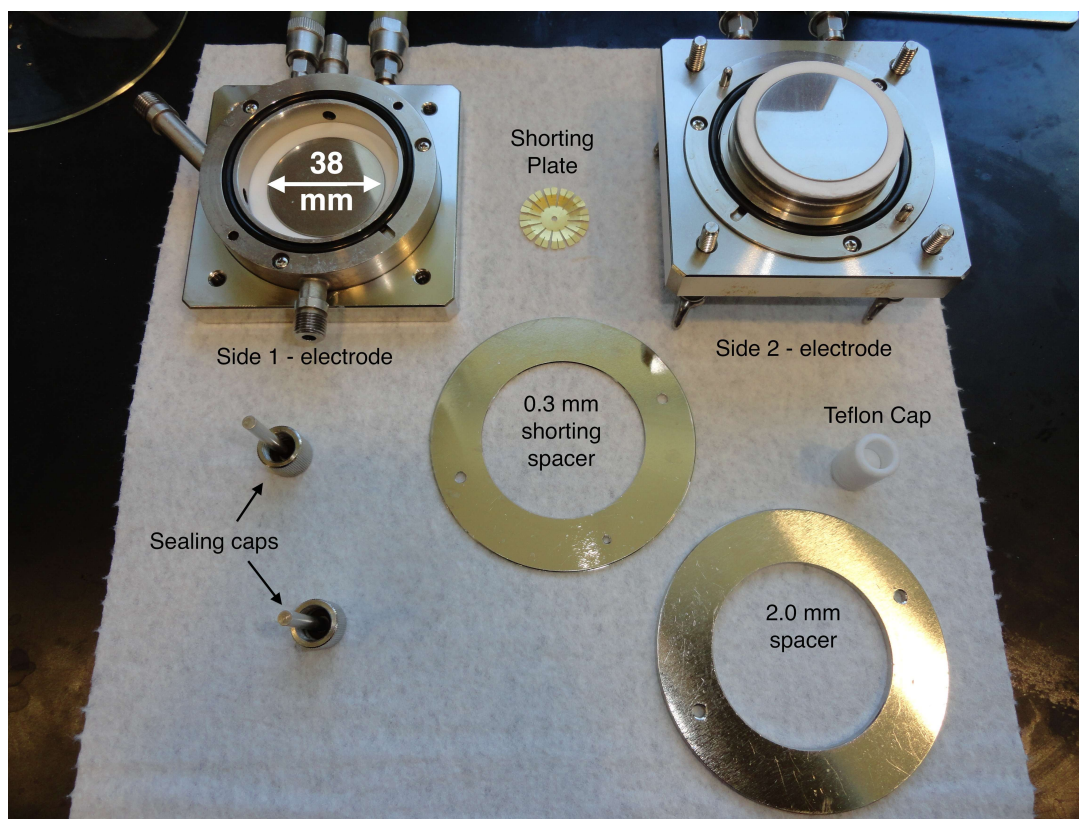
Figure A.1: Image of components of Agilent 16452A liquid test fixture. Parts are labelled in the figure.

trodes are circular disks made from nickel-plated cobalt (Fe 54 %, Co 17 %, Ni 29 %), have a diameter of 38 mm, and are in the center of the components labelled side 1-, and side 2-electrode in **Fig. A.1**. The sealing caps were screwed onto the fill ports located on the side and bottom of the side 1-electrode labelled in **Fig. A.1**. The teflon cap was designed and milled by Jeremy Jernigan of the Homer L. Dodge Department of Physics and Astronomy.[a] It fits snugly on the top fill port of side 1-electrode. The cell was assembled first using the 0.3 mm shorting spacer and the shorting plate. The assembled cell was then connected to a HP 4192 A impedance analyzer, and a zero short was performed at 10MHz inside the glovebox. This was done by connecting the appropriate

---

[a]And it is a necessity if temperature-dependent work is to be done with this apparatus.

cables to the labelled connections on the top of the test fixture. The frequency on the HP 4192 A was set to 10 mHz, the series mode and impedance mode were selected. The "zero short" was selected. The reading on the instrument went from approximately 0.3 Ω to 0.00 Ω. This step cancelled out any stray impedance due to the cables. The liquid test fixture was then disassembled, the shorting plate was removed and the shorting spacer was replaced with the 2 mm spacer (shown in the bottom left of **Fig. A.1**). The largest spacer was used in order to reduce the effects of electrode polarization.[84] The liquid test fixture was assembled, shown in **Fig. A.2**, in order: side 1-electrode,
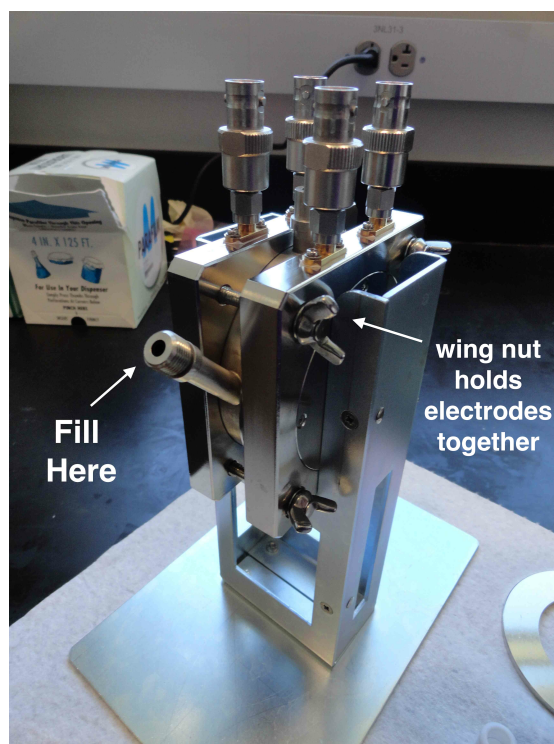

Figure A.2: Assembled Agilent 16452A liquid test fixture.

o-ring,[a] 2mm spacer, o-ring, side 2-electrode, components were then screwed together using the four attached wing nut screws, labelled in **Fig. A.2**. Once assembled, one

---

[a]The o-rings are set in place around the electrodes in **Fig. A.1**.

of the screw caps was secured to the bottom fill port. The solution to be measured was then injected into the side fill port, labelled "Fill Here" in **Fig. A.2** using a clean glass syringe. The liquid test fixture required approximately 7 mL of solution. The test fixture was filled until the solution appears at the top of the side fill port. The teflon cap, labelled in **Fig. A.1**, was then pushed over the top fill port. A small amount of solution usually came out of the side fill port. The screw cap was then secured onto the side fill port. It was essential to fill the test fixture in this order. Once the test fixture was filled, it was placed into the thermal bath (as shown below in **Fig. A.3**) by hanging it from two connectors suspended by a metal rod. The thermal bath sat
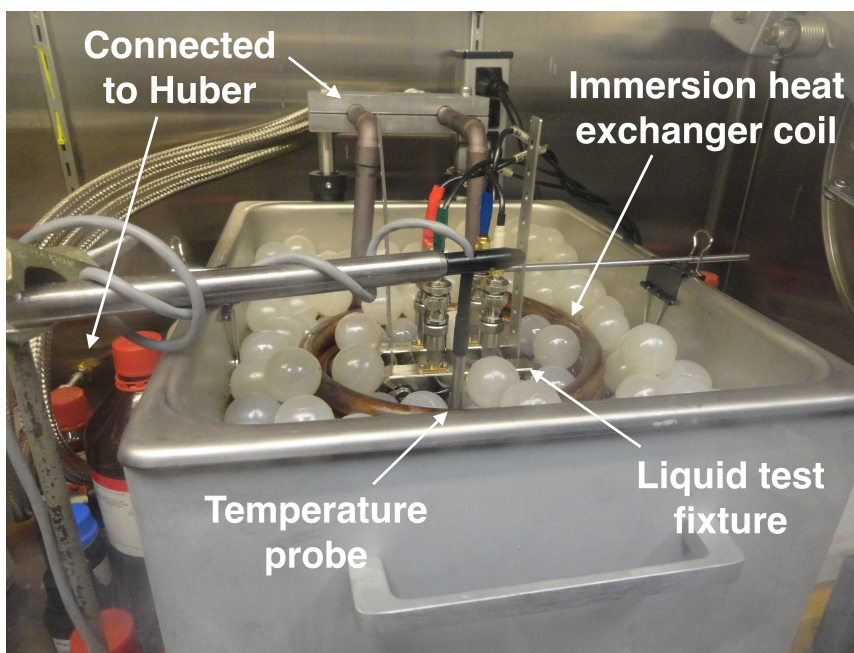

Figure A.3: Assembled Agilent 16452A liquid test fixture suspended in thermal heating fluid within immersion heat exchanger, and all contained inside the glovebox.

upon a stir-plate, contained a large stir bar, and was filled with Dynalene HT heat transfer fluid designed to accommodate a temperature range of -30 – 350°C. A Huber ministat 125 bath was used to regulate the temperature to ±0.1°C from 5–85°C, in

10°C increments. The Huber pumped a mixture of ethylene glycol and water into the glovebox through a tube connected to a copper immersion heat exchanger coil, that returns to the Huber ministat. The heat exchanger was set inside the thermal bath in the glovebox, which allows for control of the temperature of the thermal bath without disrupting the glovebox atmosphere. The liquid test fixture was placed within the inner circumference of this heat exchanger, as shown in **Fig. A.3**.

The data were collected via an automated system operated by LabView software developed by Chris Crowe of the Homer L. Dodge Department of Physics and Astronomy. As mentioned in the Acknowledgments section, the design of the glovebox-integrated temperature bath system was done by the Matt Johnson research group and I continue to be in awe of their expertise in machining and equipment design. Again, thank you gentlemen! This work would not have been possible without you.

A.2.2   Determining the conductivity and dielectric constant

The capacitance (C), conductance (G), and phase angle (θ) were all measured using the HP 4192 A impedance analyzer and the Agilent 16452A liquid test fixture as assembled in **Fig. A.3**. The measurements were taken with a logarithmic sweep over a frequency range 1 kHz to 13 MHz. The instrument was set to parallel circuit and averaging (slow) mode. The conductivity σ was calculated from the measured conductance G through the equation $\sigma = L \times G \times A^{-1}$, where L is the electrode gap (in this case determined by the size of the spacer used with the Agilent liquid test fixture, shown in **Fig. A.1**), and A is the electrode area (the area of the disks of the Agilent liquid test fixture). The static dielectric constant ε_s was calculated from the measured

capacitance C through the equation $\varepsilon_s = \alpha \times C \times C_0^{-1}$, where α is a variable to account for stray capacitance, and C_0 is the atmospheric capacitance,[85] taken as a function of temperature inside the glovebox.
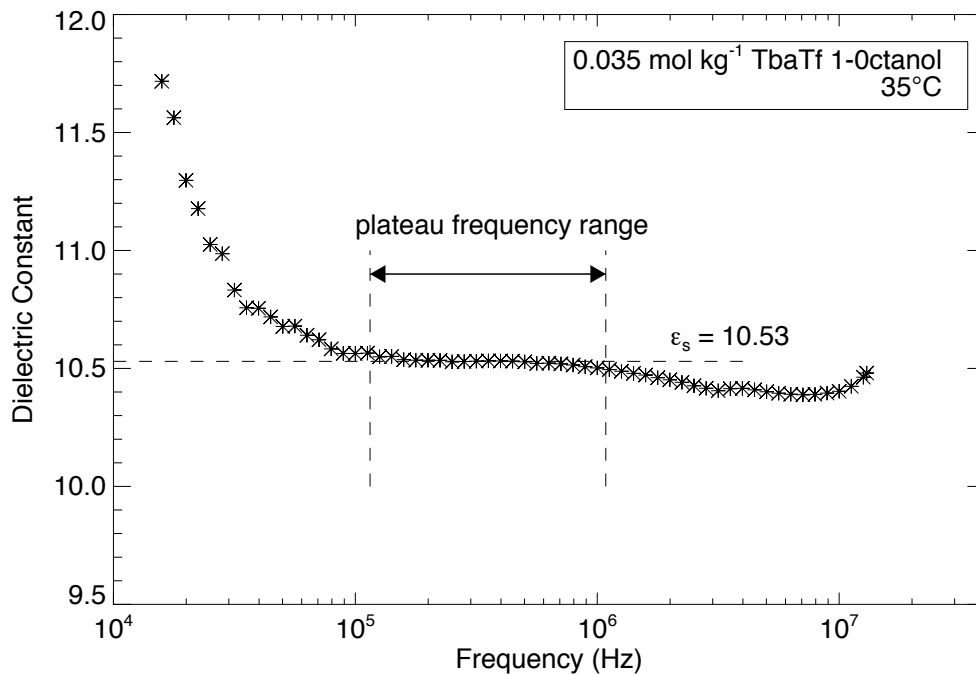

Figure A.4: Dielectric constant versus frequency for 0.035 m TbaTf 1-octanol at 35°C. The horizontal dashed line represents extrapolation of the plateau region to zero frequency. The vertical dashed lines represent the plateau frequency range.

Measuring the static dielectric constant of an ionically conducting solution is not trivial, and therefore further details for the determination of ε_s will now be given. It is straightforward to calculate ε_s in a pure solvent by using the above equation to divide the limiting low frequency value of the capacitance by the atmospheric capacitance. However, in an electrolyte the capacitance in the limit of low frequency is artificially high due to electrode polarization effects,[33,86–89] as depicted in **Fig. A.4** for 0.035 m TbaTf

1-octanol. The electrode polarization dies off as the frequency increases and a plateau region is observed. I considered the static capacitance as the value in the plateau region. In the case of 0.035 m TbaTf 1-octanol, the plateau extrapolates to a dielectric constant of 10.53, which is rounded to 10.5. This plateau region is relatively broad, such that it is straightforward to extrapolate to zero frequency. For more concentrated solutions,
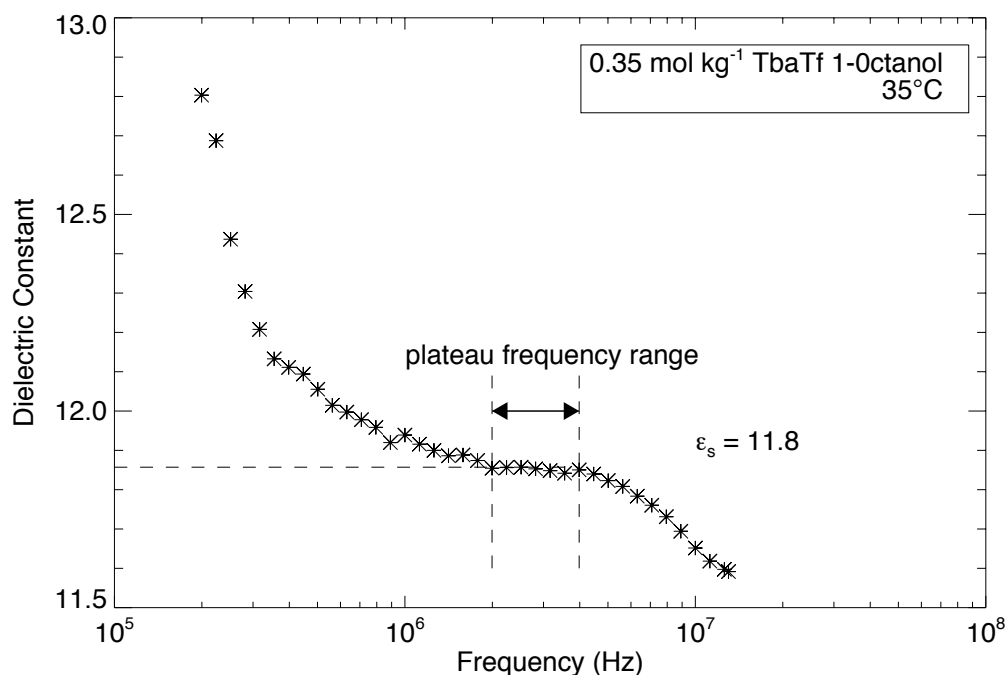

Figure A.5: Dielectric constant versus frequency for 0.035 m TbaTf 1-octanol at 35°C. The horizontal dashed line represents extrapolation of the plateau region to zero frequency. The vertical dashed lines represent the plateau frequency range.

the plateau region of the frequency narrows as illustrated in **Fig. A.5** with data for 0.35 m TbaTf 1-octanol at 35°C. This plateau region is determined by taking the square of the difference between consecutive capacitance values with frequency and isolating the minimum of the curve. A plot of the square of the difference between consecutive

values is given in **Fig. A.6** for 0.35 m TbaTf 1-octanol at 35°C. The vertical dashed lines represent the same frequency region in **Fig. A.5** and **Fig. A.6**. The minimum formed from the parabola-like shape of the curve in **Fig. A.6** denotes the plateau region from which to extrapolate to zero frequency. The same procedure is used for
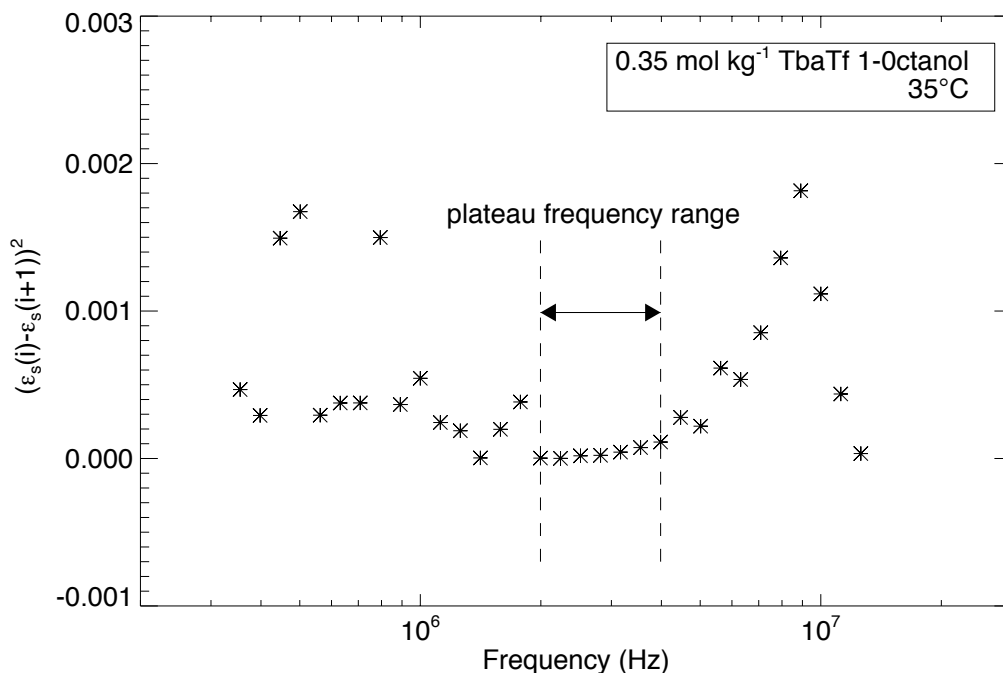

Figure A.6: Dielectric constant versus frequency for 0.035 TbaTf 1-octanol at 35°C. Dashed line represents extrapolation of plateau region to zero frequency.

determining the conductance, which also varies over frequency and has a broad plateau that is simple to determine, much like the broad plateau of **Fig. A.4**. There is an additional complication in solutions with high conductivities. The impedance analyzer models the electrolyte as a capacitor and resistor in parallel. For highly conducting solutions, the electrolyte behaves mostly as a resistor (*i.e.*, very small phase angle) and

the accuracy of the capacitance measurements deteriorates.[33,90,91] To help quantify the error in the dielectric constant measurements, ε_s for LiClO$_4$–ethyl acetate solutions at several different salt concentrations was determined. These values were compared to literature values.[37] For a 0.80 M solution at 25°C there is roughly a 0.6 percent difference between the measured ε_s and the literature value, with the measured value being higher. Therefore, the quality of the capacitance data was considered to be satisfactory if the conductivity was less than that of the 0.80 M solution (2.35×10^{-3} S cm^{-1}) and the phase angle greater than that of the 0.80 M solution ($\theta > 1.1°$). These conductivity and phase angle limitations for accurate measurement of ε_s are consistent with an additional study that compared measured σ and ε_s values to literature values for sodium iodide-methanol solutions.[92]

A.3 Pulse Field Gradient NMR

Diffusion coefficients were measured using pulsed field gradient nuclear magnetic resonance (PFG NMR) with a VarianVNMRS-400 MHz NMR and a Auto-X-Dual broadband 5 mm probe. The pure solvents were put into a glass NMR tube with a 5 mm outer diameter. The sample height within the tube was measured to 0.8 cm. The temperature was regulated from 5 – 85°C in 10°C increments using a FTS XR401 air-jet regulator. The sample was allowed to equilibrate at each temperature for 10 minutes. At each temperature, a standard Stejskal-Tanner[93] pulsed field gradient spin-echo sequence was used. The review of PFG NMR by Price[94] is an exceptional resource for this technique. The gradient field strength was varied in 0.023 T m^{-1} intervals from 0.05 – 0.63

T m^{-1}. At each interval, the signal was integrated and the resulting intensity values were plotted as the natural logarithm versus the square of the gradient field strength.

Fig. A.7 shows the data used to determine the diffusion coefficient for pure 3-hexanol
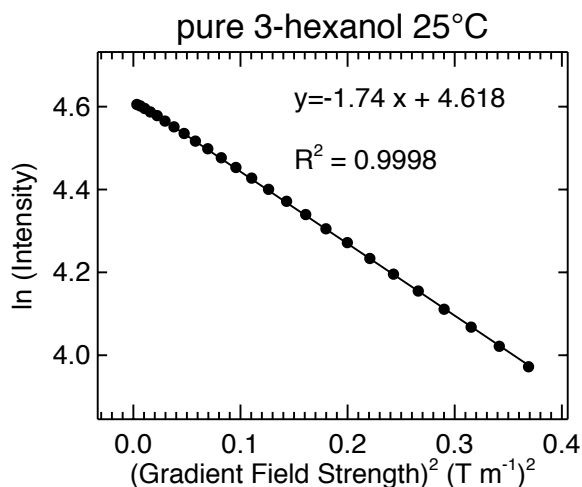

Figure A.7: ln(Intensity) versus gradient field strength for pure 3-hexanol at 25°C. The slope from the given equation was used to determine the diffusion coefficient.

at 25°C. Using **eq. A.1**, the diffusion coefficient was calculated from the slope of the linear fit.[93]

$$E = \exp[-\gamma^2 \, g^2 \, D \, \delta^2 (\Delta - \delta/3)] \quad \rightarrow \quad \ln(E) = \underbrace{-(\gamma^2 \delta^2 (\Delta - \gamma/3) \, D)}_{\text{slope in } \textbf{Fig. A.7}} \times g^2 \qquad (\textbf{A.1})$$

where E is the integrated signal intensity, γ is the gyromagnetic ratio (2.68×10^8 s^{-1} T^{-1}, for ^{1}H), g is the gradient field strength in T m^{-1}, D is the diffusion coefficient, δ is the length of the gradient pulse (which is unique to each solvent system) and Δ is the time between gradient pulses, which depends on the value of δ.

A.4 FT-IR

Infrared data were collected with a Bruker IFS66V Fourier Transform Infrared (FTIR) spectrometer with a potassium bromide beamsplitter. Data were recorded with a spectral resolution of 1 cm^{-1} over the range 500 – 4000 cm^{-1}. The data were averaged over 64 scans under N_2 purge. Samples were placed between two sodium chloride (2 mm thickness and 25 mm diameter) windows and secured in a Harrick temperature-controlled demountable liquid cell (model TFC-M25-3). The temperature was controlled using both a Neslab coolflow CFT-33 refrigerated regulator and an Omega CN9000A digital temperature controller. Due to instrument complications with the Bruker ISF66V, the room temperature 0.48 m TbaTf 1-decanol data discussed in § 5.4 was collected using a IRAffinity-1 Shimadzu FTIR. For comparison with the Bruker spectra, pure 1-decanol spectra were also collected with the Shimadzu and the average deviation of several peaks was approximately 2 cm^{-1}.

A.5 Density

Density measurements of pure solvents were made using an Anton-Paar DMA 4500M density meter with internal temperature regulation. Control samples of 2-pentanone, 2-octanone, butyl acetate, and hexyl acetate were checked against literature data and found to be within 0.1%.[80]

A.6 Data Analysis

Data were analyzed using IDL 8.0 and Microsoft Excel. For linear and non-linear least squares fitting (determining the functional form for the reference curves), MPFIT[95] was used within IDL.